SOME SPECTRAL PROBLEMS IN MATHEMATICAL PHYSICS

A Dissertation

by

NGOC THANH DO

Submitted to the Office of Graduate and Professional Studies of
Texas A&M University
in partial fulfillment of the requirements for the degree of

DOCTOR OF PHILOSOPHY

Chair of Committee,	Peter Kuchment
Committee Members,	Artem Abanov
	Gregory Berkolaiko
	Joseph Ward
Department Head,	Emil Straube

August 2016

Major Subject: Mathematics

ABSTRACT

In this dissertation we deal with some spectral problems for periodic differential operators originating from mathematical physics. We begin by using quantum graphs to model a particular graphyne and related nanotubes. The dispersion relations, and thus spectra, of periodic Schrödinger operators on these structures are analyzed. We find highly directional Dirac cones, which makes some types of graphynes fascinating. Then, we study a conjecture that has been widely assumed in solid state physics. Namely, the extrema of the dispersion relation of a generic periodic difference operator on a class of discrete graphs are proven to be non-degenerate. Here, by non-degeneracy we mean extrema having non-degenerate Hessian. Finally, we present a technique of creating and manipulating spectral gaps for a (regular) periodic quantum graph by inserting appropriate internal structures into its vertices.

DEDICATION

To my parents, Doa Do and Phuong Hoang

ACKNOWLEDGEMENTS

I do not even attempt to write down the list of all the people I want to thank as it is clearly an impossible task. Nevertheless, I try, with apologies to many, to make a very condensed acknowledgment to people that I am grateful for so many things they have done for me.

First, I would like to thank my advisor, Dr. Peter Kuchment. Thanks to you not only for being my advisor (the work of which solely was enormous), but also for being there during my ups and downs. I am indebted to you for your discussions, advice, and deep care. You shape me as a mathematician and a whole person.

I would also like to thank the rest of my PhD committee. Dr. Gregory Berkolaiko's assistance began from my early research phase and has continued all those years. Thank you for the insight gained from our discussions and your continued support. Dr. Joseph Ward was very kind to agree to be in my committee. Thank you for the time and effort spent looking into my work. Dr. Artem Abanov was the one I relied on for physics insights. Thank you for always finding time for me in your busy schedule.

I am grateful to many people from Department of Mathematics at Texas A&M University and my alma mater Southern Federal University (former Rostov State University), without whom my journey into the mathematical world would have not been possible. Special thanks to Dr. Frank Sottile, whose helpfulness, patience, and encouragement go beyond any expectation; Dr. Stephen Fulling for his great kindness. Dr. Valeriy Levenshtam, Dr. Vladimir Dybin and my late beloved teachers Dr. Igor Simonenko, Dr. Mikhail Uknovski - you will be in my heart forever. Dr. Peter Howard, our graduate advisor, does an excellent job to take the best care of us graduate students. I am personally indebted to you for being my teaching mentor and for valuable advice about job application. Ms. Monique Stewart, whom I relied on for so many things over the years, a thank to you is not even close to enough.

During my time in graduate school I have had a tremendous support. Thank to you Dr. Mila Mogilevsky for your care and love, which started before my first day in graduate school, and, without any doubt, will not end on my graduation day. Your warmth always makes me feel like being home. Dr. Dima Ryabogin, the precious nexus between me and Rostov, thank you for always being there when I need you. I want to thank to you Dr. Andrew Comech for advice and encouragement. I could not resist the temptation to mention some of my friends' names: Roma Kogan, Lien Tran, Hau Tran, Rishika Rupam, David Carroll, Shahina Rahman, Sourav Dutta, Dilber Kocak, Fatma Terzioglu, Tracy

Weyand - I have never ceased to thank life for bringing you to me. Roma, it is not an overstatement that you are one of the best awards I got for knowing Russian - I truly enjoy every moment spent with you.

Mom and Dad, it is just impossible for me to thank you enough. Your unconditional love and inspiration nurture a little shy girl become who I am today. My family, the joy, love, and happiness you give me, and even only the thought about you enlighten every single day in my life. And finally, my soul mate, Khanh Nguyen, thank you for your love and for sharing your life with me. Myself is never complete without you.

TABLE OF CONTENTS

LIST OF FIGURES

CHAPTER I

INTRODUCTION

Graphene, a monolayer of graphite, is a wonder material (e.g., [22, 32, 46]). There are manifold reasons for its becoming a rising star in the arsenal of materials science and condensed matter physics. The subject of the 2010 Nobel Prize in physics, graphene is famous for its mechanical and electrical properties, for instance super strength and high conductivity.

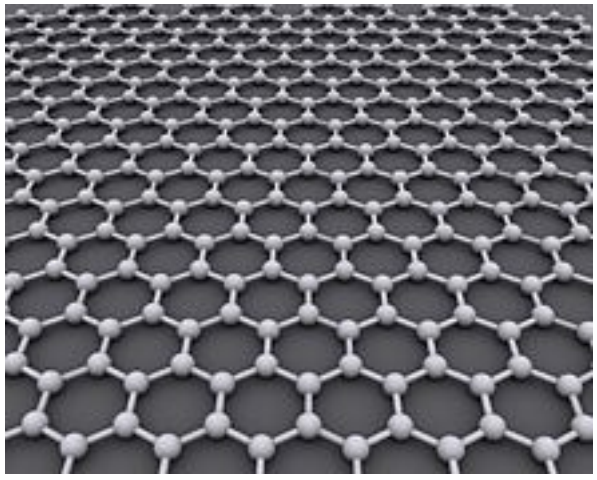

Figure I.1: Graphene is an atomic-scale honeycomb lattice made of carbon atoms [25]

Recently, researchers suggested other 2D carbon allotropes which were given the common name "graphynes." Some graphynes, which have not been synthesized yet, are claimed to be even better than graphene in terms of electrical properties (see, e.g., [4, 45]).

Carbon nanotubes are also carbon allotropes but with a cylindrical nano-structure. Similar to graphene and some of graphynes, they have extraordinary thermal, mechanical, and electrical properties, which are valuable for nano-technology, electronics, optics, and other fields of materials science. Although carbon nanotubes were discovered and studied long before the appearance of graphene (see, e.g., [28, 32]) they can be understood as sheets of graphene rolled onto a cylinder (i.e., with one of the vectors of the lattice of periods quotioned out, see, e.g., [32]). Thus, it is natural to think of graphynes nanotubes as obtained by folding a sheet of graphynes.

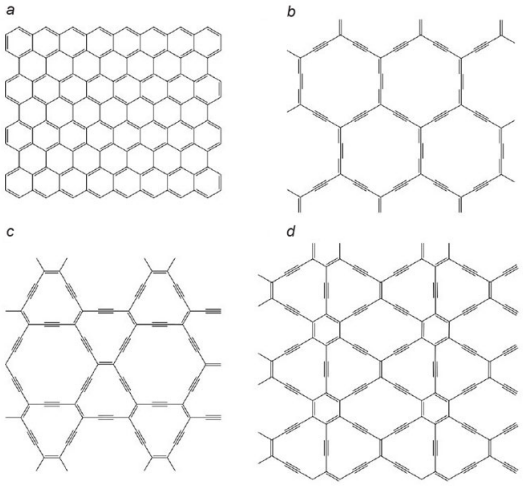

Figure I.2: Some graphyne structures[1] [27]

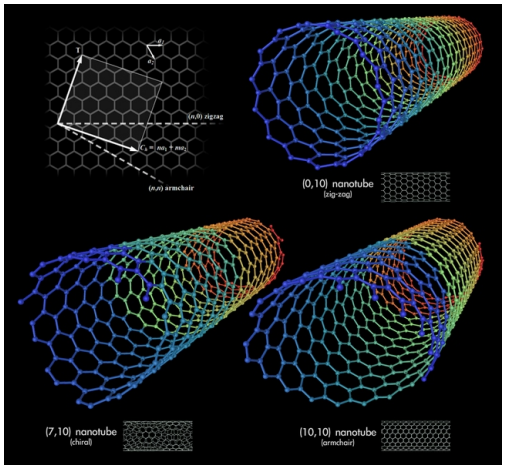

Figure I.3: Different types of carbon nanotubes [26]

The "true" quantum mechanical models of such structures are beyond our analytical and computer abilities for a foreseeable future. Therefore, various approximate models are used. Two of the most popular ones are the density functional theory and the tight binding model. Density functional theory, an approximation of the complete multiple-electron model, although is amenable to computation, is quite complex. In single-electron approximation, tight binding method (i.e. discrete graph model, e.g., [16, 59]) is easy to study, but

[1]Image reprinted with permission from "Could graphynes be better than graphene?" by Belle Dumé, 2012. Physics World (Institute of Physics), Copyright 2012 by Institute of Physics.

often is too simplistic (for example, the Schrödinger operators on graphene structure are bounded and their spectra have only two bands). Another method in the single-electron approximation, the so-called *quantum graph* (or *quantum network*) technique (see, e.g., [2, 49, 54]), falls somewhere in the middle (e.g., unlike tight binding model, it leads to unbounded Hamiltonians and infinitely many spectral bands). Quantum graph models have proven to be simple enough to study and yet preserve all essential ingredients of the dispersion relation. In particular, several studies of spectra of Schrödinger operators on graphene and graphene nanotubes have been conducted (e.g., [36, 35, 44]).

In chapter II and chapter III, using quantum graph models, we describe explicitly dispersion relations and spectra of periodic Schrödinger operators with real and even potentials on a particular graphyne and its related nanotubes respectively. The quantum graph operators on these structures have nonempty point spectra (i.e., bound states). We find these parts of the spectra and provide explicit descriptions of the corresponding eigenspaces [12, 11]. We also study *Dirac cones* of the dispersion relations of the periodic Schrödinger operators on this particular graphyne. In case of graphene, Dirac cones are mainly responsible for its wonderful electrical properties. There are several studies of dispertion relations of 2D Schrödinger operators with honeycomb symmetry, where in particular the mandatory presence of Dirac cones is proven. One should mention [59] where this was done for discrete graph model, [44] - for the quantum graph model, and [19, 20, 6] which studied the continuous model. The presence of Dirac cones is one of the features that makes some of graphynes, which do not have honeycomb symmetry, fascinating in term of electrical properties.

In chapter IV, we study an open conjecture in mathematical physics. It is conjectured that extrema of dispersion relation of a generic periodic Schödinger operator are isolated and having non-degenerate Hessian. (The other belief that each band edge of a generic periodic Schödinger operator is an extremal value of a single band function was answered positively in [34].) This conjecture is assumed, for example, when studying emergence of impurity states under localized perturbations of the periodic medium or defining the effective masses (see, e.g., [3] [37, Section 5.9]). It has been proven [21] for 2D Schrödinger operator that the extrema of the dispersion relation are generically isolated. In this dissertation, we are interested in the non-degeneracy aspect of the extrema of the dispersion relation. We prove the conjecture for periodic difference operators on discrete (combinatorial) graphs.

In the last chapter V, we study creation of gaps in the spectra of some periodic operators arising in mathematical physics. Gap existence plays important role in many areas (e.g., solid state physics [3], photonic crystal manufacturing [30, 43, 42], and in expander graphs construction [52], see also discussion in [37, Section 6.1]). It is also important for customized

designing of quantum wire circuits, which can be modeled by quantum graphs. Many efforts have been made to investigate various mechanisms of creating and manipulating the spectral gaps, for example, to make the medium periodic, to construct expander graphs, or to distribute identical resonators throughout the medium. A spider decoration, i.e. an internal structure being inserted into each vertex of a regular graph, was considered in [47]. It was proven that some special decoration will indeed open the gap in the finite quantum graph case. We extend this result in chapter V.

In the rest of this introduction we provide some preliminaries on quantum graphs and Floquet-Bloch theory, which are necessary for further study.

I.1 Quantum graphs

We consider a graph G that consists of a set of points (vertices) and a set of segments (edges) connecting some of the vertices. By $E(G)$ and $V(G)$ we denote the set of edges and vertices of G respectively. The set of edges containing a vertex u is denoted as $E(u)$. The graph G is called a *metric graph* if we define on each its edge e a coordinate x_e that identifies the edge e with a segment $[0, l_e]$ of the real axis for some $l_e > 0$. We call l_e the length of the edge e. When it does not lead to ambiguity, we will use x instead of x_e to denote the coordinate on the edge e. One can now introduce in a natural way the Hilbert space $L_2(e)$ as the space of all square integrable functions on the edge e and $H_2(e)$ as the Sobolev space of all functions on the edge e with two distributional derivatives in $L_2(e)$. We also define

$$L_2(G) = \bigoplus_{e \in E(G)} L_2(e)$$

as the space of all square integrable functions on G. *A quantum graph* [7, Section 1.4], [40, 41] is a metric graph equipped with a differential operator (which we will call the Hamitonian) and appropriate vertex conditions. Let us introduce one example of such an operator and vertex conditions. On each edge of the graph the Hamiltonian operator acts as follows

$$u(x) \mapsto -\frac{d^2 u(x)}{dx^2}$$

The domain of this operator consists of all functions $u(x)$ on G such that:

1. $u_e \in H_2(e)$, for all $e \in E(G)$,
2. $\sum_{e \in E(G)} \|u_e\|^2_{H_2(e)} < \infty$,
3. at each vertex these functions satisfy the *Neumann vertex condition*, i.e.

$u_{e_1}(v) = u_{e_2}(v)$ for any edges $e_1, e_2 \in E(v)$ and

$\sum_{e \in E(v)} u'_e(v) = 0$ for any vertex v from $V(G)$.

Here u_e is the restriction of function u on G to the edge e and u'_e is the derivative of u_e in the direction away from the vertex v. The defined Hamiltonian is unbounded and self-adjoint (see, e.g., [7, Theorem 1.4.19]).

Here is a more general Schrödinger operator

$$u(x) \mapsto -\frac{d^2u(x)}{dx^2} + V(x)u(x),$$

where $V(x)$ is an electric potential. If one wishes to consider operators that involve first order derivative term, as it is the case, for example, in magnetic Schrödinger operator, then the quantum graph needs to be directed. However, we consider neither such kind of operators nor directed quantum graphs in this dissertation. There are other types of self-adjoint vertex conditions, see, e.g., [7, Subsection 1.4.4].

I.2 Floquet-Bloch theory

Let us define a periodic quantum graph (see [7, Section 4.1]) and introduce some notions that we will need later.

Definition I.2.1. *An infinite combinatorial, metric, or quantum graph is said to be* ***periodic*** *(or* $\mathbb{Z}^n$***-periodic***$)$ *if G is equipped with an action of the free abelian group $\mathbb{Z}^n$, i.e. a mapping $(p, x) \in \mathbb{Z}^n \times G \mapsto px \in G$, such that the following properties are satisfied:*

1. ***Group action:*** *For any $p \in \mathbb{Z}^n$, the mapping $x \mapsto px$ is a bijection of G.*
   $0x = x$ for any $x \in G$, where $0 \in \mathbb{Z}^n$ is the identity element;
   $(p_1p_2)x = p_1(p_2x)$ for any $p_1, p_2 \in \mathbb{Z}^n, x \in G$.

2. ***Continuity:*** *For any $p \in \mathbb{Z}^n$, the mapping $x \mapsto px$ of G into itself is continuous.*

3. ***Faithfulness:*** *If $px = x$ for some $x \in G$, then $p = 0$.*

4. ***Discreteness:*** *For any $x \in G$, there is a neighborhood U of x such that $px \notin U$ for $p \neq 0$.*

5. ***Co-compactness:*** *The space of orbits $G/\mathbb{Z}^n$ is compact. In other words, the whole graph can be obtained by the $\mathbb{Z}^n-$shifts of a compact subset.*

6. ***Structure preservation:***
   • *px, py are connected iff x, y are connected. In particular, $\mathbb{Z}^n$ acts bijectively on the*

set of edges.

- *The action preserves the edges' lengths in the case of a metric or quantum graph.*
- *The action commutes with the Hamiltonian H.*

A simple geometric model of a periodic graph is graph G embedded into $\mathbb{R}^n$ in such a way that G is invariant under shifts by integer vectors $pe := \sum_{1\le i\le n} p_i e_i$, where $p \in \mathbb{Z}^n$ and $e = (e_1, \dots, e_n)$ - a basis of $\mathbb{R}^n$. In this case, the map $(p, x) \mapsto x + pe$ is the action of the group $\mathbb{Z}^n$ in the above definition. For $n = 1, 2$, edges of the graph G may have to cross each other when G is embedded into $\mathbb{R}^n$. When $n \ge 3$, by allowing curved edges, one can avoid such crossings.

Due to the co-compactness condition, there exists a compact part W of G such that

1. The union of all $\mathbb{Z}^n$-shitfs of W covers the whole graph G.
2. Two different $\mathbb{Z}^n$-shitfs of W have only finite number of common points, none of which are vertices.

Such a compact subset W, which is not uniquely defined, is called the *fundamental domain* (or the *Wigner-Seitz cell*) for this action of $\mathbb{Z}^n$ of G.

Floquet-Bloch theory (see, e.g., [7, Section 4.3],[51, Section XIII.16], [39, Chapter 4], [15, 38]) is the main tool to study periodic differential operators. One can think of Floquet-Bloch technique as an analog of Fourier series expansion.

Let V be a periodic function on G, i.e. $V(x + pe) = V(x)$ for $p \in \mathbb{Z}^n$, and G be a periodic metric graph equipped with a self-adjoint Schödinger operator $H = -\Delta + V(x)$ and appropriate boundary conditions. For $p = (p_1, \dots, p_n) \in \mathbb{Z}^n$ and $\theta = (\theta_1, \dots, \theta_n) \in \mathbb{C}^n$, we denote $p_1\theta_1 + \ldots + p_n\theta_n$ by $p\theta$. For $\theta = (\theta_1, \dots, \theta_n) \in \mathbb{C}^n$, the Floquet transform of a compactly supported or sufficiently fast decaying function on $V(G)$ function f is defined as follows

$$f(x) \mapsto Uf(x, \theta) = \sum_{p\in\mathbb{Z}^n} f(x - pe)e^{ip\theta}.$$

The parameter θ is called *quasimomentum* (the term comes from solid-state physics, see, e.g., [3]). By straightforward calculation we have

$$Uf(x + pe, \theta) = e^{ip\theta}Uf(x, \theta), \text{ for all } p \in \mathbb{Z}^n, \tag{I.1}$$

and

$$Uf(x, \theta + \gamma) = Uf(x, \theta), \text{ for all } \gamma \in 2\pi\mathbb{Z}^n. \tag{I.2}$$

The relation (I.1), also known as *Floquet (cyclic) condition*, shows that it is sufficient to know $Uf(x,\theta)$ for x from the fundamental domain W only. On the graph we define

The relation (I.2) means that the function $Uf(x,\theta)$ is periodic with respect to the quasi-momentum θ. Let us call $B = [-\pi,\pi)^n$ the *Brillouin zone*. Then it is enough to know $Uf(x,\theta)$ for those θ from B in order to define $Uf(x,\theta)$ completely.

Combining (I.1) and (I.2), the Floquet transform can be considered as a function of θ in B with values in a space of functions of x on compact domain W. The following theorem [23, 38, 51] is true:

Theorem I.2.2. *The transform $U : L^2(\mathbb{R}^n) \to L^2(B, L^2(W))$ is isometric and its inverse transform is $U^{-1}f(x) = \int_B f(x,\theta)d\theta$, where $f(x,\theta)$ is extended from W to all $x \in \mathbb{R}^n$ according to the Floquet condition.*

It can be understood that $L^2(\mathbb{R}^n)$ is expanded into a "continuous direct sum" over B of identical summands $L^2(W)$. One can easily check that $UH = HU$. Thus, after Floquet transform, the operator H becomes the operator of multiplication in $L^2(B, L^2(W))$. To be specific, for each $\theta = (\theta_1, \theta_2)$ in the Brillouin zone B, let $H(\theta)$ be the *Bloch Hamiltonian* that acts as H does on the domain consisting of functions $u(x)$ that belong to $H^2_{loc}(G)$ and satisfy Neumann vertex condition and the following *cyclic* (or *Floquet*) condition:

$$u(x + p_1e_1 + p_2e_2) = u(x)e^{ip\theta} = u(x)e^{i(p_1\theta_1+p_2\theta_2)}, \tag{I.3}$$

The operator $H(\theta)$, being self adjoint elliptic operator and acting on the compact metric graph W, has discrete spectrum $\{\lambda_1(\theta) \le \ldots \le \lambda_n(\theta) \le \ldots \to \infty\}$ (see, e.g., [7, Theorem 3.1.1]). We then say that the operator H is expanded into the direct integral of operators $H(\theta)$ (see, e.g., [51, 38], [7, Section 4.2]).

$$H = \int_B^{\oplus} H(\theta)d\theta.$$

As a consequence,

$$\sigma(H) = \bigcup_{\theta\in B} \sigma(H(\theta)). \tag{I.4}$$

We define the *dispersion relation* of H as the multiple-valued function that maps each quasimomentum θ to the (discrete) spectrum of $H(\theta)$. The graph of the dispersion relation is called the *dispersion surface* or the *Bloch variety*. Function $\theta \mapsto \lambda_j(\theta), j = 1, 2, \ldots,$ is called the j-th *band function* or *dispersion relation branch*. It is known (see, e.g., [31]) that band functions are continuous and piecewise analytic. The range $[a_j, b_j]$ of the j-th band function is called the j-th *spectral band*. Numbers a_j, b_j are called spectral edges and they

correspond to the extrema of the dispersion relation of H.

Similarly, in case of periodic difference operator, after the Floquet transform, the operator becomes multiplication by a matrix-valued function in $L^2(B, \mathbb{C}^{|W|})$.

From the identity (I.4), we have that a value λ belongs to the spectrum of H iff λ is in the spectrum of $H(\theta)$ for some $\theta \in B$. Thus, we switch from the spectral problem for H on the periodic graph to a set of spectral problems for $H(\theta)$ on the fundamental domain.

CHAPTER II

SPECTRAL ANALYSIS OF A GRAPHYNE STRUCTURE[1]

In this chapter, we take the quantum graph approach similar to [44] to study spectra of periodic Schrödinger operators on the simplest graphyne (see Fig. II.1) among 14 various structures suggested in [16]. It represents the 2D projection of the so called lithographite [10]. From now on, we reserve the word "graphyne" for this particular structure. We derive the dispersion relations for periodic Schrödinger operators with real and even potentials on this graphyne. From here, we extract various information about the spectral structures of the operators. Unlike similar periodic operators in $\mathbb{R}^n$, the quantum graph operators can (and often do) have point spectra (i.e., bound states). We find these parts of the spectra and provide an explicit description of the corresponding eigenspaces[2]. The presence of spectral gaps and Dirac cones is also studied. The formulations of the results involve the discriminant of the Hill operator with the potential obtained by the periodic extension of the 1D potential on a single edge.

In Section II.1 we describe the geometry of the particular graphyne structure and the operators of interest. In Section II.2 we derive the dispersion relations and the band-gap structures of the operators on the graphyne with the main results stated in Theorems II.2.5 and II.2.7. The proof of an auxiliary Proposition II.2.8 is given in Section II.3.

II.1 Quantum graph model of graphyne structure and related Schrödinger operators

In what follows, we describe quantum graph model of the graphyne structure shown in Fig. II.1. At each vertex there is a carbon atom that is bonded to three or four neighboring atoms. The chemical bonds between the atoms are represented by the edges connecting the corresponding vertices. This graphyne structure is periodic (see Section I.2). There is a free action of the group $\mathbb{Z}^2$ of integer vectors in $\mathbb{R}^2$ on G by the shifts by vectors $p_1e_1+p_2e_2$, where $(p_1, p_2) \in \mathbb{Z}^2$ and $e_1 = (\sqrt{3}, 0), e_2 = (0, 2)$. We choose the shaded domain W shown in Fig. II.1 as the fundamental domain of this action. It contains three vertices a, b, c and

[1]Part of this chapter is reprinted with permission from "Quantum graph spectra of a graphyne structure" by Ngoc Do and Peter Kuchment, 2013. *Nanoscale Systems: Mathematical Modeling, Theory and Applications*, Volume 2, Page 107-123, Copyright [2013] by Ngoc Do and Peter Kuchment.

[2]The presence of bound states is an artefact of the quasi-1D model. It, however, often indicates possible presence of very flat bands and thus resonances in the "grown up" system.

five edges f, g, h, k, l as shown in the figure. We choose the directions[3] of these edges as shown. The entire structure G can be obtained from W by $\mathbb{Z}^2$-shifts, which also define directions on all edges of the graph G. All the edges of G have length 1. We define on each directed edge e the arc length coordinate x_e that identifies it with the segment $[0, 1]$.

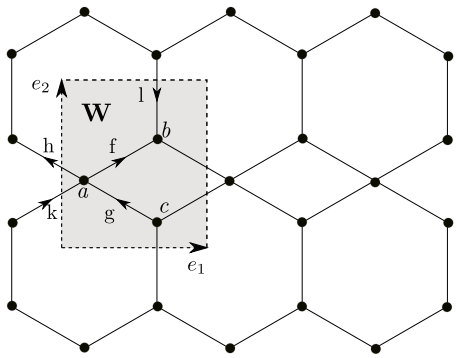

Figure II.1: The structure G and a fundamental domain W with vertices a, b, c and edges f, g, h, k, l

We now define Schrödinger operator and corresponding vertex boundary conditions. Let $q_0(x)$ be an even[4] and real L_2-function on $[0, 1]$, i.e. $q_0(x) = q_0(1 - x)$ for a.e. $x \in [0, 1]$. Using the described before identification of the directed edges with the segment $[0, 1]$, we can transfer the potential $q_0(x)$ to each edge, thus defining a potential $q(x)$ on the whole G.

It is not hard to show that the evenness assumption on q_0 implies the following property:

Lemma II.1.1. *The potential q defined as above is invariant with respect to the symmetry group of the graph G.*

Proof. We denote the shifts by the integer vectors $p_1e_1 + p_2e_2$, where $(p_1, p_2) \in \mathbb{Z}^2$, and the reflections with respect to the lines l_1 and l_2 shown in Figure II.2 by $T_{(p_1,p_2)}$ and R_1, R_2 accordingly. Let us first prove that the symmetry group of the graph G is generated by $T_{p1,p2}, R_1, R_2$ then show that the potential q is invariant under each of these transforms, which implies the lemma.

[3]The choice of the directions can be arbitrary and does not influence the results.

[4]The evenness assumption is made not only for technical convenience. Without this condition, the graph must be oriented in order to define the operator. This assumption is also needed to preserve the symmetry that we use.

Indeed, let F be an isometry from the symmetry group of the graph G. Let A_1, A_2 be the shaded hexagon and rhombus shown in the Fig. II.2 respectively. Let us denote $A_0 = A_1 \cup A_2$.

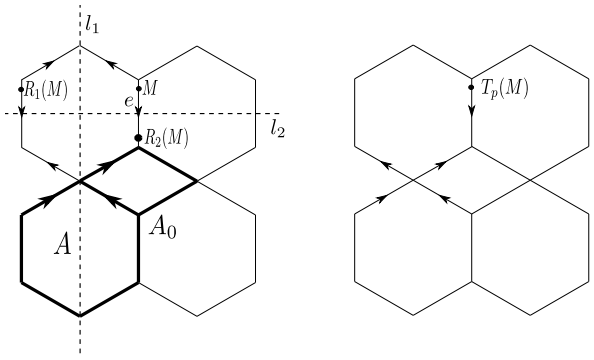

Figure II.2: A_1, A_2 are shaded hexagon and rhombus accordingly. M and its images through shifts and reflections

Since F preserves distance, $F(A_1)$ is a hexagon. Let $p_0 = (p_1^0, p_2^0) \in \mathbb{Z}^2$ such that $R(A_1) := T_{p_0}(F(A_1))$ coincides with A_1 as hexagons. Since R preserves distance, $R(A_0)$ is one of the forms shown in Figure II.3.

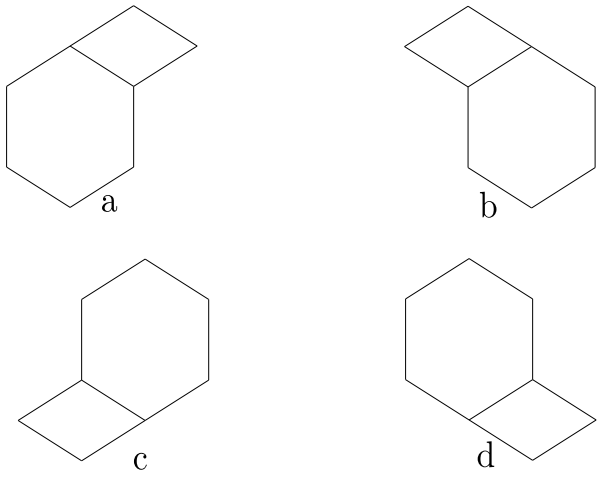

Figure II.3: Possible images of A_0 after an isometry from the symmetry group of G

As $R = T_{p_0} \cdot F$, we have $F = T_{-p_0} \cdot R$.

If $R(A_0)$ is of the form a shown in Fig. II.3 then $R = Id$, thus $F = T_{p_0}$.

If $R(A_0)$ is of the form b shown in Fig. II.3 then $R = R_1$, thus $F = T_{p_0} \cdot R_1$.

If $R(A_0)$ is of the form c shown in Fig. II.3 then $R = R_1 \cdot R_2$, so $F = T_{p_0} \cdot R_1 \cdot R_2$.

If $R(A_0)$ is of the form d shown in Fig. II.3 then $R = R_2$, so $F = T_{p_0} \cdot R_2$.

So one can always represent the isometry F as a combination of a shift T_p and reflections R_1, R_2 for some $p \in \mathbb{Z}^2$.

Now we just need to check that the potential q is invariant with respect to each of the transforms T_p and R_1, R_2.

Let $M \in e, e \in E(G)$, be some point on the graph G. Since the directions on all edges of the graph G are defined periodically from the directions of edges inside the fundamental domain, $x_e(M) = x_{T_p(e)}(T_p(M))$. Thus,

$$q(M) = q_0(x_e(M)) = q_0(x_{T_p(e)}(T_p(M))) = q(T_p(M)),$$

i.e. the potential q is invariant with respect to the shifts T_p.

A similar argument proves the invariance of the potential q with respect to the reflection R_1.

For the reflection R_2, due to the direction of edges, we have $x_{R_2(e)}(R_2(M)) = 1 - x_e(M)$. Since q_0 is even, $q(x_{R_2(e)}(R_2(M))) = q_0(x_{R_2(e)}(R_2(M))) = q_0(1 - x_e(M)) = q_0(x_e(M)) = q(M)$. Thus, the potential q is also invariant with respect to the reflection R_2. □

We are now ready to construct the Schrödinger operator H in $L_2(G)$, whose spectral properties will be studied in this chapter. The operator H acts on each edge as follows:

$$Hu(x) = -\frac{d^2u(x)}{dx^2} + q(x)u(x). \tag{II.1}$$

Its domain $D(H)$ consists of all functions $u(x)$ on G such that:

1. $u_e \in H_2(e)$, for all $e \in E(G)$,
2. $\sum_{e \in E(G)} \|u_e\|^2_{H_2(e)} < \infty$,
3. at each vertex these functions satisfy Neumann vertex conditions, i.e. $u_e(v) = u_{e'}(v)$, $\forall e, e' \in E(v)$ and $\sum_{e \in E(v)} u'_e(v) = 0$.

The defined operator is known to be unbounded and self-adjoint (e.g. [7, Theorem 1.4.19]). It is also invariant with respect to all symmetries of the graph G.

II.2 Spectral analysis of the graphyne operator

In this section we study the spectrum of the operator H. Let us describe first the main steps of our approach. Using the Floquet-Bloch technique I.2, we reduce our consideration to a family of spectral problems on the fundamental domain W. Then, using the standard Hill's operator theory [15, 51], we switch to a discrete problem (e.g., [48], [7, Section 3.6]). Finally, the discrete problem can be analyzed rather explicitly.

Let us get to some detail now. For each $\theta = (\theta_1, \theta_2)$ in the Brillouin zone $B = [-\pi, \pi)^2$, let $H(\theta)$ be the Bloch Hamiltonian that acts as (II.1) on the domain consisting of functions $u(x)$ that belong to $H^2_{loc}(G)$ and satisfy Neumann vertex condition and the following cyclic (or Floquet) condition:

$$u(x + p_1 e_1 + p_2 e_2) = u(x)e^{ip\theta} = u(x)e^{i(p_1\theta_1 + p_2\theta_2)}, \tag{II.2}$$

for all $(p_1, p_2) \in \mathbb{Z}^2$ and all $x \in G$.

From the Floquet-Bloch theory, we have

$$\sigma(H) = \bigcup_{\theta \in B} \sigma(H(\theta)).$$

It is well-known (e.g., [40], [7, Theorem 3.1.1]) that the operators $H(\theta)$, $\theta \in B$, has purely discrete spectrum $\sigma(H(\theta)) = \{\lambda_1(\theta) \leq \ldots \leq \lambda_n(\theta) \leq \ldots \to \infty\}$. The spectrum of H is the range of the dispersion relation for θ changing in the Brillouin zone B. Thus, we now concentrate on studying the spectra of $H(\theta)$ for $\theta \in B$, i.e. on solving the eigenvalue problem:

$$H(\theta)u = \lambda u, \lambda \in \mathbb{R}, \tag{II.3}$$

for $u \in H_2(W)$ satisfying the cyclic condition at the boundary and Neumann vertex conditions inside W.

Combining the vertex and cyclic conditions we have:

$$\begin{cases} u_f(0) = u_g(1) = u_h(0) = u_k(1) =: A \\ u'_f(0) - u'_g(1) + u'_h(0) - u'_k(1) = 0 \\ u_f(1) = u_l(1) = u_h(1)e^{i\theta_1} =: B \\ u'_f(1) + u'_l(1) + u'_h(1)e^{i\theta_1} = 0 \\ u_g(0) = u_k(0)e^{i\theta_1} = u_l(0)e^{-i\theta_2} =: C \\ u'_g(0) + u'_k(0)e^{i\theta_1} + u'_l(0)e^{-i\theta_2} = 0. \end{cases}$$

We will need another auxiliary operator. Let us denote by H^D the *Dirichlet Hamiltonian* on $[0,1]$ that acts as (II.1) with Dirichlet boundary conditions $u(0) = u(1) = 0$. We also denote by Σ^D the (discrete) spectrum of H^D For each $\lambda \notin \Sigma^D$, there exist two linearly independent solutions φ_0, φ_1 such that $\varphi_0(0) = \varphi_1(1) = 1, \varphi_0(1) = \varphi_1(0) = 0$. We omit the letter λ in the notations $\varphi_{0,\lambda}, \varphi_{1,\lambda}$ unless we want to emphasize their dependence on λ. We use notations φ_0, φ_1 for analogous functions on each edge of W under fixed λ and fixed identification of these edges with the segment $[0,1]$, which should not lead to confusion. Then for $\lambda \notin \Sigma^D$ solution of (II.3) can be represented as follows:

$$\begin{cases} u_f = A\varphi_0 + B\varphi_1 \\ u_g = C\varphi_0 + A\varphi_1 \\ u_k = Ce^{-i\theta_1}\varphi_0 + A\varphi_1 \\ u_h = A\varphi_0 + Be^{-i\theta_1}\varphi_1 \\ u_l = Ce^{i\theta_2}\varphi_0 + B\varphi_1. \end{cases}$$

Continuity and eigenvalue equation on each edge are already satisfied. What we need to check is the zero flux condition at each of the three vertices in W:

$$\begin{cases} A(2\varphi'_0(0) - 2\varphi'_1(1)) + (B\varphi'_1(0) - C\varphi'_0(1))(1 + e^{-i\theta_1}) = 0 \\ A\varphi'_0(1)(1 + e^{i\theta_1}) + 3B\varphi'_1(1) + Ce^{i\theta_2}\varphi'_0(1) = 0 \\ A\varphi'_1(0)(1 + e^{i\theta_1}) + Be^{-i\theta_2}\varphi'_1(0) + 3C\varphi'_0(0) = 0. \end{cases} \tag{II.4}$$

Due to the evenness of the function q_0, we have $\varphi'_1(1) = -\varphi'_0(0)$ and $\varphi'_1(0) = -\varphi'_0(1)$ Thus, (II.4) becomes

$$\begin{cases} -4A\varphi'_1(1) + B\varphi'_1(0)(1 + e^{-i\theta_1}) + C\varphi'_1(0)(1 + e^{-i\theta_1}) = 0 \\ A\varphi'_1(0)(1 + e^{i\theta_1}) - 3B\varphi'_1(1) + Ce^{i\theta_2}\varphi'_1(0) = 0 \\ A\varphi'_1(0)(1 + e^{i\theta_1}) + Be^{-i\theta_2}\varphi'_1(0) - 3C\varphi'_1(1) = 0. \end{cases} \tag{II.5}$$

Since $\varphi_1'(0) \neq 0$, we can define

$$\eta(\lambda) := \frac{\varphi_{1,\lambda}'(1)}{\varphi_{1,\lambda}'(0)}, \tag{II.6}$$

then (II.5) is reduced to

$$\begin{cases} -4\eta(\lambda)A + (1+e^{-i\theta_1})B + (1+e^{-i\theta_1})C = 0 \\ (1+e^{i\theta_1})A - 3\eta(\lambda)B + e^{i\theta_2}C = 0 \\ (1+e^{i\theta_1})A + e^{-i\theta_2}B - 3\eta(\lambda)C = 0. \end{cases}$$

The determinant of this system is

$$-4[9\eta^3(\lambda) - \eta(\lambda) - (\cos\theta_1 + 1)(3\eta(\lambda) + \cos\theta_2)].$$

These calculations prove the following:

Lemma II.2.1. *A point $\lambda \notin \Sigma^D$ is in the spectrum of the Schrödinger operator H if and only if there exists $\theta = (\theta_1, \theta_2) \in B$ such that $x = \eta(\lambda)$ is a root of the equation*

$$9x^3 - x - (\cos\theta_1 + 1)(3x + \cos\theta_2) = 0. \tag{II.7}$$

Let us now extend q_0 periodically from $[0,1]$ to q_{per} on $\mathbb{R}$ and consider the *Hill operator* H^{per} on $\mathbb{R}$ as below:

$$H^{per}u(x) = -\frac{d^2u(x)}{dx^2} + q_{per}(x)u(x).$$

The monodromy matrix[5] $M(\lambda)$ of H^{per} is defined by the following formula

$$\begin{bmatrix} \varphi(1) \\ \varphi'(1) \end{bmatrix} = M(\lambda) \begin{bmatrix} \varphi(0) \\ \varphi'(0) \end{bmatrix},$$

where φ satisfies the differential equation

$$-\frac{d^2\varphi(x)}{dx^2} + q_0(x)\varphi(x) = \lambda\varphi(x) \text{ on } \mathbb{R}. \tag{II.8}$$

Discriminant (or *Lyapunov function*) $trM(\lambda)$ of the Hill operator H^{per} is denoted by $D(\lambda)$. The next proposition ([44, Proposition 3.4]) collects some well-known results about the spectra of Hill operators [15]:

Lemma II.2.2.

[5] I.e. Monodromy matrix is the matrix that transforms the Cauchy data $(u(0)\ \ u'(0))^\tau$ of the solution of $H_{per}u = \lambda u$ at zero to the data $(u(1)\ \ u'(1))^\tau$ at the end of the period.

1. *The spectrum $\sigma(H^{per})$ of H^{per} is purely absolutely continuous.*

2. *$\sigma(H^{per}) = \{\lambda \in \mathbb{R} \big| |D(\lambda)| \leq 2\}$.*

3. *$\sigma(H^{per})$ consists of the union of closed non-overlapping (although, possibly touching) and non-zero length finite intervals (bands) $B_{2k} := [a_{2k}, b_{2k}], B_{2k+1} := [b_{2k+1}, a_{2k+1}]$ such that*

$$a_0 < b_0 \leq b_1 < a_1 \leq a_2 < b_2 \leq \dots$$

and $\lim\limits_{k\to\infty} a_k = \infty$.
The (possibly empty) segments (b_{2k}, b_{2k+1}) and (a_{2k}, a_{2k+1}) are called the spectral gaps.
Here, $\{a_k\}$ and $\{b_k\}$ are the spectra of the operators with periodic and anti-periodic conditions on $[0, 1]$ correspondingly.

4. *Let $\lambda_k^D \in \Sigma^D$ be the k^{th} Dirichlet eigenvalue labeled in increasing order. Then, λ_k^D belongs to (the closure of) the k^{th} gap. When q_0 is even, λ_k^D coincides with an edge of the k-th gap.*

5. *If λ is in the interior of the k^{th} band B_k, then $D'(\lambda) \neq 0$, and $D(\lambda)$ is a homeomorphism of the band B_k onto $[-2, 2]$. Moreover, $D(\lambda)$ is decreasing on $(-\infty, b_0)$ and (a_{2k}, b_{2k}) and is increasing on (b_{2k+1}, a_{2k+1}). It has a simple extremum in each spectral gap $[a_k, a_{k+1}]$ and $[b_k, b_{k+1}]$.*

6. *The dispersion relation for H^{per} is given by*

$$D(\lambda) = 2\cos\theta,$$

where θ is the one-dimensional quasimomentum.

Claim (4) of the lemma about the even potential case can be explained as follows: let $u(x)$ be the eigenfunction of the Hill operator H^{per} corresponding to the k^{th} Dirichlet eigenvalue λ_k^D, i.e.

$$H^{per}u(x) = \lambda_k^D u(x), u(0) = u(1) = 0.$$

Then $u(1-x)$ is also an eigenfunction corresponding to that eigenvalue. Either $u(x) + u(1-x)$ or $u(x) - u(1-x)$ is nonzero and therefore will be an eigenfunction corresponding to λ_k^D. Since $u(x) + u(1-x)$ is periodic and $u(x) - u(1-x)$ is anti-periodic, λ_k^D must coincide with an edge of the k^{th} gap.

The following relation between function $\eta(\lambda)$ (see (II.6)) and the discriminant $D(\lambda)$ of H^{per}

is well-known [15, 44] and easy to establish:

$$\eta(\lambda) = \frac{1}{2} D(\lambda). \tag{II.9}$$

Therefore, according to the statement (2) of Lemma II.2.2 and equality (II.9), one just needs to analyze the roots of the cubic equation (II.7).

So far we have just dealt with λ not in the Dirichlet spectrum Σ^D of H^D. Now let us consider the exceptional values $\lambda \in \Sigma^D$.

We introduce the following notion first:
Definition II.2.3. *An eigenfunction is said to be a* simple loop state *if it is supported on a single hexagon or rhombus of the structure G and vanishes at all vertices (see Fig. II.4).*

We can now describe what happens for $\lambda \in \Sigma^D$.
Lemma II.2.4. *Each $\lambda \in \Sigma^D$ is an eigenvalue of infinite multiplicity of the operator H. The corresponding eigenspace is generated by*[6] *the simple loop states.*

Proof. For each $\lambda \in \Sigma^D$, let ψ_λ be the corresponding eigenfunction of operator H^D. Since q_0 is even, one can assume the function ψ_λ to be either even or odd. For an odd eigenfunction ψ_λ, we repeat it on each edge of a hexagon/rhombus; for an even eigenfunction ψ_λ - repeat around a hexagon/rhombus with an alternating sign. In both cases we get an eigenfunction of H that lives only on one particular loop. Thus, $\lambda \in \sigma_{pp}(H)$.

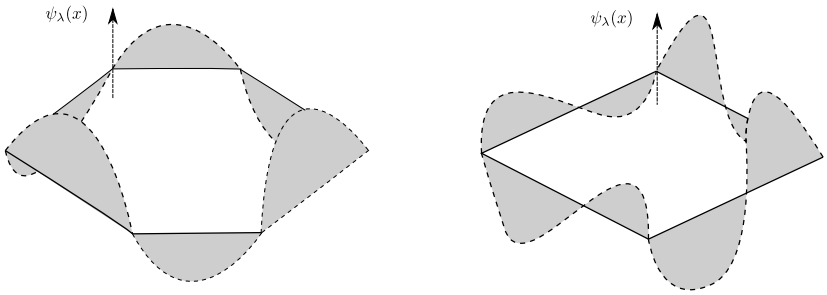

Figure II.4: Simple loop states constructed from even function on $[0, 1]$ for hexagon and odd function on $[0, 1]$ for rhombus

Let us prove infinite multiplicity of the eigenvalues $\lambda \in \Sigma^D$, which is a well-known feature of periodic problems. Let $M_\lambda \subset L_2(G)$ be the corresponding eigenspace and γ be some period

[6] I.e., is the closed linear hall of ...

vector of G. The shift operator S_γ by γ acts in M_λ as an unitary operator. Suppose that M_λ is finite dimensional, then S_γ has an eigenfunction $f \in M_\lambda \subset L_2(G)$ corresponding to an eigenvalue μ such that $|\mu| = 1$. On the other hand, f is multiplied by μ when shifted by the vector γ. Since $|\mu| = 1$, f clearly cannot belong to $L_2(G)$, which leads to contradiction. Thus, $\lambda \in \Sigma^D$ are eigenvalues of infinite multiplicity.

In order to prove that the eigenspace is generated by simple loop states with hexagonal and rhomboidal supports, it is enough to prove that these simple loop states generate all compactly supported eigenfunctions in the eigenspace M_λ. Indeed, as it is shown in [41] (see also [7, Theorem 4.5.2]), linear combinations of compactly supported eigenfunctions are dense in the space M_λ.

First, we notice that each compactly supported eigenfunction φ of H vanishes at all vertices. Indeed, due to connectedness of G, there must be a "boundary" vertex v of the support that is connected by an edge with a vertex w outside the support. We claim that $\varphi(v) = 0$. Otherwise, we have an edge such that the function vanishes at one end, w (corresponding to $x = 0$), and does not vanish at the other end. We introduce a basis of solutions of (II.3), functions c_λ and s_λ, such that $c_\lambda(0) = 1, s_\lambda(0) = s_\lambda(1) = 0$ (such non-trivial function s_λ exists for $\lambda \in \Sigma^D$). The eigenfunction φ can be represented as $\varphi(x) = Ac_\lambda(x) + Bs_\lambda(x)$. In particular, $0 = \varphi(0) = A$, and so $0 \neq \varphi(1) = Bs_\lambda(1) = 0$, which leads to contradiction. Repeating this argument, we conclude that the eigenfunction φ vanishes at all vertices. Besides, the support of φ cannot have a vertex of degree 1. (Otherwise, due to Neumann boundary condition, both function and its derivative will vanish at that vertex, which makes function to be equal to zero.)

Now one needs to prove that φ can be represented as a combination of simple loop states. Consider the external boundary of the support of φ, which is a closed circuit C of edges, containing the whole support inside. The interior of this curve is a union of N elementary hexagons and/or rhombuses of the graph G. We begin with a boundary edge $e_0 \in C$. One of the N internal hexagonal or rhomboidal loops must contain e_0. Let φ_0 be the simple loop state that coincides with φ on the edge e_0 and is extended to that loop as described before. Function $\varphi - \varphi_0$ will be the new eigenfunction with a smaller support (number of loops $N - 1$). Continuing this process (see Fig.II.5), we will eventually represent the eigenfunction φ as a combination of simple loop states.

In the next theorem, which is our main result of this section, we describe the dispersion relation and the structure of the spectrum of the operator H.

Let $F(\theta)$ be the triple-valued function providing for each θ the three roots of the equation (II.7). By Proposition II.2.8, which we will formulate and prove later, function F is real-

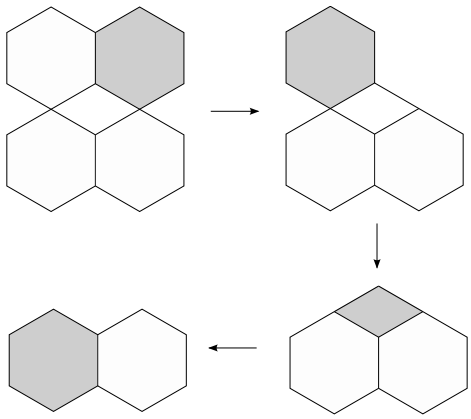

Figure II.5: An example of deleting simple loop states (the dark ones) from the support of an eigenfunction

valued in the Brillouin zone. Assume $F(\theta) = (F_1(\theta), F_2(\theta), F_3(\theta))$, where $F_1(\theta) \le F_2(\theta) \le F_3(\theta)$ for all $\theta \in B$. Then we have

Theorem II.2.5.

1. *The singular continuous spectrum $\sigma_{sc}(H)$ is empty.*

2. *The dispersion relation of operator H consists of the following two parts:*
   i) pairs (θ, λ) such that $0.5D(\lambda) \in F(\theta)$ (or, $\lambda \in D^{-1}(2F(\theta))$), where θ changing in the Brillouin zone;
   and
   ii) the collection of flat (i.e., θ-independent) branches $\lambda \in \Sigma^D$.

3. *The absolutely continuous spectrum $\sigma_{ac}(H)$ has band-gap structure and is the same (as the set) as the spectrum $\sigma(H^{per})$ of the Hill operator H^{per} with potential obtained by extending periodically q_0 from $[0, 1]$. In particular,*

$$\sigma_{ac}(H) = \{\lambda \in \mathbb{R} \big| \, |D(\lambda)| \le 2\},$$

   where $D(\lambda)$ is the discriminant of H^{per}.

4. *The bands of $\sigma(H)$ do not overlap (but can touch). Each band of $\sigma(H^{per})$ consists of three touching bands of $\sigma(H)$.*

5. *The pure point spectrum $\sigma_{pp}(H)$ coincides with Σ^D and belongs to the union of the edges of spectral gaps of $\sigma(H^{per}) = \sigma_{ac}(H)$.*
   Eigenvalues $\lambda \in \Sigma^D$ of the pure point spectrum are of infinite multiplicity and the

corresponding eigenspaces are generated by simple loop (hexagon or rhombus) states.

6. *Spectrum $\sigma(H)$ has gaps if and only if $\sigma(H^{per})$ has gaps.*

The statements of the theorem are illustrated in Fig. II.6.

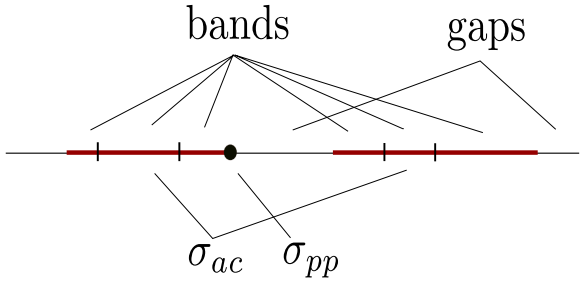

Figure II.6: The bold segments are the bands of $\sigma(H^{per})$. Each of them is split into three touching bands of $\sigma(H)$. One eigenvalue at the end of a band is also shown.

Proof. The first claim about emptiness of the singular continuous spectrum of the Schrödinger operator H is well-known[7].

Let first $\lambda \notin \Sigma^D$. Then, according to Lemma II.2.1, (θ, λ) is in the dispersion surface of H iff $\eta(\lambda)$ is a root of (II.7) for this θ. In other words, due to (II.9), $0.5D(\lambda)$ must be one of the three values of $F(\theta)$. Hence, this is equivalent to $D(\lambda) \in 2F(\theta)$, or $\lambda \in D^{-1}(2F(\theta))$.

If $\lambda \in \Sigma^D$, then according to Lemma II.2.4, (θ, λ) is in the dispersion surface for any θ from the Brillouin zone.

This proves the second statement of the theorem.

According to the Lemmas II.2.2 and II.2.4 we have

$$\Sigma^D \subset \sigma(H), \Sigma^D \subset \sigma(H^{per}), \tag{II.10}$$

and

$$\sigma(H^{per}) = \{\lambda \in \mathbb{R} \big| \, |D(\lambda)| \leq 2\}.$$

[7]It goes back to the famous L. Thomas' absolute continuity theorem [57]. See, e.g., [51, Section XIII.6], [7, Theorem 4.4.1], or [37, Section 6.3] and references therein.

For $\lambda \notin \Sigma^D$, λ is in the spectrum of H iff $\eta(\lambda)$ is a root of equation (II.7) for some θ. Proposition II.2.8 below shows, in particular, that all roots of equation (II.7) belong to $[-1,1]$ and cover this interval. Thus, λ is in the spectrum of H iff $|\eta(\lambda)| \leq 1$. Since $D(\lambda) = 2\eta(\lambda)$, this means that $\sigma(H)\backslash\Sigma^D = \sigma(H^{per})\backslash\Sigma^D$ and, by closure, $\sigma(H) = \sigma(H^{per})$.

The same Proposition II.2.8 shows that the graph of the triple-valued function $F(\theta)$ does not have any flat branches outside the set of values Σ^D. Thus, the spectrum of H is absolutely continuous outside Σ^D. This argument, together with Lemma II.2.4, finishes the proof of the statements (3) and (5) of the theorem.

From statement (2), the dispersion relation of H consists of the variety $\lambda = D^{-1}(2F_j(\theta)), j \in \overline{1,3}$, and collection of flat branches $\lambda \in \Sigma^D$ located at some edges of spectral bands.

According to Lemma II.2.2, function $D(\lambda)$ is a monotonic homeomorphism from each spectral band of the Hill operator onto $[-2,2]$. Besides, the ranges of functions $2F_1, 2F_2$, and $2F_3$ are all in $[-2,2]$. Thus, part of the spectrum $\sigma(H^{per})$ that corresponds to each band of the Hill operator H^{per} coincides as a set with the part of the absolutely continuous spectrum $\sigma_{ac}(H)$ that consists of three bands. In another words, the operator H has "three times more" non-flat bands than the Hill operator H^{per} does.

The function D^{-1} is multiple-valued, thus producing infinitely many bands for any $2F_j, j = \overline{1,3}$. Two such spectral bands (pre-images of the same $2F_j(B)$) clearly cannot overlap because function $D(\lambda)$ is monotonic on each band. Two spectral bands which are pre-images of $2F_j(B)$ and $2F_i(B)$ for different $i, j \in \overline{1,3}$, also cannot overlap because the ranges of functions $F_j, j = \overline{1,3}$, belong to $[-1,1]$ and do not overlap by Proposition II.2.8 below. One should notice that although spectral bands do not overlap, they still can touch each other as we will see shortly. This can happen at points (θ, λ) such that $D(\lambda) = \pm 2$ or $\pm 2/3$. This proves the statement (4) of the theorem.

Since the spectra of H and H^{per} coincide as sets, we get the last statement of the theorem. □

Corollary II.2.6.

1. *Unless the potential q_0 is constant, the spectrum $\sigma(H)$ has at least one gap.*
2. *For a* generic *smooth potential q_0, all possible gaps in $\sigma(H)$ are open.*

Proof. The first claim of the Corollary follows from the last statement of Theorem II.2.5 and Borg's theorem [9]. Similarly, the second claim follows from Simon's genericity result [56] instead of Borg's theorem. □

Graphene has captured physicists' interest because of its unusual electronic properties. These properties are caused by the occurrence of so-called *conical singularities* or *Dirac points*. Roughly speaking, Dirac point is point where two spectral bands touch and locally form a cone (also known as Dirac cone). We are interested in conical singularities that are stable under small perturbation of the potential not breaking the symmetry.

In the next theorem, we will take a closer look at the spectral bands of the operator H. Moreover, we will specify all the conical singularities in the Brillouin zone B and describe how the spectral bands behave near these points.

In what follows, we will use the notation

$$\theta_0 := \arccos(-1/3).$$

Theorem II.2.7.

1. *In the free case, i.e., when the potential q_0 is equal to zero, the Bloch variety of H has conical singularities at the following points:*

   i) $(\theta, \lambda) = (0, 0, (2(k+1)\pi)^2)$, *at which* $D(\lambda) = 2$,

   ii) $(\theta, \lambda) = (0, \pm\pi, ((2k+1)\pi)^2)$, *at which* $D(\lambda) = -2$,

   iii) $(\theta, \lambda) = (\pm\theta_0, 0, (\theta_0 + 2k\pi)^2)$, *at which* $D(\lambda) = -2/3$,

   iv) $(\theta, \lambda) = (\pm\theta_0, \pm\pi, (2\pi - \theta_0 + 2k\pi)^2)$, *at which* $D(\lambda) = 2/3$, *for* $k = 0, 1, 2, \ldots$

2. *When we turn on a small potential $q_0 \neq 0$, the conical singularities corresponding to $|D(\lambda)| = 2$ will generically split into two smooth branches, thus, open a gap. The conical singularities that occur when $|D(\lambda)| = 2/3$ are stable under small perturbation by a potential q of the type considered.*

Before proving this theorem, we need to explore some properties of function $F(\theta)$.

Proposition II.2.8.

1. *Function $F(\theta)$ is real-valued for θ in the Brillouin zone B.*

2. *Let $F(\theta) = (F_1(\theta), F_2(\theta), F_3(\theta))$, where $F_1(\theta) \leq F_2(\theta) \leq F_3(\theta)$ for all $\theta \in B$. Then, the ranges of functions F_1, F_2, F_3 are $[-1, -1/3], [-1/3, 1/3]$, and $[1/3, 1]$ correspondingly.*

3. *Function F_1 attains its maximal value at $(\theta_1, 0)$ for $\theta_1 \in [-\pi, -\theta_0] \cup [\theta_0, \pi]$ or $(\pm\pi, \theta_2)$ for $\theta_2 \in [-\pi, \pi]$ and minimal value at $\theta = (0, \pm\pi)$.*

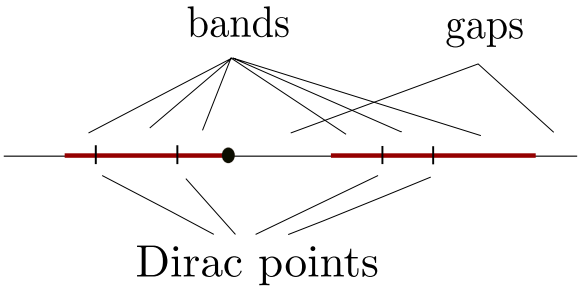

Figure II.7: The stable Dirac points are located at the points where three bands of $\sigma(H)$ touch to form a band of $\sigma(H^{per})$.

Function F_2 attains its maximal value at $(\theta_1, \pm\pi)$ for $\theta_1 \in [-\theta_0, \theta_0]$ and minimal value at $\theta = (\theta_1, 0)$ for $\theta_1 \in [-\theta_0, \theta_0]$.

Function F_3 attains its maximal value at $(0, 0)$ and minimal value at $(\theta_1, \pm\pi)$ for $\theta_1 \in [-\pi, -\theta_0] \cup [\theta_0, \pi]$ or $(\pm\pi, \theta_2)$ for $\theta_2 \in [-\pi, \pi]$.

4. *The linear level sets of function $F(\theta)$ inside B are*

$\{(\pm\pi, \theta_2), \theta_2 \in [-\pi, \pi]\}$,

$\{(\theta_1, \pm\pi), \theta_1 \in [-\pi, \pi]\}$,

$\{(\theta_1, \pm\pi/2), \theta_1 \in [-\pi, \pi]\}$,

$\{(\theta_1, 0), \theta_1 \in [-\pi, \pi]\}$.

Function $F(\theta)$ does not have any flat branches.

Proof of this proposition will be given in Section II.3.

Proof of Theorem II.2.7

1. In the free case, $D(\lambda) = 2\cos\sqrt{\lambda}$ (see, e.g., [15]), so we have

$$\cos\sqrt{\lambda} = F_j(\theta), j = 1, 2, 3. \tag{II.11}$$

As it was proven in Theorem II.2.5, spectral bands do not overlap. It is still possible that these bands touch each other at their edges. We will prove this indeed happens and at these points the spectral bands have conical form.

According to (II.11), all non-flat spectral bands are

$$\lambda_{6k+j} = (\arccos(F_j(\theta)) + 2k\pi)^2, \lambda_{6k+3+j} = (2\pi - \arccos(F_j(\theta)) + 2k\pi)^2,$$

for all $j = \overline{1,3}, k = 0, 1, 2, \ldots$

Thus, for $k = 0, 1, 2, \ldots$, we have

i) Bands $\lambda_{6k+4}, \lambda_{6k+7}$ touch each other at $(0, 0, (2(k+1)\pi)^2)$, for which $D(\lambda) = 2$.

ii) Bands $\lambda_{6k+3}, \lambda_{6k+6}$ touch each other at $(0, \pm\pi, ((2k+1)\pi)^2)$, for which $D(\lambda) = -2$.

iii) Bands $\lambda_{6k+2}, \lambda_{6k+3}$ touch each other at $(\pm\theta_0, 0, (\theta_0 + 2k\pi)^2)$ while bands $\lambda_{6k+5}, \lambda_{6k+6}$ touch each other at $(\pm\theta_0, 0, (-\theta_0 + (2k+2)\pi)^2)$. At these points $D(\lambda) = -2/3$.

iv) Bands $\lambda_{6k+1}, \lambda_{6k+2}$ touch each other at $(\pm\theta_0, \pm\pi, (\pi - \theta_0 + 2k\pi)^2)$ while $\lambda_{6k+4}, \lambda_{6k+5}$ touch each other at $(\pm\theta_0, \pm\pi, (\pi + \theta_0 + 2k\pi)^2)$. At these points $D(\lambda) = 2/3$.

Let us now look at the structure near the touching points. One needs to deal with each case above separately. Since the argument we use for i) and iii) are similar to those needed for ii) and iv), for the sake of brevity, we will consider only cases i) and iii).

i) Let $(\theta, \lambda) = (0, 0, \lambda_0)$ where $\lambda_0 = (2(k+1)\pi)^2, k \in \mathbb{N}$. Then,

$$\frac{D(\lambda)}{2} = \cos\sqrt{\lambda} = 1 + a_2(\lambda - \lambda_0)^2 + o((\lambda - \lambda_0)^2), \tag{II.12}$$

for $\lambda \to \lambda_0$ where $a_2 = -1/8\lambda_0 < 0$,

$$\cos\theta_1 = 1 - \frac{\theta_1^2}{2} + o(\theta_1^2), \text{ for } \theta_1 \to 0 \tag{II.13}$$

and

$$\cos\theta_2 = 1 - \frac{\theta_2^2}{2} + o(\theta_2^2), \text{ for } \theta_2 \to 0. \tag{II.14}$$

Since $0.5D(\lambda)$ is a root of the equation (II.7), we have

$$9\left(\frac{D(\lambda)}{2}\right)^3 - \frac{D(\lambda)}{2} = (\cos\theta_1 + 1)\left(3\frac{D(\lambda)}{2} + \cos\theta_2\right). \tag{II.15}$$

Plugging expressions (II.12), (II.13), and (II.14) into (II.15) and simplify the expression, one obtains the following formula:

$$A(\lambda - \lambda_0)^2 + 2\theta_1^2 + \theta_2^2 = o(\theta_1^2) + o(\theta_2^2) + o((\lambda - \lambda_0)^2), \tag{II.16}$$

for $(\theta,\lambda)\to(0,0,\lambda_0)$, where $A=20a_2<0$. Equation (II.16) shows that the spectral bands touching at the point $(\theta,\lambda)=(0,0,\lambda_0)$ have the conical form. In other words, the Bloch variety of operator H has conical singularity at $(\theta,\lambda)=(0,0,\lambda_0)$.

iii) Let now $(\theta,\lambda)=(\theta_0,0,\lambda_0)$, where $\lambda_0=(\theta_0+2k\pi)^2, k=0,1,2,\ldots$. We have

$$\frac{D(\lambda)}{2}=-\frac{1}{3}+a_1(\lambda-\lambda_0)+a_2(\lambda-\lambda_0)^2+o((\lambda-\lambda_0)^2),$$

$$\text{for } \lambda\to\lambda_0, \text{ where } a_1=0.5D'(\lambda_0),$$

$$\cos\theta_1=-\frac{1}{3}+b_1(\theta_1-\theta_0)+b_2(\theta_1-\theta_0)^2+o((\theta_1-\theta_0)^2),$$

$$\text{for } \theta_1\to\theta_0 \text{ where } b_1=-\sin\theta_0,$$

and

$$\cos\theta_2=1-\frac{\theta_2^2}{2}+o(\theta_2^2), \text{ for } \theta_2\to 0.$$

Analogously to part i), we substitute these formulas into (II.15) to obtain

$$\frac{(A(\lambda-\lambda_0)+b_1(\theta_1-\theta_0))^2}{4}-\frac{B(\theta_1-\theta_0)^2}{4}-\frac{\theta_2^2}{3}=$$

$$=o(\theta_2^2)+o((\theta_1-\theta_0)^2)+o((\lambda-\lambda_0)^2),$$

for $(\theta,\lambda)\to(\theta_0,0,\lambda_0)$, where $A=6a_1$ and $B=b_1^2>0$. Since $D'(\lambda)\neq 0$ if $D(\lambda)\neq\pm 2$ according to Lemma II.2.2, $D'(\lambda_0)\neq 0$ and so $A=6a_1=3D'(\lambda_0)\neq 0$. Thus, two spectral bands which touch at the point $(\theta_0,0,\lambda_0)$ form a cone about that point. The Bloch variety of operator H has conical singularity at $(\theta_0,0,\lambda_0)$.

The same argument applies when $(\theta,\lambda)=(-\theta_0,0,\lambda_0)$.

2. When we turn on a small potential, since $D'(\lambda_0)\neq 0$ for $\lambda_0=D^{-1}(\pm 2/3)$, we can repeat the calculation in part iii), and find conical singularities at $\theta=(\pm\theta_0,0)$ or $(\pm\theta_0,\pm\pi)$ (at these points $|D(\lambda)|=2/3$).

As it was shown in [56], for almost every C^∞ periodic potential q_0 on $\mathbb{R}$, all the gaps of the Hill operator H^{per} open (at the edges of the gaps $D(\lambda)=\pm 2$). Since the spectrum $\sigma(H)$ has gaps iff $\sigma(H^{per})$ has gaps, this implies that all conical singularities in the free case with $D(\lambda)=\pm 2$ will generically split into two smooth branches and open a gap when we perturb the potential a little bit. □

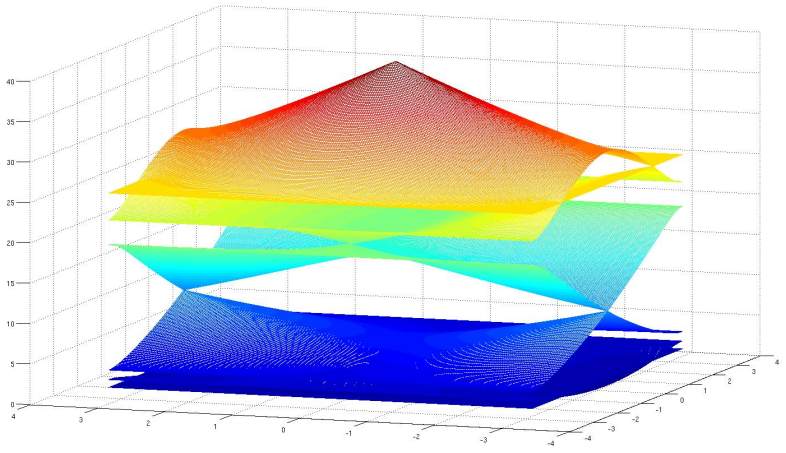

Figure II.8: Bloch variety of operator H in the free case

II.3 Proof of Proposition II.2.8

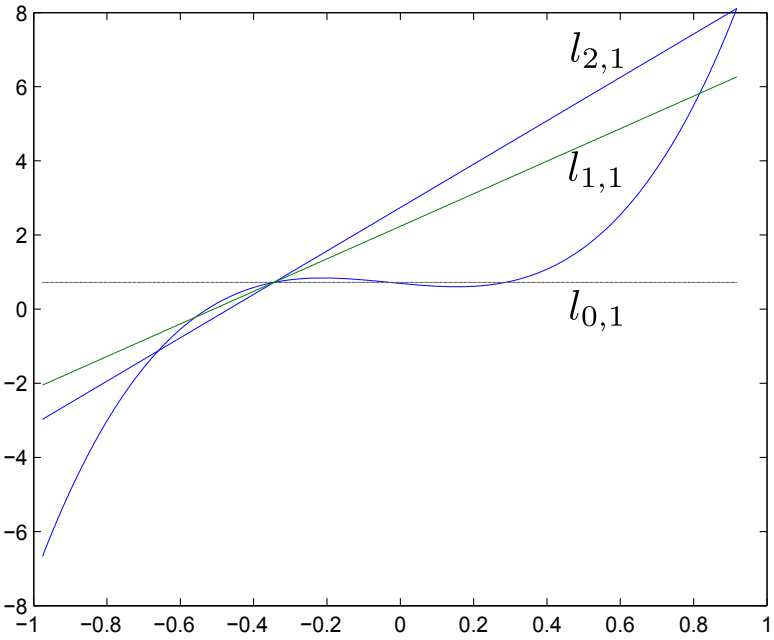

Figure II.9: The line $l_{1,1}$ lies between $l_{0,1}$ and $l_{2,1}$ and thus has nonempty intersections with I_1, I_2 and I_3

Proof. 1. We will use the following notations $a := \cos\theta_1 + 1$, $b := \cos\theta_2$, then $a \in [0, 2], b \in [-1, 1]$. Equation (II.7) becomes:

$$9x^3 - x = a(3x + b). \tag{II.17}$$

Denote $l_{a,b}$ as the graph of function $y = a(3x + b)$ and I_1, I_2, I_3 as parts of the graph of function $y = 9x^3 - x$ restricted to $[-1, -1/3]$, $[-1/3, 1/3]$ and $[1/3, 1]$ correspondingly, $I := I_1 \cup I_2 \cup I_3$. Then I_1, I_2, I_3 are all connected.

One can notice that the line $l_{0,1}$ intersects with I_1, I_2, I_3 when $x = -1/3, 0, 1/3$ correspondingly while the line $l_{2,1}$ intersects with I_1, I_2, I_3 when $x = -2/3, 1/3, 1$ respectively. When slope $3a$ of the line $l_{a,1}$ changes from 0 to 6, the line $l_{a,1}$ rotates from the line $l_{0,1}$ to the line $l_{2,1}$ around point $(-1/3, 0)$ as shown in Fig. II.9. Thus, the line $l_{a,1}$ intersects with each of I_1, I_2, I_3 for all values $a \in [0, 2]$. Applying the same argument for the line $l_{a,-1}$, we also have that the line $l_{a,-1}$ intersects with each of I_1, I_2, I_3 for all $a \in [0, 2]$.

Besides, for $a \in [0, 2], b \in (-1, 1)$, three lines $l_{a,1}, l_{a,b}$ and $l_{a,-1}$ are parallel and $l_{a,b}$ lies between the other two. Both lines $l_{a,1}$ and $l_{a,-1}$ intersect with each of I_1, I_2, I_3, and so the line $l_{a,b}$ also intersects with each of I_1, I_2, I_3, see illustration in case $a = 1/2$ in Fig. II.10. This means equation (II.17) has three real roots for all $a \in [0, 2]$, $b \in [-1, 1]$. Thus, all roots of equation (II.7) are real and so function $F(\theta)$ has only real values for all $\theta \in B$.

2. For each $a \in [0, 2]$, $b \in [-1, 1]$, the line $l_{a,b}$ intersects with each of I_1, I_2, I_3. By our notation, I_1, I_2, I_3 are parts of the graph of function $y = 9x^3 - x$ restricted to $[-1, -1/3]$, $[-1/3, 1/3]$ and $[1/3, 1]$ correspondingly. Thus, the ranges of functions F_1, F_2 and F_3 are $[-1, -1/3], [-1/3, 1/3]$ and $[1/3, 1]$ respectively.

3. In what follows, we will find out when function F_3 attains its maximal and minimal values. The similar argument applies for functions F_1 and F_2.

From part 2 we know that maximal value of F_3 is 1 and its minimal value is $1/3$.

Plugging $x = 1$ into equation (II.17) we have $a(3 + b) = 8$, which occurs only when $a = 2, b = 1$, i.e. $\theta = (0, 0)$. So function F_1 attains its maximum at $(0, 0)$.

Similarly, we plug $x = 1/3$ into the equation (II.17) to obtain $a(1 + b) = 0$, i.e. either $a = 0$ or $b = -1$. Now for each case when $a = 0$ or $b = -1$, solve equation (II.17), we will see that the biggest root of equation (II.17) is equal to $1/3$ when $a = 0, b \in [-1, 1]$ or $a \in [0, 2/3], b = -1$. This means function F_3 attains its minimum at $(\pm\pi, \theta_2)$ for $\theta_2 \in [-\pi, \pi]$ or $(\theta_1, \pm\pi)$ for $\theta_1 \in [-\pi, -\theta_0] \cup [\theta_0, \pi]$.

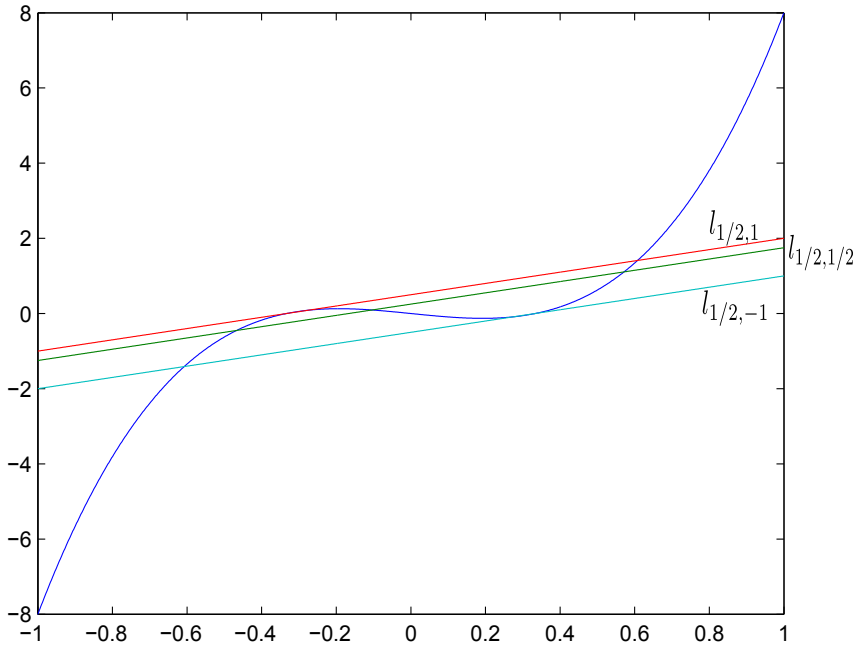

Figure II.10: The line $l_{1/2,1/2}$ is parallel to $l_{1/2,1}$ and $l_{1/2,-1}$, thus intersects with I_1, I_2, I_3

4. Let us denote the linear level set of function $F(\theta)$ as L (if such a set exists).

$$L := \{(\theta_1, \theta_2) \in B | p_1^0 \theta_1 + p_2^0 \theta_2 = 2k_0\pi\}, p_0 = (p_1^0, p_2^0) \in \mathbb{Z}^2 \backslash \{(0,0)\}, k_0 \in \mathbb{Z}.$$

For all θ belonging to L, equation (II.7) has (at least) a constant solution, namely c. Then

$$9c^3 - c = (\cos\theta_1 + 1)(3c + \cos\theta_2), \text{ for all } (\theta_1, \theta_2) \in L. \tag{II.18}$$

If $p_2^0 = 0$, then the linear level set $L = \{(2k_0\pi/p_1^0, \theta_2), \theta_2 \in [-\pi, \pi]\}$. Since all values in (II.18) are constant except θ_2 changing from $-\pi$ to π, the expression (II.18) is true only if $\cos\theta_1 + 1 = 0$. This would mean $\theta_1 = \pm\pi$, i.e. $L = \{(\pm\pi, \theta_2), \theta_2 \in [-\pi, \pi]\}$.

In case $p_2^0 \neq 0$, the linear level set L can be rewritten as

$$L = \left\{ (\theta_1, \theta_2) \in B \middle| \theta_2 = \frac{-p_1^0\theta_1 + 2k_0\pi}{p_2^0} \right\}$$

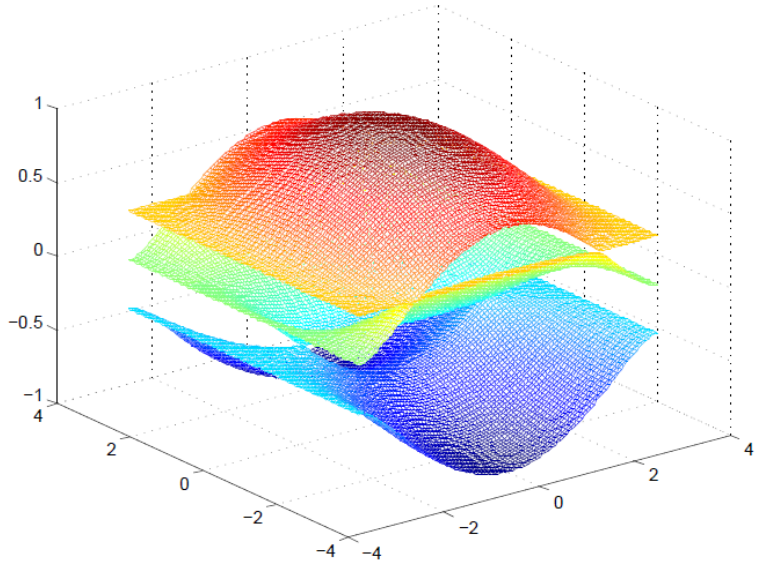

Figure II.11: Graph of root function for equation (II.7)

and so (II.18) becomes

$$9c^3 - c = (\cos\theta_1 + 1)\left(3c + \cos\frac{-p_1^0\theta_1 + 2k_0\pi}{p_2^0}\right), \text{ for all } \theta_1 \in [-\pi, \pi].$$

Since c is a constant and θ_1 runs from $-\pi$ to π, we have

$$9c^3 - c = (\cos\pi + 1)\left(3c + \cos\frac{-p_1^0\pi + 2k_0\pi}{p_2^0}\right) = 0.$$

Thus by solving the equation $9c^3 - c = 0$, we conclude that constant c can be $0, 1/3$ or $-1/3$. Plugging each value of c into (II.18), we can get all the linear level sets of $F(\theta)$ as below:

$\{(\pm\pi, \theta_2), \theta_2 \in [-\pi, \pi]\}$,

$\{(\theta_1, \pm\pi), \theta_1 \in [-\pi, \pi]\}$,

$\{(\theta_1, \pm\pi/2), \theta_1 \in [-\pi, \pi]\}$,

$\{(\theta_1, 0), \theta_1 \in [-\pi, \pi]\}$.

As a consequence, function $F(\theta)$ does not have any flat branches. □

CHAPTER III

ON GRAPHYNE NANOTUBES[1]

III.1 Carbon nanotube structures and related Schrödinger operators

While in the previous chapter we studied the spectra of the Schrödinger operators on the periodic graphyne structure shown in Fig. III.1, now we introduce carbon nanotubes related to that structure, which also carry similar Schrödinger operators. Studying the spectra of the latter ones is our goal.

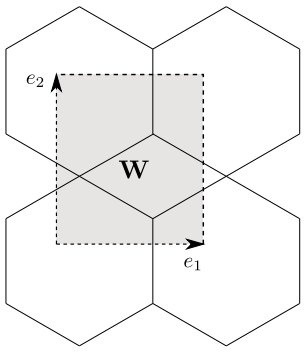

Figure III.1: Graph G and a fundamental domain W

As before the vectors e_1 and e_2 generate the square *lattice* of shifts that leave the geometry invariant. Let $p = (p_1, p_2) \in \mathbb{Z}^2 \backslash \{(0,0)\}$, then $pe := p_1 e_1 + p_2 e_2$ belongs to the latice of translation symmetries of the graphyne G. This means $G + pe = G$. We define ι_p to be the equivalence relation that identifies vectors $z_1, z_2 \in G$ if $z_2 - z_1 = kpe$ for some integer k. Then *nanotube* T_p is the graph obtained as the quotient of G with respect to this equivalence relation:

$$T_p := G/\iota_p.$$

Let us recall that $q_0(x)$ is a real, even, square integrable function on $[0,1]$ and $q(x)$ is the transferred potential of q_0 on all edges of T_p.

[1]Part of this chapter is reprinted with permission from "On the quantum graph spectra of graphyne nanotubes" by Ngoc Do, 2015. *Analysis and Mathematical Physics Journal*, Volume 1, Page 39-65, Copyright [2015] by Analysis and Mathematical Physics Journal

In chapter II, the operator

$$Hu(x) := -\frac{d^2u(x)}{dx^2} + q(x)u(x)$$

on the graphyne G was defined and studied. Analogously, we introduce the nanotube Schrödinger operator H_p that acts on each edge in the same way as H does:

$$H_p u(x) = -\frac{d^2u(x)}{dx^2} + q(x)u(x) \tag{III.1}$$

and whose domain $D(H_p)$ is the set of all functions $u(x)$ on T_p [2] such that:

1. $u_e := u|_e \in H_2(e)$, for all $e \in E(T_p)$,
2. $\sum_{e\in E(T_p)} \|u_e\|^2_{H_2(e)} < \infty$,
3. at each vertex these functions satisfy the Neumann vertex condition, i.e. $u_e(v) = u_{e'}(v)$, $\forall e, e' \in E(v)$ and $\sum_{e\in E(v)} u'_e(v) = 0$..

Understanding the spectra $\sigma(H_p)$ of these nanotube operators is our task here.

III.2 Spectral analysis of graphyne nanotube operators

The questions we address here are about the structure of the absolute continuous, singular continuous, and pure point spectrum of H_p, as well as spectral gaps opening.

In this section, we study the spectra of the operator H_p acting on the nanotube $T_p = T_{(p_1,p_2)}$ for some $p = (p_1, p_2) \in \mathbb{Z}^2$. If p is a zero vector, instead of a nanotube one gets the whole graphyne G, so we will always assume, without repeating this every time, that $p \neq (0, 0)$.

The standard Floquet-Bloch theory (see Section I.2) gives the following direct integral decomposition of the graphyne operator H:

$$H = \int_B^{\oplus} H(\theta)d\theta.$$

Here $H(\theta)$ is the Bloch Hamiltonian that acts as H does on the domain consisting of functions $u(x)$ that belong to $H^2_{loc}(G)$ and satisfy Neumann vertex conditions and Floquet condition.

Since functions on T_p are in one-to-one correspondence with p-periodic functions u on G, i.e. u such that $u(x+p_1e_1+p_2e_2) = u(x)$, only the values of *quasimomenta* θ satisfying the

[2] Equivalently, one can say that $u(x)$ is a function on G such that $u(x + kpe) = u(x)$ for all $k \in \mathbb{Z}$.

condition $p\theta = p_1\theta_1 + p_2\theta_2 \in 2\pi\mathbb{Z}$ will enter the direct integral expansion of H_p. Denoting by B_p the set

$$\{(\theta_1, \theta_2) \in B | p\theta = p_1\theta_1 + p_2\theta_2 = 2k\pi, k \in \mathbb{Z}\}, \tag{III.2}$$

one obtains the direct integral decomposition for H_p:

$$H_p = \int_{B_p}^{\oplus} H(\theta) d\theta.$$

As a consequence (see, e.g., [7, Section 4.2]),

$$\sigma(H_p) = \bigcup_{\theta \in B_p} \sigma(H(\theta)). \tag{III.3}$$

Moreover, the dispersion relation of H_p is the dispersion relation of H restricted to B_p.

We now need to recall some notations and results from chapter II that describe the spectrum and the dispersion relation of the operator H.

We extend the potential $q_0(x)$ on $[0, 1]$ to a 1-periodic function $q_{per}(x)$ on $\mathbb{R}$ and denote by $D(\lambda) = trM(\lambda)$ the discriminant (or the Lyapunov function) of the periodic Sturm-Liouville operator

$$H^{per} := -\frac{d^2}{dx^2} + q_{per}(x).$$

Here $M(\lambda)$ is the monodromy matrix for this operator.

As before, by Σ^D we denote the (discrete) spectrum of the operator $-d^2/dx^2 + q_0(x)$ on $[0, 1]$ with Dirichlet conditions at the ends of this segment.

Let us recall that the triple-valued function $F(\theta) := (F_1(\theta), F_2(\theta), F_3(\theta))$ on B provides for each θ the three (real) roots of the equation

$$9x^3 - x - (\cos\theta_1 + 1)(3x + \cos\theta_2) = 0,$$

where $F_1 \leq F_2 \leq F_3$ for each value of θ.

We can now quote the main result from the previous chapter, which describes the spectral structure of the graphyne operator H:

Theorem II.7

1. *The singular continuous spectrum $\sigma_{sc}(H)$ is empty.*

2. *The dispersion relation of operator H consists of the following two parts:*
   i) pairs (θ, λ) such that $D(\lambda) \in 2F(\theta)$ (or, $\lambda \in D^{-1}(2F(\theta))$), where θ is changing in the Brillouin zone;
   and
   ii) the collection of flat (i.e., θ-independent) branches (θ, λ) such that $\lambda \in \Sigma^D$.

3. *The absolutely continuous spectrum $\sigma_{ac}(H)$ has band-gap structure and is (as the set) the same as the spectrum $\sigma(H^{per})$ of the Hill operator H^{per} with potential obtained by extending periodically q_0 from $[0, 1]$. In particular,*

$$\sigma_{ac}(H) = \{\lambda \in \mathbb{R} \big| \, |D(\lambda)| \leq 2\},$$

   where $D(\lambda)$ is the discriminant of H^{per}.

4. *The bands of $\sigma(H)$ do not overlap but can touch. Each band of $\sigma(H^{per})$ consists of three touching bands of $\sigma(H)$.*

5. *The pure point spectrum $\sigma_{pp}(H)$ coincides with Σ^D and belongs to the union of the edges of spectral gaps of $\sigma(H^{per}) = \sigma_{ac}(H)$.*
   Eigenvalues $\lambda \in \Sigma^D$ of the pure point spectrum are of infinite multiplicity and the corresponding eigenspaces are generated by simple loop (i.e., supported on a single hexagon or rhombus) states.

6. *Spectrum $\sigma(H)$ has gaps if and only if $\sigma(H^{per})$ has gaps* [3].

Since, in order to obtain the dispersion relation for the nanotube operator H_p, we need to restrict this relation to the subset B_p of the Brillouin zone B, the previous theorem provides a good start. Indeed, we see that Σ^D belongs to the pure point spectrum $\sigma_{pp}(H_p)$ and the rest of the spectrum is defined by $D^{-1}(2F(B_p))$. However, further analysis is still needed, since during the restriction to B_p new gaps might open and new bound states might appear. These effects are expected to depend upon the vector p, i.e. on the type of the nanotubes (for the "usual" nanotubes the names "zig-zag," "armchair," and "chiral" are used, but they are not applicable in our situation).

In what follows, we will study the range of the function F restricted to B_p. According to (III.2), in the $\theta_1\theta_2$-coordinate system, B_p is a set of points belonging to a family of parallel lines restricted to the Brillouin zone B. If the slope of these lines is negative, we reflect B_p over the θ_2-axis to make the slope positive. Let us denote the set of segments from B_p

[3] It is well known that for any non-constant potential q, the spectrum $\sigma(H^{per})$ has some gaps (see [15]). Moreover, for a generic potential q, all gaps are open (see [56]).

with positive slope as R_p, then $R_p = \{(\theta_1, \theta_2) \in B : |p_2|\theta_2 = |p_1|\theta_1 - 2k\pi, k \in \mathbb{Z}\}$. Since $F(\theta_1, \theta_2) = F(-\theta_1, \theta_2)$ for all (θ_1, θ_2), we have $F(B_p) = F(R_p)$.

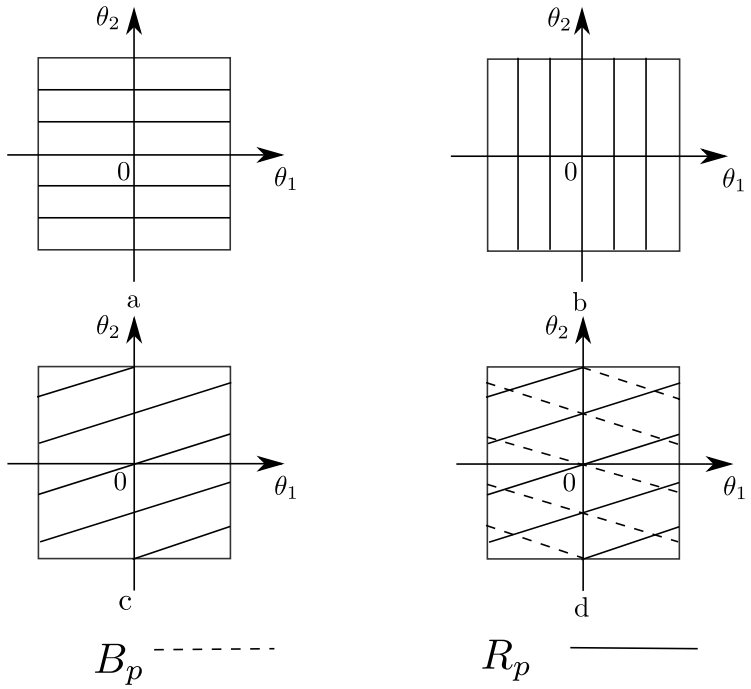

Figure III.2: R_p and B_p coincide when $p_1p_2 \leq 0$ (cases a, b, c) or are symmetric w.r.t. the θ_2-axis (d)

We denote by N_p the set of points from R_p that belong to lines with non-negative θ_1-intercept (or nonpositive θ_2-intercept in case lines from R_p are parallel to θ_1-axis). Then $N_p = \{(\theta_1, \theta_2) \in B : |p_2|\theta_2 = |p_1|\theta_1 - 2k\pi, k = 0, 1, \ldots\}$. Since $F(\theta_1, \theta_2) = F(-\theta_1, -\theta_2)$ for all (θ_1, θ_2), $F(R_p) = F(N_p)$.

Let $V_q := \{(\theta_1, \theta_2) \in B : q_2\theta_2 = q_1\theta_1 - 2k\pi, k = 0, 1, \ldots\}$, where $q = (q_1, q_2)$. The above argument proves that $F(B_p) = F(V_q)$ for $q = (q_1, q_2) := (|p_1|, |p_2|)$. Thus, it is sufficient to study the range of function $F(\theta)$ restricted to V_q for nonnegative q_1, q_2.

Let us denote $l_0 = [q_1\theta_0/2\pi]$. Below we state three lemmas about the range of functions $F_j, j = \overline{1,3}$, proofs of which will be provided in Section III.3.

Lemma III.2.1. *If $q_2 = 0$ and $q_1 > 1$, then*

$$F_1(V_q) = [-1, F_1(2l_0\pi/q_1, 0)] \cup [F_1(2(l_0 + 1)\pi/q_1, \pi), -1/3].$$

If $q_2 = 0$ *and* $q_1 = 1$*, then* $F_1(V_q) = [-1, -2/3]$.

If $q_2 \neq 0$ *is even, then* $F_1(V_q) = \left[-1, -\frac{1}{3}\right]$.

If q_2 *is odd, then* $F_1(V_q) = [a, -1/3]$ *for some* $a := \min F_1(V_q) \in (-1, -2/3]$. *In particular, if* $q_1 = 0$ *then* $a = F_1(0, -2[q_2/2]\pi/q_2)$

Lemma III.2.2. *If* $q_1 \leq 1$ *and* q_2 *is odd, then* $F_2(V_q) = [-1/3, a]$ *for some* $a \in [0, 1/3)$. *Otherwise* $F_2(V_q) = [-1/3, 1/3]$.

Lemma III.2.3. *If* $q_2 = 0$ *and* $q_1 > 1$ *then*

$$F_3(V_q) = [1/3, F_3(2(l_0 + 1)\pi/q_1, 0)] \cup [F_3(2l_0\pi/q_1, \pi), 1].$$

If $q_2 = 0$ *and* $q_1 = 1$ *then* $F_3(V_q) = [2/3, 1]$.

Otherwise $F_3(V_q) = [1/3, 1]$.

Taking into account that $F(B_p) = F(V_q)$ for $q = (|p_1|, |p_2|)$, we summarize results of above lemmas in Fig. III.3

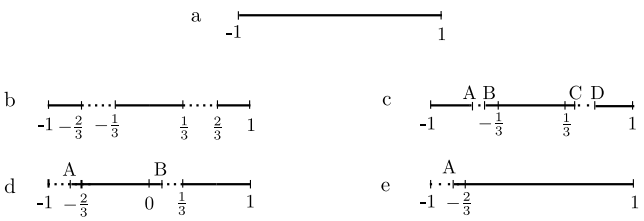

Figure III.3: Functions $F_j, j = \overline{1,3}$, have values in $[-1, 1]$. The bold segments are $F(\theta)$. The dotted intervals do not belong to the union of the ranges of $F_j, j = \overline{1,3}$. a) $p_2 \neq 0$ even, b) $p_2 = 0$, $p_1 = \pm 1$, c) $p_2 = 0$, $|p_1| > 1$, d) p_2 odd, $|p_1| \leq 1$, e) p_2 odd, $|p_1| > 1$

Notice that in the case c where $p_2 = 0$ and $|p_1| > 1$ either or both dotted intervals may vanish.

As it was pointed out before, Σ^D belongs to the pure point spectrum of H_p. Extra pure point spectrum appears if some non-constant branch of the dispersion relation of H has constant restriction on B_p. This can happen only on the linear level sets of functions $F_j, j = \overline{1,3}$, inside B. In Proposition II.2.8 we described all such sets:

1. $A_1 = \{(\pm\pi, \theta_2), \theta_2 \in [-\pi, \pi]\}$,
2. $A_2 = \{(\theta_1, \pm\pi), \theta_1 \in [-\pi, \pi]\}$,

3. $A_3 = \{(\theta_1, 0), \theta_1 \in [-\pi, \pi]\}$,

4. $A_4 = \{(\theta_1, \pm\pi/2), \theta_1 \in [-\pi, \pi]\}$.

Let us now deal with the additional pure point spectrum that arises due to the presence of linear level sets. First, we build compactly supported eigenfunctions corresponding to those extra eigenvalues. Then, we prove that these functions generate all compactly supported eigenfunctions in the corresponding eigenspaces.

We look at the first linear level set $A_1 = \{(\pm\pi, \theta_2), \theta_2 \in [-\pi, \pi]\}$. Let $p = (2N, 0)$ for some postivive integer N, then A_1 can be rewritten as $\{\theta | p\theta \pm 2N\pi = 0\}$. On this line $F_1(\theta) = -1/3, F_2(\theta) = 0$, and $F_3(\theta) = 1/3$.

Let us recall that for each $\lambda \notin \Sigma^D$ functions φ_0, φ_1 are two linearly independent solutions of the equation

$$-\frac{d^2u}{dx^2} + q_0(x)u = \lambda u \tag{III.4}$$

such that $\varphi_{0,\lambda}(0) = \varphi_{1,\lambda}(1) = 1, \varphi_{0,\lambda}(1) = \varphi_{1,\lambda}(0) = 0$. Also, function $\eta(\lambda)$ is defined as follows $\eta(\lambda) := \varphi'_{1,\lambda}(1)/\varphi'_{1,\lambda}(0)$. Then (Lemma II.2.1), λ is in the spectrum of H if and only if there exists $\theta = (\theta_1, \theta_2) \in B$ such that $\eta(\lambda) = F_j(\theta)$ for some $j \in \overline{1,3}$. We will first consider those values of λ such that $\eta(\lambda) = F_2(\theta) = 0$, i.e.

$$\frac{\varphi'_{1,\lambda}(1)}{\varphi'_{1,\lambda}(0)} = 0 \text{ or } \varphi'_{1,\lambda}(1) = 0.$$

As it was said before, we now build a compactly supported eigenfunction , namely $g(x)$, corresponding to these λ of operator $H_{(2N,0)}$. Let g be equal to φ_1 on four edges directed toward the vertex A and be equal to $-\varphi_1$ on four edges directed toward B and C (see Fig. III.4). One can easily check that the Neumann boundary conditions satisfied at vertex A.

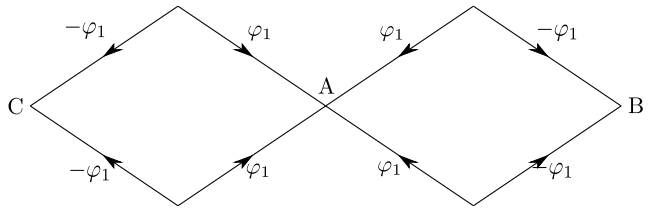

Figure III.4: Piece of rhombus bracelet function corresponding to $p = (2N, 0)$ and $\eta(\lambda) = 0$

We extend this piece of function g to the whole nanotube by repeating it N times horizontally. Outside this band of rhombuses around the nanotube, function g is defined to be

equal to zero. The defined function g is periodic with period $2e_1$ and satisfies the Neumann boundary conditions at all vertices. Thus, it is a compactly supported eigenfunction for the nanotube $T_{(2N,0)}$ corresponding to those λ such that $\eta(\lambda) = 0$. We call the constructed function the *rhombus bracelet function*.

In Fig. III.5, III.6, III.7 one can find similar functions built on a piece of the nanotube structure, extensions of which will serve as the compactly supported eigenfunctions corresponding to the additional eigenvalues.

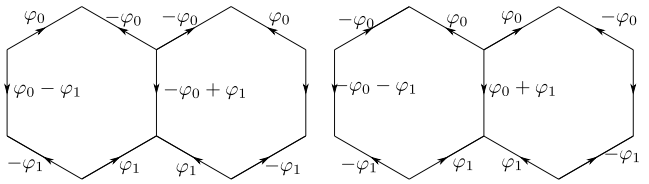

Figure III.5: Piece of hexagon bracelet functions of type a ($\eta(\lambda) = -1/3$) or type b ($\eta(\lambda) = -1/3$) in case $p = (2N, 0)$

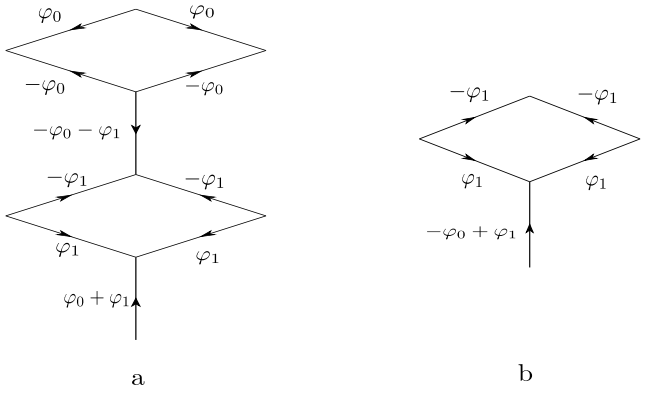

Figure III.6: a. Piece of mushroom function in case $p = (0, N)$ for N - a multiple of 2 and $\eta(\lambda) = 1/3$ and b. piece of flower function in case $p = (0, N)$ for integer N and $\eta(\lambda) = -1/3$

More specifically, for $p = (2N, 0)$, where N is some nonzero integer, we repeat the piece of functions in Fig. III.5 N times horizontally and make it equal to zero elsewhere. The obtained functions are compactly supported eigenfunctions corresponding to λ such that $\eta(\lambda) = F_1(\theta) = -1/3$ (on the left) and $\eta(\lambda) = F_3(\theta) = 1/3$ (on the right). For the

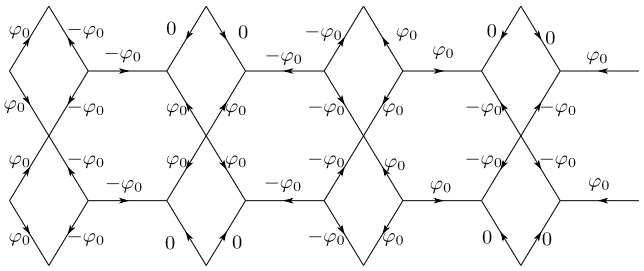

Figure III.7: Piece of double-band function in case $p = (0, N)$ for N - a multiple of 4 and $\eta(\lambda) = 0$

second linear level set $A_2 = \{(\theta_1, \pm\pi), \theta_1 \in [-\pi, \pi]\}$, we have $p = (0, 2N)$, where N is some nonzero integer. In this case, we has to repeat function from Fig. III.6a N times vertically and make it equal to zero elsewhere. The obtained function is a compactly supported eigenfunction corresponding to λ such that $\eta(\lambda) = 1/3$. Analogously, $p = (0, N)$ corresponds to the third linear level set $A_3 = \{(\theta_1, 0), \theta_1 \in [-\pi, \pi]\}$. One first needs to repeat the piece of function from Fig. III.6b N times vertically and make it equal to zero beyond that in order to get a compactly supported eigenfunction corresponding to λ with $\eta(\lambda) = -1/3$. The last linear level set, $A_4 = \{(\theta_1, \pm\pi/2), \theta_1 \in [-\pi, \pi]\}$, corresponds to $p = (0, 4N)$, where N is some nonzero integer. One again repeat the piece of function from Fig. III.7 N times horizontally and make it equal to zero outside the double-band in order to obtain an eigenfunction corresponding to eigenvalues λ with $\eta(\lambda) = 0$. We accordingly call functions from Fig. III.5 *hexagon bracelet functions of type a and b*, from Fig. III.6 - *mushroom function* and *flower function* accordingly, and from Fig. III.7 - *double-band function*.

Now one needs to prove that these functions generate all compactly supported eigenfunctions of the corresponding eigenspaces.

Indeed, let g be a compactly supported eigenfunction of $H_{(2N,0)}$ corresponding to those eigenvalues λ such that $\eta(\lambda) = 0$ and P - the lowest point on the boundary of the support of g (think about the nanotube $T_{(2N,0)}$ as a vertical tube). Since the nanotube structure is periodic, without loss of generality, P can be one of three points D, E, or I shown in the Fig. III.8.

The point P cannot be E since it would make $g|_e(E) = g'|_e(E) = 0$, as a result of which, $g|_e \equiv 0$ - contradiction.

Fig. III.9 shows what we obtain when trying to construct the compactly supported eigenfunction using Neumann vertex conditions if P is I.

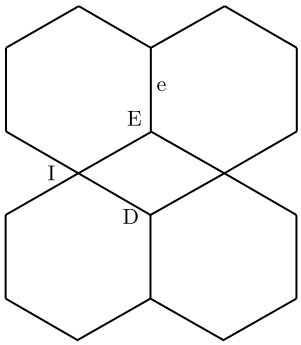

Figure III.8: Three possible locations (D, E or I) of the lowest point on the boundary of the compactly supported eigenfunction in case $p = (2N, 0)$

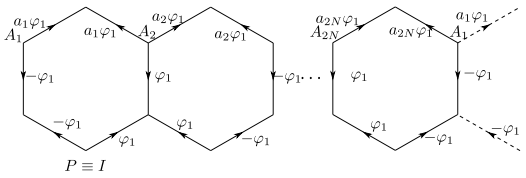

Figure III.9: Construction of a compactly supported eigenfunction (if such a function exists) when P concides with I in case $p = (2N, 0)$ and $\eta(\lambda) = 0$

From the Neumann boundary conditions at vertices $A_j, j = \overline{1, 2N}$, we have

$$a_1 + a_2 + 1 = 0,$$

$$a_2 + a_3 - 1 = 0,$$

$$\dots$$

$$a_{2N-1} + a_{2N} + 1 = 0,$$

$$a_{2N} + a_1 - 1 = 0.$$

Let us number above formulas, starting from 1. Then, the sum of odd-ordered formulas gives us $a_1 + a_2 + \ldots + a_{2N} + n = 0$ while the sum of even-ordered formulas gives us $a_1 + \ldots + a_{2N} - n = 0$, which lead to contradiction. Thus, I cannot be the lowest point on the support of function g.

Therefore, D must be the lowest point on the boundary of the support of function g. Extending from D a function with band of rhombuses support and substracting it from g,

we will get a new function with smaller support. The lowest point in the support of this new function (this is also an eigenfunction corresponding to the same eigenvalue, provided that it is nonzero) must be "another" point D. Continuing this procedure, we will eventually get zero function, which implies that g is a combination of rhombus bracelet eigenfunctions.

In case $p = (2N, 0)$, N - nonzero integer, and $\eta(\lambda) = F_1(\theta) = -1/3$ or $\eta(\lambda) = F_3(\theta) = 1/3$, we use the same technique. The only difference is the lowest point on the boundary is now I. Point E cannot be the lowest point by the same reason as before and point D - by contradiction obtained from Fig. III.10.

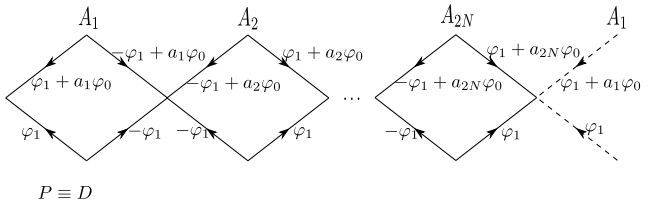

Figure III.10: Construction of a compactly supported eigenfunction (if such a function exists) when P concides with D in case $p = (2N, 0)$ and $\eta(\lambda) = \pm 1/3$

In all other cases, we also use the "lowest point" argument. The symmetry of the structure once again implies that the lowest point on the boundary of compactly supported eigenfunction can locate at D, E, or I (see Fig. III.11).

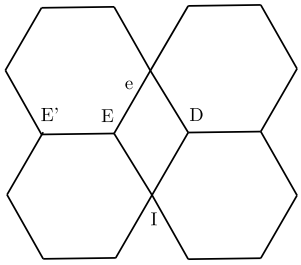

Figure III.11: Three possible locations of the lowest point on the boundary of the compactly supported eigenfunctions in case $p = (0, N)$ for $N \in \mathbb{Z}$

Both D and E are excluded by the same reason. For instance, if E is the lowest point, then $g|_e(E) = g|_e(E') = 0$ (otherwise due to the first Neumann boundary condition E will

not be the lowest point). From here we have $g|_e \equiv 0$, which leads to contradiction. The lowest point, thus, should be I.

The eliminating process for $p = (0, N), N \in \mathbb{Z}$, $\eta(\lambda) = -1/3$ or $p = (0, 2N), N \in \mathbb{Z}$, $\eta(\lambda) = 1/3$ occurs exactly the same as in the previous cases.

Now, we consider the case when $p = (0, 4N), N \in \mathbb{Z}$, $\eta(\lambda) = 0$. We claim that there does not exist a compactly supported eigenfunction of height $|e_1|$. Indeed, suppose the contrary, Fig. III.12 shows what we may obtain when constructing such a function. Then, there would not be such an a that the Neumann boundary conditions satisfied at both points A and B. This implies that any compactly supported eigenfunction corresponding to λ with $\eta(\lambda) = 0$ has at least height $2|e_1|$.

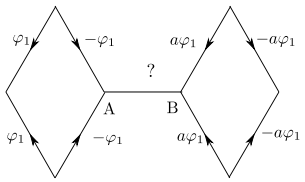

Figure III.12: Situation when trying to construct a compactly supported eigenfunction of height $|e_1|$

The eliminating process would then be similar to what happened before. (Since the minimum height of any nonzero compactly supported eigenfunction is $2|e_1|$, when we substract function of double-band type from the original eigenfunction, there is no need to worry that the support of the new eigenfunction will exceed the old one's.)

Let Σ^0 be the extra pure point spectrum which occurs due to the linear level set(s) of function F. Recall that $D(\lambda) = 2\eta(\lambda)$. Then the above argument proves the following:
Lemma III.2.4.

1. *If $p = (2N, 0)$ for some nonzero $N \in \mathbb{Z}$, then $\Sigma^0 = D^{-1}(\{\pm 2/3, 0\})$.*

   The eigenspace corresponding to λ with $D(\lambda) = 0$ is generated by the rhombus bracelet functions. The eigenspaces corresponding to λ with $D(\lambda) = -2/3$ or $2/3$ are generated by the hexagon bracelet functions of type a or b accordingly.

2. *If $p = (0, N)$ for some odd N, then $\Sigma^0 = D^{-1}(\{-2/3\})$.*
   If $p = (0, N)$ for some N which is a multiple of 2 but not a multiple of 4, then

$\Sigma^0 = D^{-1}(\{\pm 2/3\})$.
If $p = (0, N)$ *for some* N *which is a multiple of* 4, *then* $\Sigma^0 = D^{-1}(\{\pm 2/3, 0\})$.

In all cases, the eigenspace corresponding to λ *with* $D(\lambda) = -2/3$ *is generated by the flower functions. The eigenspace corresponding to* λ *with* $D(\lambda) = 2/3$ *is generated by the mushroom functions and the one corresponding to* λ *with* $D(\lambda) = 0$ *is generated by the double-band functions.*

We are now ready to formulate the main result about the spectra of carbon nanotubes. Let us first recall some necessary notations. Vector $pe := p_1 e_1 + p_2 e_2$ is the translation vector that defines the nanotube T_p. Function q_0 is a real, even, L_2-function on $[0, 1]$. The Hamiltonian H_p is defined on $L_2(T_p)$ with potential q transfered from q_0 to each edge. The set B_p is the subset of the Brillouin zone B as defined in (III.2). The Hill operator H^{per} has potential q_{per}, which is periodic extension of q_0 and $D(\lambda)$ - its discriminant. By simple loop state we mean an eigenfunction of operator H with Dirichlet boundary condition whose support is a hexagon or rhombus (see Fig. III.13). We also introduce the so-called *tube loop eigenfunction*, support of which is a loop of edges around the tube.

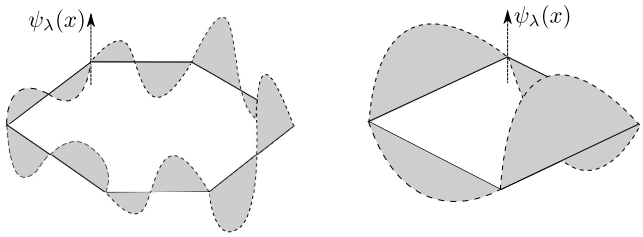

Figure III.13: Simple loop states constructed from odd function on $[0, 1]$ for hexagon and even function on $[0, 1]$ for rhombus

Theorem III.2.5.

1. *The singular continuous spectrum* $\sigma_{sc}(H_p)$ *is empty.*

2. *The nonconstant part of the dispersion relation for the Hamiltonian* H_p *is described by the following formula*

$$D(\lambda) \in 2F(\theta), \theta \in B_p \text{ or } \lambda \in D^{-1}(2F(\theta)), \theta \in B_p. \tag{III.5}$$

3. *The absolutely continuous spectrum* $\sigma_{ac}(H_p)$ *has band gap structure. All bands do not overlap. If* p_2 *is nonzero and even, then* $\sigma_{ac}(H_p) = \sigma(H^{per})$. *Otherwise, there may*

be additional gaps opened inside spectral bands H^{per}. In particular,

i. If $p_2 = 0$ and $p_1 = \pm 1$, then $\sigma_{ac}(H_p) = D^{-1}(\{[-2, -4/3] \cup [-2/3, 2/3] \cup [4/3, 2]\})$. There is two gaps opened in each spectral band of H^{per}.

ii. If $p_2 = 0$ and $p_1 \neq \pm 1$, then $\sigma_{ac}(H_p) = D^{-1}(A)$, where

$$A = [-2, 2F_1(\tfrac{2l_0\pi}{p_1}, 0)] \cup [2F_3(\tfrac{2l_0\pi}{p_1}, \pi), 2] \cup [2F_1(\tfrac{2(l_0+1)\pi}{p_1}, \pi), 2F_3(\tfrac{2(l_0+1)\pi}{p_1}, 0)].$$

If $F_1(\frac{2l_0\pi}{p_1}, 0) < F_1(\frac{2(l_0+1)\pi}{p_1}, \pi)$ there is a gap opened in each band of H^{per}.
If $F_3(\frac{2(l_0+1)\pi}{p_1}, 0) < F_3(\frac{2l_0\pi}{p_1}, \pi)$ there is a gap opened in each band of H^{per}.

iii. If p_2 is odd and $|p_1| \leq 1$, then for $B = [2 \min F_1(B_p), 2 \max F_2(B_p)] \cup [2/3, 2]$ we have $\sigma_{ac}(H_p) = D^{-1}(B)$. There is always two gaps opened in each band of H^{per}.

iv. If p_2 is odd and $|p_1| > 1$, then $\sigma_{ac}(H_p) = D^{-1}(C)$ where $C = [2 \min F_1(B_p), 2]$. Only one gap is opened in each band of H^{per}.

4. The pure point spectrum of H_p contains the pure point spectrum Σ^D of H.

i. If p is not of the form $(2N, 0)$ or $(0, N)$ for some nonzero integer N, then these two sets concide. The eigenvalues from Σ^D are of infinite multiplicity and the corresponding eigenspaces are spanned by the simple loop state eigenfunctions and the tube loop eigenfunctions.

ii. If $p = (2N, 0)$ or $(0, N)$ for some nonzero N, then, besides Σ^D, the nanotube operator H_p has extra pure point spectrum, which is denoted by Σ^0. All eigenvalues are of infinite multiplicity. Description of these extra eigenvalues and their corresponding eigenspaces are provided in Lemma III.2.4.

Proof. The first claim is a well-known fact about singular continuous spectrum of Schrödinger operator (see [57],[7, Theorem 4.4.1], [51, Section XIII.6] [37, Section 6.3]).

The second claim follows from the formula (III.3) and claim 2i of II.2.5.

The fact that absolutely continuous spectrum $\sigma_{ac}(H_p)$ has band gap structure and all bands do not overlap is also a consequence of formula (III.3) and claims (3) and (4) of II.2.5.

Gaps will be opened when the ranges of functions F_1, F_2, and F_3 restricted on B_p create gaps in the interval $[-1, 1]$. The rest of this claim therefore follows directly from lemmas III.2.1, III.2.2, III.2.3 (result of which was briefly described in Fig. III.3).

As it was mentioned before, the pure point spectrum of H_p always contains the Dirichlet spectrum Σ^D. The claim about infinite multiplicity of eigenvalues in both cases is known to

be true for periodic problems (see, e.g., Lemma II.2.4). Extra pure point spectrum occurs only if there is some linear level set. This happens when $p = (2N, 0)$ or $(0, N)$ for some nonzero N. The next part of claim (4) is proved similarly as for the analogous one from Lemma II.2.4. The only difference is that the eliminating process may end up with a tube loop eigenfunction.

The last part of the claim is contained in Lemma III.2.4. □

III.3 Proofs of supporting lemmas

In what follows, we denote the graph of the line $q_2\theta_2 = q_1\theta_1 - 2k\pi$ and its restriction to V_q by $t_{q,k}$ and $T_{q,k}$ accordingly. Let us recall that by θ_0 we denote $\arccos(-1/3)$.

Lemma III.2.1 *If $q_2 = 0$ and $q_1 > 1$, then*

$$F_1(V_q) = [-1, F_1(2l_0\pi/q_1, 0)] \cup [F_1(2(l_0+1)\pi/q_1, \pi), -1/3].$$

If $q_2 = 0$ and $q_1 = 1$, then $F_1(V_q) = [-1, -2/3]$.

If $q_2 \neq 0$ is even, then $F_1(V_q) = \big[-1, -\frac{1}{3}\big]$.

If q_2 is odd, then $F_1(V_q) = [a, -1/3]$ for some $a := \min F_1(V_q) \in (-1, -2/3]$. In particular, if $q_1 = 0$ then $a = F_1(0, -2[q_2/2]\pi/q_2)$

Proof. First of all we notice the following:

i. For fixed $\theta_1 = \theta_1^0 \neq \pm\pi$, function $F_1(\theta_1^0, \theta_2)$ is decreasing on $[0, \pi]$.

ii. For fixed $\theta_2 = \theta_2^0$, function $F_1(\theta_1, \theta_2^0)$ is non-decreasing on $[0, \pi]$.

Indeed, $F_1(\theta_1, \theta_2)$ is the smallest value of $x-$ coordinates of intersections of graphs of functions $f(x) = 9x^3 - x$ and $g(x) = (\cos\theta_1 + 1)(3x + \cos\theta_2)$. If we fix $\theta_1 := \theta_1^0 \neq \pm\pi$, then the slope $3(\cos\theta_1^0 + 1)$ is constant and positive. As a consequence, $y-$intercept $(\cos\theta_1^0 + 1)\cos\theta_2$ decreases on $[0, \pi]$, which make function F_1 decrease on $[0, \pi]$. (In case $\theta_1 = \pm\pi$, function F_1 is constant and equal to $-1/3$.)

Now if we fix $\theta_2 := \theta_2^0$, then the $x-$intercept $-(\cos\theta_2^0)/3$ of $g(x)$ will be constant and belongs to the interval $[-1/3, 1/3]$. The slope $3(\cos\theta_1 + 1)$ of function $g(x)$ is decreasing on $[0, \pi]$, thus $F_1(\theta_1, \theta_2^0)$ is nondecreasing on $[0, \pi]$.

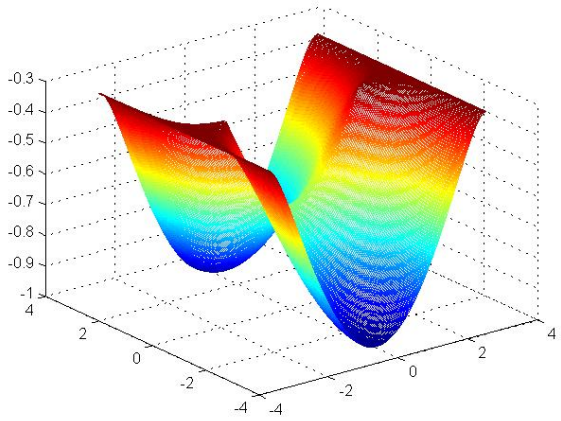

Figure III.14: Graph of function F_1

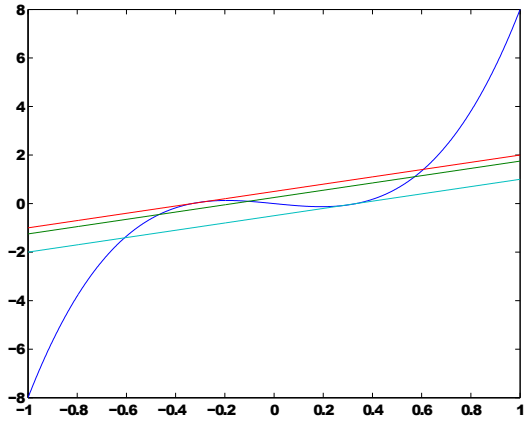

Figure III.15: The constant slope and decreasing θ_2-intercept make F_1 decrease

We first consider the case $q_2 = 0$. Then,

$$V_q = \{(\theta_1, \theta_2) \in B : \theta_1 = \frac{2k\pi}{q_1}, k = 0, 1, 2, \ldots\}.$$

The most right interval $T_{q,k}$ of V_q is $T_{q,[\frac{q_1}{2}]}$. Thus,

$$F_1(V_q) = F_1\Big(\bigcup_{0 \le k \le \left[\frac{q_1}{2}\right]} T_{q,k}\Big) = \bigcup_{0 \le k \le \left[\frac{q_1}{2}\right]} F_1(T_{q,k}).$$

Since $T_{q,k} = \left\{ \dfrac{2k\pi}{q_1} \right\} \times [-\pi, \pi]$ and $F_1(\theta_1, \theta_2) = F_1(\theta_1, -\theta_2)$,

$$F_1(T_{q,k}) = F_1\left(\left\{ \frac{2k\pi}{q_1} \right\} \times [-\pi, \pi] \right) = F_1\left(\left\{ \frac{2k\pi}{q_1} \right\} \times [0, \pi] \right).$$

Now, according to the remark above, for fixed k, $\theta_1 = 2k\pi/q_1$, we have

$$F_1(T_{q,k}) = \left[F_1\left(\frac{2k\pi}{q_1}, \pi \right), F_1\left(\frac{2k\pi}{q_1}, 0 \right) \right].$$

(In case $\theta_1 = \pi$ the segment boils down to the one-point set $\{-1/3\}$.) Therefore,

$$F_1(V_q) = \bigcup_{0 \le k \le \left[\frac{q_1}{2}\right]} \left[F_1\left(\frac{2k\pi}{q_1}, \pi \right), F_1\left(\frac{2k\pi}{q_1}, 0 \right) \right].$$

Recall that $l_0 = [q_1\theta_0/2\pi]$, the interval $T_{q,k}$ intersects with $\theta_2 = \pi$ at $\theta_1 = 2k\pi/q_1 < \theta_0$ for all $k \in [0, l_0]$. Function F_1 is non-decreasing on $[0, \pi]$ for fixed θ_2, thus for all $k \in [0, l_0]$

$$-1 = F_1(0, \pi) < F_1(2k\pi/q_1, \pi) \le -2/3 = F_1(\theta_0, \pi)$$

and

$$F_1(0, 0) = -2/3 \le F_1(2k\pi/q_1, 0) \le F_1(2l_0\pi/q_1, 0).$$

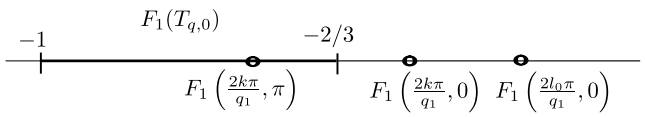

Figure III.16: Case $q_2 = 0$.$F_1(T_{q,0}) = [-1, -2/3]$, $F_1(2k\pi/q_1, \pi)$ are on the right of $-2/3$ and $F_1(2k\pi/q_1, 0) \le F_1(2l_0\pi/q_1, 0)$ are on the left of $-2/3$ for all $k \in [0, l_0]$

As a consequence (see Fig. III.16), for $q = (q_1, 0)$,

$$\bigcup_{0 \le k \le l_0} F_1(T_{q,k}) = [-1, F_1(2l_0\pi/q_1, 0)]. \tag{III.6}$$

For all $q_1 \ge 6$ we have $1 \le q_1/2 - q_1\theta_0/2\pi$, which implies the existence of an integer k such that $l_0 < k \le [q_1/2]$. It is not difficult to check that the latter claim is also true for

$1 < q_1 \leq 5$. Thus, for all $q_1 > 1$, there exists k such that $T_{q,k}$ belongs to V_q and lies on the right of the line $\theta_1 = \theta_0$ (see Fig. III.17).

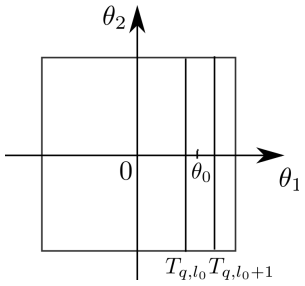

Figure III.17: Case $q_2 = 0, q_1 > 1$. Point $(\theta_0, 0)$ lies between two lines t_{q,l_0} and t_{q,l_0+1}

For such k, we have $2k\pi/q_1 > \theta_0$. Since function F_1 is non-decreasing on $[0, \pi]$ for fixed θ_2, we have

$$F_1(\theta_0, 0) = -1/3 \leq F_1(2k\pi/q_1, 0) \leq -1/3 \text{ i.e. } F_1(2k\pi/q_1, 0) = -1/3$$

and

$$F_1(2(l_0+1)\pi/q_1, \pi) \leq F_1(2k\pi/q_1, \pi) \text{ for all } k \in [l_0+1, [q_1/2]].$$

Thus, for $q = (q_1, 0)$

$$\bigcup_{l_0 < k \leq \left[\frac{q_1}{2}\right]} F_1(T_{q,k}) = \left[F_1\left(\frac{2(l_0+1)\pi}{q_1}, \pi\right), -\frac{1}{3}\right]. \tag{III.7}$$

Combining (III.6) and (III.7), we obtain that

$$F_1(V_q) = [-1, F_1(2l_0\pi/q_1, 0)] \cup [F_1(2(l_0+1)\pi/q_1, \pi), -1/3].$$

If $q_1 = 1$, then $V_q = T_{q,0}$, which leads to $F_1(V_q) = F_1(T_{q,0}) = [-1, -2/3]$.

Now let us study the case when $q_2 = 2k_0$ for some nonzero integer k_0 (see Fig. III.18). Note that $(0, -\pi) \in T_{q,k_0}$, thus $-1 = F_1(0, -\pi) \in F_1(T_{q,k_0})$.

If T_{q,k_0} intersects with $\theta_1 = \pi$ at some point (π, θ_2^0), then $F_1(\pi, \theta_2^0) = -1/3$. As a consequence, $F_1(V_q) \supset F_1(T_{q,k_0}) = [-1, -1/3]$ or $F_1(V_q) = [-1, -1/3]$. If T_{q,k_0} intersects with $\theta_2 = \pi$ at (b_0, π), then t_{q,jk_0} intersects with $\theta_2 = -\pi$ and $\theta_2 = \pi$ at $(a_j, -\pi)$ and

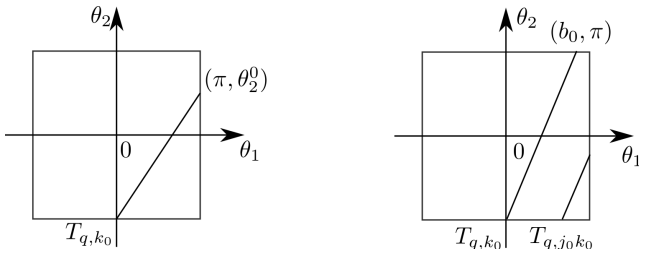

Figure III.18: Different situations occur for even $q_2 = 2k_0$. T_{q,k_0} intersects with $\theta_1 = \pi$ on the left and with $\theta_2 = \pi$ on the right

(b_j, π) accordingly, where $a_j = (j-1)b_0/2$ and $b_j = (j+1)b_0/2$. There exists a smallest $j_0 \in \mathbb{N}, j_0 \geq 2$, such that T_{q,j_0k_0} intersects with both $\theta_2 = -\pi$ at $(a_{j_0}, -\pi)$ and $\theta_1 = \pi$ at (π, θ_2^0). Note that $0 < a_j < a_{j+1} = b_{j-1}$ for all $j \geq 1$, thus according to the second remark,

$$F_1(a_j, -\pi) < F_1(a_{j+1}, -\pi) = F_1(a_{j+1}, \pi) = F_1(b_{j-1}, \pi).$$

We then have

$$\begin{aligned}
&[-1, -1/3] \subset \\
&\subset [-1, F_1(b_0, \pi)] \cup \Big(\bigcup_{1 \leq j < j_0} [F_1(b_{j-1}, \pi), F_1(b_j, \pi)] \Big) \cup [F_1(b_{j_0-1}, \pi), -1/3] \\
&\subset [-1, F_1(b_0, \pi)] \cup \Big(\bigcup_{1 \leq j < j_0} [F_1(a_j, -\pi), F_1(b_j, \pi)] \Big) \cup [F_1(a_{j_0}, -\pi), -1/3] \\
&\subset \bigcup_{0 \leq j \leq j_0} F_1(T_{q,jk_0}) \subset F_1(V_q),
\end{aligned}$$

i.e. $F_1(V_q) = [-1, -1/3]$.

We will now study the last case when q_2 is odd, namely $q_2 = 2k_0 + 1, k_0 \in \mathbb{N}$. Since q_2 is odd, V_q contains neither $(0, \pi)$ nor $(0, -\pi)$, the minimum of $F_1(V_q)$ is some $a \in (-1, -2/3]$ (since $F_1(0, 0) = -2/3$). One should be able to find a on T_{q,k_0} or T_{q,k_0+1} which are closest to $(0, -\pi)$.

If $q_1 = 0$, then $V_q = \{[-\pi, \pi] \times \{-2k\pi/q_2\}, k = 0, \ldots, [q_2/2]\}$. Since $F_1(\theta_1, \theta_2) = F_1(-\theta_1, -\theta_2)$, $F_1(V_q) = \cup_{0 \leq k \leq [q_2/2]} F_1([0, \pi] \times \{2k\pi/q_2\})$. Moreover, function F_1 is non-decreasing on $[0, \pi]$ for fixed θ_2, thus,

$$F_1(V_q) = \cup_{0 \leq k \leq [q_2/2]} [F_1(0, 2k\pi/q_2), F_1(\pi, 2k\pi/q_2)].$$

For $\theta_1 = \pi$, $F_1 \equiv -1/3$. Besides, function $F_1(0, \theta_2)$ is decreasing on $[0, \pi]$, we have

$$F_1(V_q) = \bigcup_{0 \le k \le [q_2/2]} \big[F_1\big(0, 2k\pi/q_2\big), -1/3\big] = \big[F_1\big(0, 2[q_2/2]\pi/q_2\big), -1/3\big].$$

Now we consider the case when $q_1 \neq 0$. Let $k_1 \in \mathbb{N}$ such that function F_1 attains its minimum a on T_{q,k_1}. If T_{q,k_1} intersects with $\theta_1 = \pi$, then we have $[a, -1/3] \subset F_1(T_{q,k_1}) \subset F_1(V_q)$, i.e. $F_1(V_q) = [a, -1/3]$. Otherwise, let $k_2 \in \mathbb{N}$ such that T_{q,k_2} is the most left segment from V_q having nonempty intersection with $\theta_1 = \pi$ (see Fig. III.19).

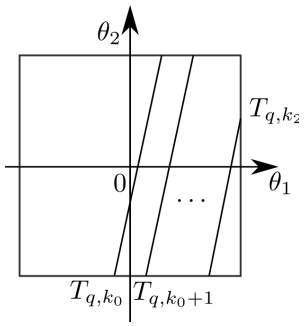

Figure III.19: q_2 is odd and q_1 is nonzero. T_{q,k_2} is the most left segment from V_q having nonempty intersection with $\theta_1 = \pi$

Let $(a_k, -\pi)$ and (b_k, π) be intersection of $t_{q,k}$ with $\theta_2 = -\pi$ and $\theta_2 = \pi$ accordingly. Then,

$$a_{k_0+1} = \frac{\pi}{q_1} \le \frac{(2k_0+1)\pi}{q_1} = b_0 \le b_{k_1},$$

and

$$a_k = \frac{(2k - q_2)\pi}{q_1}, b_k = \frac{(q_2 + 2k)\pi}{q_1},$$

which imply that $0 < a_k \le b_{k-1} < b_k$ for $k \ge k_0 + 1$.

Since function F_1 is non-decreasing on $[0, \pi] \times \{\pi\}$, we have

$$F_1(a_{k_0+1}, -\pi) = F_1(a_{k_0+1}, \pi) \le F_1(b_{k_1}, \pi),$$

and

$$F_1(a_k, -\pi) = F_1(a_k, \pi) \le F_1(b_{k-1}, \pi) \le F_1(b_k, \pi),$$

which makes $[F_1(b_{k-1}, \pi), F_1(b_k, \pi)] \subset [F_1(a_k, -\pi), F_1(b_k, \pi)] \subset F_1(T_{q,k})$ for $k \ge k_0 + 1$. Thus,

$[a, -1/3]$
$= [a, F_1(a_{k_0+1}, -\pi)] \cup [F_1(a_{k_0+1}, -\pi), F_1(b_{k_0+1}, \pi)] \cup$
$\cup (\cup_{k_0+1<k<k_2} [F_1(b_{k-1}, \pi), F_1(b_k, \pi)]) \cup [F_1(b_{k_2-1}, \pi), -1/3]$
$\subset [a, F_1(b_{k_1}, \pi)] \cup F_1(T_{q,k_0+1}) \cup (\cup_{k_0+1<k<k_2} F_1(T_{q,k})) \cup [F_1(a_{k_2}), -1/3] \subset$
$\subset F_1(T_{q,k_1}) \cup (\cup_{k_0+1 \le k \le k_2} F_1(T_{q,k}))$
$\subset F_1(V_q)$
i.e. $F_1(V_q) = [a, -1/3]$.

Minimum value of $F_1(V_q)$ does not exceed $-2/3 = F_1(0, 0)$ in all cases. □

Lemma III.2.2 *If $q_1 \le 1$ and q_2 is odd, then $F_2(V_q) = [-1/3, a]$ for some $a \in [0, 1/3)$. Otherwise, $F_2(V_q) = [-1/3, 1/3]$.*

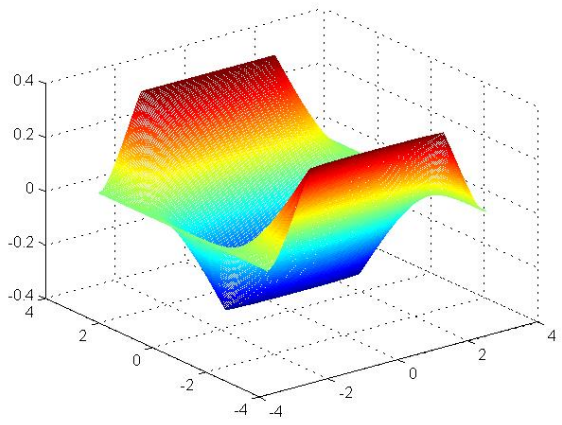

Figure III.20: Graph of function F_2

Proof. If $q_2 \neq 0$ and $\dfrac{q_1}{q_2} \ge \dfrac{\pi}{\theta_0}$ or $q_2 = 0$, then $T_{q,0}$ intersects with $\theta_2 = \pi$ at (θ_1^0, π) for some $\theta_1^0 \in [0, \theta_0]$. Thus, $F_2(T_{q,0}) = [-1/3, 1/3]$, i.e. $F_2(V_q) = [-1/3, 1/3]$.

If $q_2 \neq 0$ and $1 < q_1/q_2 < \pi/\theta_0$, then $T_{q,0}$ and $\theta_2 = \pi$ intersect at (θ_1^0, π) for some $\theta_1^0 \in (\theta_0, \pi)$. Thus, $[-1/3, 0] \subset F_2(T_{q,0})$. Also since $q_1 \ge 2, q_2 \ge 1$, which follows from inequality $1 < q_1/q_2$, we have

$$k_0 := \left[\frac{q_1\theta_0 + q_2\pi}{2\pi}\right] \ge \left[\frac{2\theta_0 + \pi}{2\pi}\right] \ge 1. \tag{III.8}$$

Two lines t_{q,k_0} and $\theta_2 = -\pi$ intersect at $(\theta_1^0, -\pi), \theta_1^0 = \dfrac{-q_2\pi + 2k_0\pi}{q_1}$.

From (III.8) one have

$$k_0 \leq \frac{q_1\theta_0 + q_2\pi}{2\pi} < k_0 + 1,$$

therefore,

$$-\theta_0 < \theta_0 - \frac{2\pi}{2} \leq \theta_0 - \frac{2\pi}{q_1} = \frac{-q_2\pi + q_1\theta_0 + q_2\pi - 2\pi}{q_1} < \frac{-q_2\pi + 2k_0\pi}{q_1},$$

and

$$\frac{-q_2\pi + 2k_0\pi}{q_1} \leq \frac{-q_2\pi + q_1\theta_0 + q_2\pi}{q_1} = \theta_0,$$

i.e. $\theta_1^0 \in [-\theta_0, \theta_0]$ and so $(\theta_1^0, -\pi) \in V_q$. Let $C = (0, \pi), O = (0, 0)$, A, E are intersection points of t_{q,k_0} with two lines $\theta_2 = 0$ and $\theta_2 = \pi$ correspondingly as shown in the Fig. III.21.

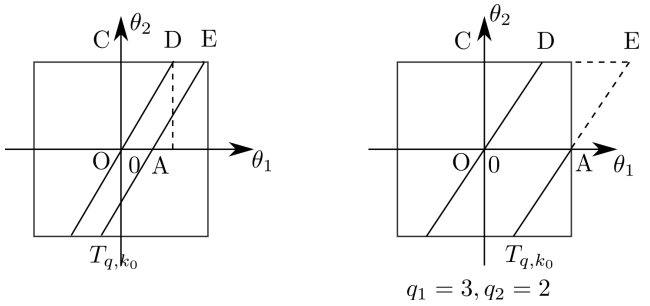

Figure III.21: $q_2 \neq 0$ and $1 < q_1/q_2 < \pi/\theta_0$. On the left $0A \leq \theta_0$ while on the right is one case when $OA > \theta_0$. Here $k_0 = [(q_1\theta_0 + q_2\pi)/2\pi]$

If $OA \leq \theta_0$, then $A \in V_q$ and $F_2(A) = -1/3$. Thus, $[-1/3, 1/3] \subset F_2(T_{q,k_0})$, i.e. $F_2(V_q) = [-1/3, 1/3]$. If $OA > \theta_0$, then $CE = CD + DE = CD + OA > \theta_0 + \theta_0 > \pi$, which means the point E lies outside Brillouin zone B. In this case, T_{q,k_0} intersects with $\theta_1 = \pi$ at (π, θ_2^0) for some $\theta_2^0 \in [-\pi, 0]$, thus $[0, 1/3] = [F_2(\pi, \theta_2^0), F_2(\theta_1^0, -\pi)] \subset F_2(T_{q,k_0})$. We also have that $F_2(V_q) = [-1/3, 1/3]$ since

$$[-1/3, 1/3] = [-1/3, 0] \cup [0, 1/3] \subset F_2(T_{q,0}) \cup F_2(T_{q,k_0}) \subset F_2(V_q).$$

Now we consider the case when $q_2 \neq 0, q_1/q_2 \leq 1$, and $q_1 > 1$. Since

$$\frac{q_2\pi + q_1\theta_0}{2\pi} - \frac{q_2\pi - q_1\theta_0}{2\pi} = \frac{q_1\theta_0}{\pi} \geq \frac{2\theta_0}{\pi} > 1,$$

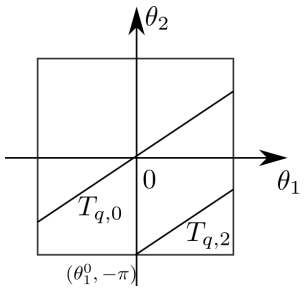

Figure III.22: $T_{q,0}$ and T_{q,k_0} in case $q_1/q_2 \leq 1$ and $q_1 > 1$ (here $p = (2,3), k_0 = 2$)

we can choose an integer k_0 such that

$$0 < \frac{q_2\pi - q_1\theta_0}{2\pi} \leq k_0 \leq \frac{q_2\pi + q_1\theta_0}{2\pi}.$$

For chosen k_0, two lines t_{q,k_0} and $\theta_2 = -\pi$ intersect at the point $(\theta_1^0, -\pi)$ for some $\theta_1^0 \in [-\theta_0, \theta_0]$.

Then $F_2(V_q) = [-1/3, 1/3]$ because

$$[-1/3, 1/3] = [-1/3, 0] \cup [0, 1/3] \subset F_2(T_{q,0}) \cup F_2(T_{q,k_0}) \subset F_2(V_q).$$

The only case left to be considered is $q_1 \leq 1$ and $q_2 \neq 0$.

If $q_1 = 0$ and q_2 is even, the interval $T_{q,[q_2/2]}$ concides with $[-\pi, \pi] \times \{\pi\}$, so

$$[-1/3, 1/3] = [-1/3, 0] \cup [0, 1/3] \subset F_2(T_{q,0}) \cup F_2(T_{q,[q_2/2]}) \subset F_2(V_q).$$

If $q_1 = 0$ and q_2 is odd, namely $q_2 = 2k_0 + 1, k_0 \in \mathbb{N}$, V_q does not intersect with $\theta_2 = \pm\pi$, thus $a := \max F_3(V_q) \in [0, 1/3)$.

Let $k \in \mathbb{N}$ such that $a \in F_2(T_{q,k})$. One would expect that $k = k_0$ which makes $t_{q,k}$ be closest to $\theta_2 = -\pi$. We have $[0, a] \subset F_2(T_{q,k})$, therefore

$$[-1/3, 0] \cup [0, a] \subset F_2(T_{q,0}) \cup F_2(T_{q,k}) \subset F_2(V_q) \text{ i.e. } F_2(V_q) = [-1/3, a].$$

If $q_1 = 1$ and $q_2 \neq 0$ even, i.e. $q_2 = 2k_0$ for some $k_0 \in \mathbb{N}, k_0 > 0$, then $F_2(T_{q,k_0}) = [0, 1/3]$.

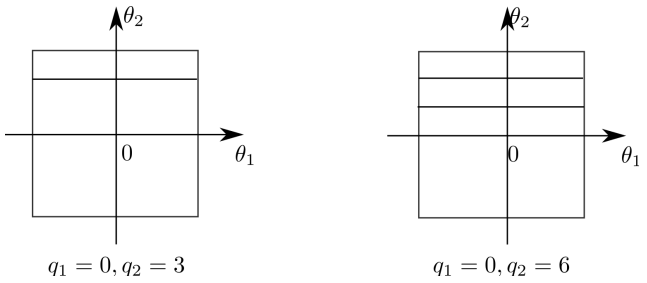

Figure III.23: Different cases occur when $q_1 = 0$. On the left q_2 is odd and on the right q_2 is even

As a consequence,

$$[-1/3, 1/3] = [-1/3, 0] \cup [0, 1/3] \subset F_2(T_{q,0}) \cup F_2(T_{q,k_0}) \subset F_2(V_q),$$

which means that $F_2(V_q) = [-1/3, 1/3]$.

If $q_1 = 1$ and q_2 is odd, namely, $q_2 = 2k_0 + 1, k_0 \in \mathbb{N}$, V_q again does not contains any point from $[-\theta_0, \theta_0] \times \{\pm\pi\}$, so $a := \max F_2(V_q) \in [0, 1/3)$. Let $k \in \mathbb{N}$ such that $a \in F_2(T_{q,k})$, since $(2k_0 + 1)(\pm\pi) \neq \theta_1 - 2k\pi$ for $\theta_1 \neq \pm\pi$, $T_{q,k}$ intersects with $\theta_1 = \pm\pi$, and so $[0, a] \subset F_2(V_q)$.

As a consequence,

$$[-1/3, a] = [-1/3, 0] \cup [0, a] \subset F_2(T_{q,0}) \cup F_2(T_{q,k}) \subset F_2(V_q).$$

Thus, $F_2(V_q) = [-1/3, a]$ for $a \in [0, 1/3)$. □

Lemma III.2.3 *If $q_2 = 0$ and $q_1 > 1$, then*

$$F_3(V_q) = [1/3, F_3(2(l_0 + 1)\pi/q_1, 0)] \cup [F_3(2l_0\pi/q_1, \pi), 1].$$

If $q_2 = 0$ and $q_1 = 1$ then $F_3(V_q) = [2/3, 1]$.

Otherwise $F_3(V_q) = [1/3, 1]$.

Proof. In this proof we will need the following remarks:

i. For fixed θ_2^0, function $F_3(\theta_1, \theta_2^0)$ is non-increasing on $[0, \pi]$.

ii. For fixed θ_1^0, function $F_3(\theta_1^0, \theta_2)$ is decreasing on $[0, \pi]$.

These claims can be justified using the same argument as in Lemma III.2.1.

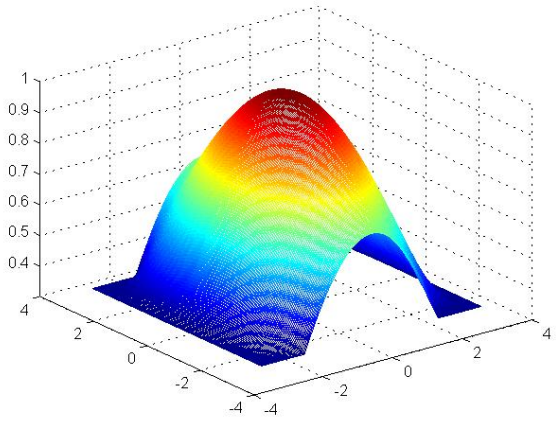

Figure III.24: Graph of function F_3

Note that function F_3 always attains its maximum at $(0, 0)$.

If $q_2 = 0$, then

$$V_q = \{\{2k\pi/q_1\} \times [-\pi, \pi], 0 \le k \le [q_1/2]\}.$$

Since $F_3(\theta_1, \theta_2) = F_3(\theta_1, -\theta_2)$, we have

$$F_3(V_q) = F_3(\{\{2k\pi/q_1\} \times [0, \pi], 0 \le k \le [q_1/2]\}).$$

Thus, according to the last remark,

$$F_3(V_q) = \bigcup_{0 \le k \le [q_1/2]} [F_3(2k\pi/q_1, \pi), F_3(2k\pi/q_1, 0)].$$

For all k such that $0 \le k \le l_0 = [q_1\theta_0/2\pi]$, we have

i. $F_3(T_{q,0}) = [2/3, 1]$,

ii. $F_3(2l_0\pi/q_1, \pi) \le F_3(2k\pi/q_1, \pi) < 2/3 = F_3(0, \pi)$ according to the first remark,

iii. $2/3 = F_3(\theta_0, 0) \le F_3(2k\pi/q_1, 0)$.

Therefore,

$$\bigcup_{0 \le k \le l_0} F_3(T_{q,k}) = [F_3(2l_0\pi/q_1, \pi), 1]. \tag{III.9}$$

From Lemma III.2.1 we know that when $q_1 > 1$ there must be some $k \in (l_0, [q_1/2]]$. For

these k, we have $\theta_0 < 2k\pi/q_1 \leq \pi$, which implies $1/3 = F_3(\pi,\pi) \leq F_3(2k\pi/q_1,\pi) \leq F_3(\theta_0,\pi) = 1/3$ or $F_3(2k\pi/q_1,\pi) = 1/3$. Besides, $F_3(2k\pi/q_1,0) \leq F_3(2(l_0+1)\pi/q_1,0)$ from the first remark. Thus,

$$\bigcup_{l_0<k\leq\left[\frac{q_1}{2}\right]} \left[\frac{1}{3}, F_3\left(\frac{2k\pi}{q_1},0\right)\right] = \left[\frac{1}{3}, F_3\left(\frac{2(l_0+1)\pi}{q_1},0\right)\right]. \tag{III.10}$$

Combining equations (III.9) and (III.10), we obtain that

$$F_3(V_q) = [1/3, F_3(2(l_0+1)\pi/q_1,0)] \cup [F_3(2l_0\pi/q_1,\pi),1].$$

In case $q_1 = 1$, $V_q = T_{q,0}$, and so $F_3(V_q) = [2/3,1]$.

Now we consider the case when $q_2 \neq 0$.

If the slope q_1/q_2 of $t_{q,k}$ is less or equal than π/θ_0, then the interval $T_{q,0}$ intersects either with the line $\theta_1 = \pi$ at (π,θ_2^0) for some $\theta_2 \in [0,\pi]$ or with the line $\theta_2 = \pi$ at (θ_1^0,π) for some $\theta_1^0 \geq \theta_0$ (see Fig. III.25). Since $F_3(\theta_1^0,\pi) = F_3(\pi,\theta_2^0) = 1/3$, the range of F_3 restricted to $T_{q,0}$ is $[1/3,1]$, and thus $F_3(V_p) = [1/3,1]$.

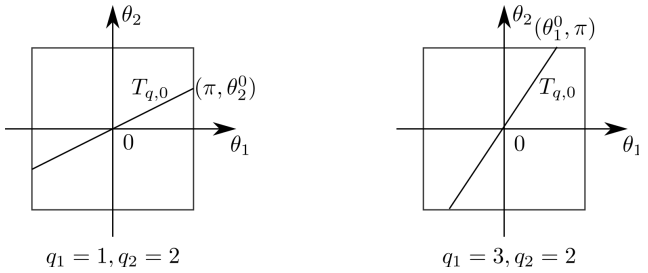

Figure III.25: q_2 is nonzero and $q_1/q_2 \leq \pi/\theta_0$. On the left $T_{q,0}$ intersects with $\theta_1 = \pi$ and on the right it intersects with $\theta_2 = \pi$ at (θ_1^0,π) where $\theta_1^0 > \theta_0$

If q_1/q_2 is larger than π/θ_0, then the interval $T_{q,0}$ intersects with the line $\theta_2 = \pi$ at (θ_1^0,π), where $0 < \theta_1^0 < \theta_0$. Thus $F_3(T_{q,0})$, and thus, $F_3(V_q)$, contain $[a,1]$ for $a = F_3(\theta_1^0,\pi) \in (F_3(\theta_0,\pi), F_3(0,\pi)) = (1/3, 2/3)$ according to the first remark.

In case $q_1 \geq 4$ and $q_2 > 1$, let $k_0 = \left[\frac{q_1\theta_0}{2\pi}\right]$, then

$$k_0 \leq \frac{q_1\theta_0}{2\pi} < k_0 + 1.$$

Two lines t_{q,k_0} and $\theta_2 = 0$ intersect at $(2k_0\pi/q_1, 0)$. Since

$$0 \leq \frac{2k_0\pi}{q_1} \leq \theta_0,$$

according to the first remark, we have

$$b := F_3\left(\frac{2k_0\pi}{q_1}, 0\right) > \frac{2}{3}.$$

Two lines t_{q,k_0} and $\theta_2 = \pi$ intersect at the point $((q_2 + 2k_0)\pi/q_1, \pi)$. Since

$$\theta_0 < \frac{2(1+k_0)\pi}{q_1} = \frac{(2k_0+2)\pi}{q_1} \leq \frac{(q_2+2k_0)\pi}{q_1},$$

the interval T_{q,k_0} intersects either with the line $\theta_2 = \pi$ at (θ_1^0, π) for some $\theta_0 < \theta_1^0 < \pi$ or with the line $\theta_1 = \pi$ at (π, θ_2^0) for some $\theta_2^0 \in [0, \pi]$ (see Fig. III.26).

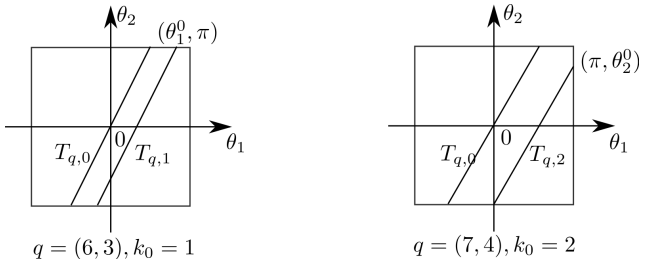

Figure III.26: $T_{q,0}$ and T_{q,k_0} in different cases for $q_1/q_2 > \pi/\theta_0$ and $q_1 \geq 4, q_2 > 1$. On the left T_{q,k_0} intersects with $\theta_2 = \pi$ at (θ_1^0, π) for $\theta_1^0 > \theta_0$ while on the right T_{q,k_0} intersects with $\theta_1 = \pi$

In both cases,

$$[1/3, 1] = [1/3, b] \cup [a, 1] \subset F_3(T_{q,k_0}) \cup F_3(T_{q,0}) \subset F_3(V_q),$$

i.e. $F_3(V_q) = [1/3, 1]$.

Now one need to consider the case when $q_1 \geq 4$ and $q_2 = 1$ or $q_1 < 4$ and $q_1/q_2 > \pi/\theta_0$. Note that for $q_1 < 4$, since $q_1/q_2 > \pi/\theta_0$, q_2 can be 1 and $q_1 > 1$. Thus, it is enough to study the range of function F_3 restricted to V_q for $q = (q_1, 1)$ with $q_1 > 1$.

For each $k \in \mathbb{N}, k > 0$, the line $t_{q,k}$ intersects with $\theta_2 = -\pi$ at $((2k-1)\pi/q_1, -\pi)$ and with $\theta_2 = \pi$ at $((2k+1)\pi/q_1, \pi)$. When both intersection points are in V_q, we have

$[b_k, a_k] \subset F_3(T_{q,k})$, where

$$a_k := F_3\left(\frac{(2k-1)\pi}{q_1}, -\pi\right), b_k := F_3\left(\frac{(2k+1)\pi}{q_1}, \pi\right).$$

On the other hand,

$$F_3\left(\frac{(2k+1)\pi}{q_1}, \pi\right) = F_3\left(\frac{(2k+1)\pi}{q_1}, -\pi\right), \text{ i.e. } a_{k+1} = b_k.$$

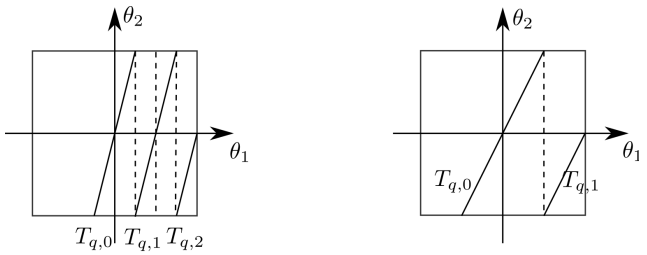

Figure III.27: $T_{q,k}$ for $k = \overline{0, k_0}$ in different cases when $q_1 > 1, q_2 = 1$

Besides, $[b_0, 1] \subset F_3(T_{q,0})$ and there must be some k_0 such that t_{q,k_0} intersects with $\theta_1 = \pi$ inside V_q, i.e. $[1/3, a_{[q_1/2]}] \subset F_3(T_{q,k_0})$. Therefore,

$$[1/3, 1] = \bigcup_{0 \le k < k_0} [b_k, a_k] \cup [b_0, 1] \cup [1/3, a_{k_0}] \subset \bigcup_{0 \le k \le k_0} F_3(T_{q,k}),$$

so $F_3(V_q) = [1/3, 1]$. □

CHAPTER IV

SPECTRAL EDGE NON-DEGENERACY

There are quite a few features (called *threshold properties*) of elliptic periodic operators that depend upon spectral behavior near spectral edges (see [37]). Below, we state an open conjecture about some spectral edge properties. We then sketch the approach that we have used to attack this conjecture and a partial result obtained.

Consider the periodic Schrödinger operator $H_V = -\Delta + V(x)$ on $\mathbb{R}^n$ for $n \geq 2$, where the potential $V(x)$ is real-valued and $\mathbb{Z}^n$-periodic, i.e. $V(x) = V(x+e)$ for all $e \in \mathbb{Z}^n$. For each quasimomentum $\theta \in \mathbb{R}^n$, we define the Bloch operator $H_V(\theta) = (-i\nabla + \theta)^2 + V(x)$ acting on the torus $\mathbb{T}^n = \mathbb{R}^n/\mathbb{Z}^n$. The spectrum of the operator $H_V(\theta)$ is real and discrete:

$$\sigma(H_V(\theta)) = \{\lambda_j(\theta, V)/\lambda_1(\theta, V) \leq \ldots \leq \lambda_m(\theta, V) \leq \ldots \to \infty\}.$$

By Floquet-Bloch theory (see Section I.2), $H_V = \int_B^{\oplus} H_V(\theta)d\theta$ for $B = [-\pi, \pi)^n$. As a consequence,

$$\sigma(H_V) = \bigcup_{\theta \in B} \sigma(H_V(\theta)). \tag{IV.1}$$

Let us recall that multi-valued function $\theta \mapsto (\lambda_1(\theta), \lambda_2(\theta), \ldots)$ is called the dispersion relation of H_V. Each function $\theta \mapsto \lambda_j(\theta), j = 1, 2, \ldots$, is called the j-th band function and its extrema - spectral edges. The following can occur at a spectral edge value λ_0 (of the band function $\lambda_j(\theta)$ at θ^0):

1. The extremum λ_0 is not simple, i.e. is attained by more than one band function.

2. The extremum λ_0 of a single band function is non-isolated, i.e. in every neighborhood U of θ^0 there exists $\theta' \neq \theta^0$ such that $\lambda_j(\theta') = \lambda_0$.

3. The extremum is isolated, but degenerate, i.e. the determinant of the Hessian matrix $(\frac{\partial^n \lambda_j}{\partial\theta_{i_1}\ldots\partial\theta_{i_n}})_{i_1,\ldots,i_n=1}^n$ at θ^0 is zero.

The following conjecture [58] is believed to be true.

Conjecture IV.0.1. *The dispersion relation of a generic periodic Schrödinger operator has only single, isolated, and non-degenerate extrema.*

The notion of "genericity" has not been defined precisely. However, one can understand the conjecture as follows: "*The set of all periodic potentials such that the related Schrödinger*

operators have only simple, isolated, and non-degenerate extrema is a residual set[1] *in an appropriate space of periodic functions.*"

The conjecture is often assumed in mathematics and physics literature [37, Section 7] (e.g., in studying homogenization, Green's function asymptotics, Liouville type theorems, Anderson localization, in defining effective masses in solid state physics).

The result of [34] establishes that the extrema of the dispersion relation of a generic periodic Schrödinger operator are simple. Recently Filonov and Kackovskii have proven [21] that the extrema of the dispersion relation of a generic periodic 2D Schrödinger operator are isolated. In this chapter, we are only interested in the non-degeneracy aspect and assume, due to [34], that the extrema under consideration are simple.

In what follows, we prove the conjecture for periodic difference operators on a class of discrete (combinatorial) graphs. To be specific, we consider periodic combinatorial graphs (see Section I.2). There is a free action on the graph of the group $\mathbb{Z}^2$ by the shifts through vectors $p_1e_1 + p_2e_2$, where $(p_1, p_2) \in \mathbb{Z}^2$ and (e_1, e_2) is a basis of $\mathbb{R}^2$. There are two vertices in the fundamental domain W of the graph as shown in Fig. IV.1.

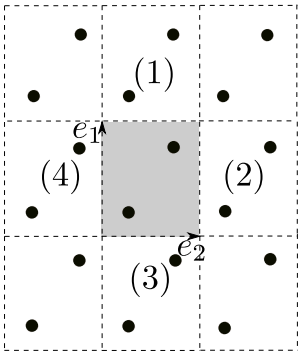

Figure IV.1: There are 2 vertices (atoms) in the fundamental domain

Vertices from W are allowed to connect to each other or to vertices from shifted copies having common boundary edges with W (i.e. copies(1), (2), (3), (4) shown in Fig. IV.1). No loops or multiple edges are allowed. Graphene [22] is one example in this class of graphs.

Each graph is equipped with a periodic weight function that assigns to each edge a positive number. We study Laplacian operators on these graphs and prove that the dispersion

[1] A residual set is the intersection of a countable collection of open, dense sets.

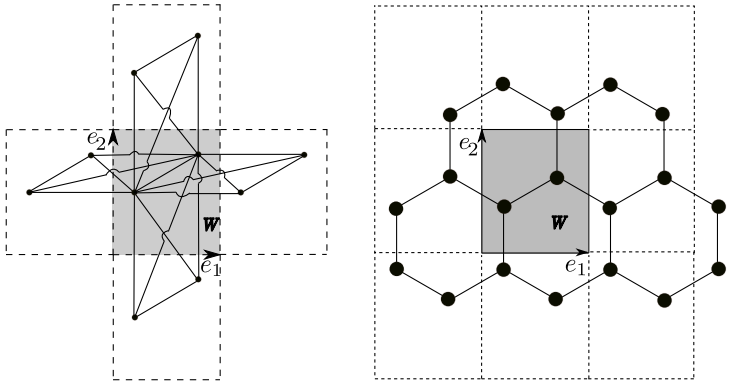

Figure IV.2: Left: vertices from W are connected to each other or to vertices from shifted copies (1), (2), (3), (4); Right: graphene - an example of graphs under consideration

relation of such a generic (with respect to the weights) Laplacian has only non-degenerate extrema.

A zero weight on an edge can be considered to be equivalent to the removal of the edge. Thus, for convenience, graph under consideration can be thought of as a graph with all possible edges presenting to which non-negative constant weights are assigned. From now on, we study the periodic discrete graph G with shaded fundamental domain W as shown in Fig. IV.3. The fundamental domain W contains two vertices C, D and nine edges.

Let us denote the set of non-negative real numbers by $\mathbb{R}_0^+$. Given $\alpha = (\alpha_1, \ldots, \alpha_9) \in (\mathbb{R}_0^+)^9$, we can assign the weights $\alpha_i, i = \overline{1,9}$, to nine edges from the fundamental domain W as shown in Fig. IV.3. The entire structure G and all edges' weights can be obtained from W by $\mathbb{Z}^2$-shifts of the fundamental domain. We can now define a Laplace-Beltrami operator L_α acting on the graph G as follows

$$L_\alpha f(u) = \sum_{e=(u,v)\in E(G)} \alpha(e)(f(u) - f(v)), \tag{IV.2}$$

where $\alpha(e)$ is the weight of edge e. When it does not lead to confusion, we will use the notation L instead of L_α.

For each $\theta = (\theta_1, \theta_2)$ from the Brillouin zone $B = [-\pi, \pi)^2$, let $L(\theta)$ be the Bloch Laplacian

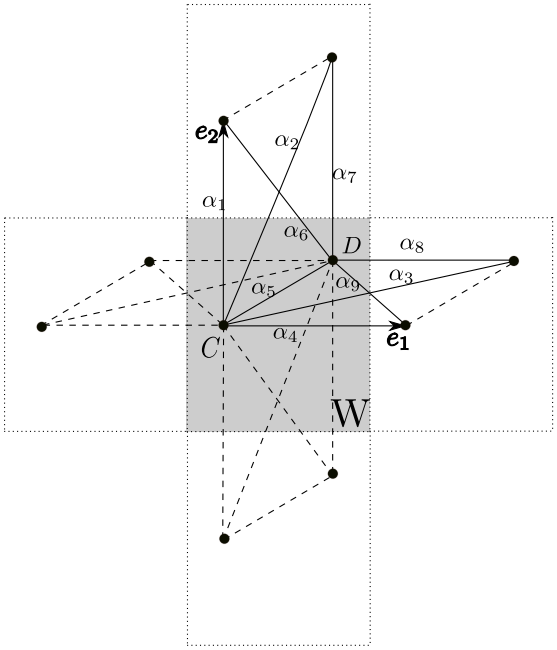

Figure IV.3: The structure G and a fundamental domain W with vertices (atoms) C, D and nine edges

that acts as (IV.2) on the set of functions defined on G and satisfying the Floquet condition

$$f(u + p_1e_1 + p_2e_2) = f(u)e^{i(p_1\theta_1+p_2\theta_2)}$$

for all $(p_1, p_2) \in \mathbb{Z}^2$ and all $u \in V(G)$. Such functions f are determined uniquely by their restrictions to the fundamental domain W. The Laplacian L is decomposed into the direct integral

$$L = \int_B^{\oplus} L(\theta)d\theta.$$

In particular, $\sigma(L) = \bigcup_{\theta\in B} \sigma(L(\theta))$.

Since there are only two vertices inside the fundamental domain, operator $L(\theta), \theta \in B$, acts in 2D and thus has a spectrum $\sigma(L(\theta)) = \{\lambda_1(\theta), \lambda_2(\theta)\}$, where $\lambda_1(\theta) \le \lambda_2(\theta)$.

Below we specify our notion of "genericity."

Definition IV.0.2. *It is said that a generic operator* $\{L_\alpha, \alpha \in (\mathbb{R}_0^+)^9\}$ *has a property* ι

if the set of α such that L_α does not have property ι is a semi-algebraic subset of positive codimension in $(\mathbb{R}_0^+)^9$.

Our main result is the following theorem:

Theorem IV.0.3. *The dispersion relation of the operator L_α, for a generic $\alpha \in (\mathbb{R}_0^+)^9$, has only non-degenerate extrema.*

Proof. Instead of $\theta \in B$, it is more convenient to consider the pair $z = (z_1, z_2) := (e^{i\theta_1}, e^{i\theta_2})$ of *Floquet multipliers*. Notice that:

$$\frac{\partial \lambda}{\partial \theta_j} = ie^{i\theta_j} \frac{\partial \lambda}{\partial z_j}, j = \overline{1,2}, \tag{IV.3}$$

and

$$\frac{\partial^2 \lambda}{\partial \theta_1^2} \frac{\partial^2 \lambda}{\partial \theta_2^2} - \left(\frac{\partial^2 \lambda}{\partial \theta_1 \partial \theta_2} \right)^2 = e^{2i(\theta_1+\theta_2)} \left[\frac{\partial^2 \lambda}{\partial z_1^2} \frac{\partial^2 \lambda}{\partial z_2^2} - \left(\frac{\partial^2 \lambda}{\partial z_1 \partial z_2} \right)^2 \right]. \tag{IV.4}$$

For each $z \in \mathbb{T} = \{(z_1, z_2) : |z_1| = |z_2| = 1\}$, we denote by $\Lambda_\alpha(z)$ the operator that acts as (IV.2) on the set of functions defined on G and satisfying condition

$$f(u + p_1 e_1 + p_2 e_2) = z_1^{p_1} z_2^{p_2} f(u).$$

Then, the spectrum $\sigma(\Lambda_\alpha(z))$ of $\Lambda_\alpha(z)$ coincides with $\sigma(L_\alpha(\theta))$ for $\theta \in B$ such that $(z_1, z_2) = (e^{i\theta_1}, e^{i\theta_2})$.

From (IV.3) and (IV.4), the dispersion relation of L_α has a degenerate extremum if and only if there exists $z = (z_1, z_2) \in \mathbb{T}$ and $\lambda \in \mathbb{R}$ such that $\lambda \in \sigma(\Lambda_\alpha(z))$,

$$\frac{\partial \lambda}{\partial z_j} = 0, j = \overline{1,2}, \tag{IV.5}$$

and

$$\frac{\partial^2 \lambda}{\partial z_1^2} \frac{\partial^2 \lambda}{\partial z_2^2} - \left(\frac{\partial^2 \lambda}{\partial z_1 \partial z_2} \right)^2 = 0 \tag{IV.6}$$

By P we denote the set of $(\alpha_1, \ldots, \alpha_9, \lambda, z_1, z_2) \in \mathbb{C}^{12}$ intersecting with $\mathbb{T}$ such that $\lambda \in \sigma(\Lambda_\alpha(z))$ satisfying (IV.5) and (IV.6). Let us sketch the proof of the theorem, which consists of three steps:

1. Obtain an algebraic variety $\mathbb{P}$ that contains P.
2. Show that all components of $\mathbb{P}$ having non-empty intersections with P are of dimension at most 8.

3. Prove that by projecting these components to $\mathbb{C}^9$ that contains the weight parameters space $(\mathbb{R}_0^+)^9$, we get a semi-algebraic subset of positive codimention in $\mathbb{C}^9$, which implies the desired result.

The two dimensional operator $\Lambda_\alpha(z)$ acts as follows

$$
\begin{aligned}
&(\Lambda_\alpha(z)f)(C)\\
&= \alpha_1(f(C) - f(C)z_2) + \alpha_2(f(C) - f(D)z_2) + \alpha_5(f(C) - f(D))\\
&+\alpha_3(f(C) - f(D)z_1) + \alpha_4(f(C) - f(C)z_1) + \alpha_1(f(C) - f(C)z_2^{-1})\\
&+\alpha_6(f(C) - f(D)z_2^{-1}) + \alpha_4(f(C) - f(C)z_1^{-1}) + \alpha_9(f(C) - f(D)z_1^{-1}),\\
&\text{and}\\
&(\Lambda_\alpha(\theta)f)(D)\\
&= \alpha_6(f(D) - f(C)z_2) + \alpha_7(f(D) - f(D)z_2) + \alpha_8(f(D) - f(D)z_1)\\
&+\alpha_9(f(D) - f(C)z_1) + \alpha_5(f(D) - f(C)) + \alpha_7(f(D) - f(D)z_2^{-1})\\
&+\alpha_2(f(D) - f(C)z_2^{-1}) + \alpha_3(f(D) - f(C)z_1^{-1}) + \alpha_8(f(D) - f(D)z_1^{-1}).
\end{aligned}
$$

Let $A_\alpha(z) = (a_{ij})_{i,j=1}^2$ be the matrix of the operator $\Lambda_\alpha(z)$. Then,

$$
\begin{aligned}
a_{11} &= 2\alpha_1 + \alpha_2 + \alpha_3 + 2\alpha_4 + \alpha_5 + \alpha_6 + \alpha_9 - \alpha_1(z_2 + z_2^{-1}) - \alpha_4(z_1 + z_1^{-1}),\\
a_{12} &= -(\alpha_2 z_2 + \alpha_6 z_2^{-1} + \alpha_3 z_1 + \alpha_9 z_1^{-1} + \alpha_5),\\
a_{21} &= -(\alpha_2 z_2^{-1} + \alpha_3 z_1^{-1} + \alpha_6 z_2 + \alpha_9 z_1 + \alpha_5),\\
a_{22} &= \alpha_6 + 2\alpha_7 + 2\alpha_8 + \alpha_9 + \alpha_5 + \alpha_2 + \alpha_3 - \alpha_7(z_2 + z_2^{-1}) - \alpha_8(z_1 + z_1^{-1})
\end{aligned}
$$

As a consequence, the spectrum of $\Lambda_\alpha(z)$ is the set of eigenvalues of matrix $A_\alpha(z)$. Like before, when it does not lead to the confusion, we will use the notation $A(z)$ instead of $A_\alpha(z)$. Then, λ belongs to the spectrum of $\Lambda(z)$ if and only if

$$\lambda^2 - \lambda TrA(z) + \det A(z) = 0. \tag{IV.7}$$

Differentiating (IV.7) with respect to $z_j, j = \overline{1,2}$, and combining the results with (IV.5) and (IV.6), we have

$$\lambda\frac{\partial(TrA)}{\partial z_j} - \frac{\partial(\det A)}{\partial z_j} = 0, j = \overline{1,2}, \tag{IV.8}$$

and

$$(2\lambda - TrA)^2 . \left(\frac{\partial^2 \lambda}{\partial z_1^2} \frac{\partial^2 \lambda}{\partial z_2^2} - \left(\frac{\partial^2 \lambda}{\partial z_1 \partial z_2} \right)^2 \right) = \left(\lambda \frac{\partial^2 (TrA)}{\partial z_1^2} - \frac{\partial^2 (\det A)}{\partial z_1^2} \right) . \left(\lambda \frac{\partial^2 (TrA)}{\partial z_2^2} - \frac{\partial^2 (\det A)}{\partial z_2^2} \right) - - \left(\lambda \frac{\partial^2 (TrA)}{\partial z_1 \partial z_2} - \frac{\partial^2 (\det A)}{\partial z_1 \partial z_2} \right)^2 . \tag{IV.9}$$

The left-hand side of identity (IV.9) is equal to zero according to (IV.6). Thus, we have

$$\left(\lambda \frac{\partial^2 (TrA)}{\partial z_1^2} - \frac{\partial^2 (\det A)}{\partial z_1^2} \right) . \left(\lambda \frac{\partial^2 (TrA)}{\partial z_2^2} - \frac{\partial^2 (\det A)}{\partial z_2^2} \right) - - \left(\lambda \frac{\partial^2 (TrA)}{\partial z_1 \partial z_2} - \frac{\partial^2 (\det A)}{\partial z_1 \partial z_2} \right)^2 = 0. \tag{IV.10}$$

Thus, the dispersion relation of Laplacian L have degenerate extremum only if system of equations (IV.7), (IV.8), and (IV.10) in variables λ, z_1, z_2 has solution such that λ is real and $(z_1, z_2) \in \mathbb{T}$. The left hand sides of equations (IV.7), (IV.8), and (IV.10) are rational functions in variables $\alpha_1, \ldots, \alpha_9, \lambda, z_1, z_2$, denominators of which are of the form $z_1^{n_1} z_2^{n_2}$ for some $n_1, n_2 \in \mathbb{N}$. Let $(\alpha_1, \ldots, \alpha_9, \lambda, z_1, z_2) \in V := \mathbb{C}^{12}$ and $\mathbb{P}$ be the algebraic variety (the joint zero set) of the polynomials-numerators of (IV.7), (IV.8), and (IV.10). Then, $P = \mathbb{P} \cap \mathbb{T}$. Consider the space $S := \mathbb{C}^9$ of weight parameters $(\alpha_1, \ldots, \alpha_9)$. Let $\pi : V \to S$ be the natural projection that omits coordinates λ, z_1, z_2.

We will prove that $\pi(P)$ has codimension at least 1 in S. We first need to explore some properties of $\mathbb{P}$.

Lemma IV.0.4. *The dimensions of all components of $\mathbb{P}$ having non-empty intersections with P in V are at most 8.*

This result is obtained by Bertini$^{\text{TM}}$software [5]. The algebraic variety $\mathbb{P}$ is decomposed into union of smooth manifolds of different dimensions. According to our computation, the components that have non-empty intersections with the torus $\mathbb{T}$ are of dimensions at most 8.

The dimensions of the projections of these components to the weight parameters space S are also at most 8. Indeed, let O be an arbitrary point from a component of $\mathbb{P}$ that has non-empty intersection with P. Let us denote the dimension of the component containing

O by m, then $m \leq 8$. There exists a smooth submersion

$$f := u \in U \subset \mathbb{C}^m \mapsto (f_1, \ldots, f_{12}) \in V_O \subset V,$$

where V_O is a neighborhood of O in V, such that $\alpha_j = f_j, j = \overline{1,9}, \lambda = f_{10}, z_1 = f_{11}$, and $z_2 = f_{12}$. The projection of V_O to S is $\{(f_1(u), \ldots, f_9(u)), u \in V_O\}$, and thus has dimension at most 8. Therefore, the projections of those components of $\mathbb{P}$ having non-empty intersections with P has positive codimension in the ambient space S.

On the other hand, the set P is defined by polynomial equations and inequalities. By Tarski - Seidenberg theorem (see, e.g., [8, 24]), its projection down to the weight parameters space $(\mathbb{R}_0^+)^9$ is also defined by polynomial equations and inequalities, i.e. is a semi-algebraic set. □

CHAPTER V

GAP OPENING

Existence of spectral gaps attracts a lot of interests in many fields ranging from solid state physics to photonic crystal theory, waveguides, expanders and Ramanujan graphs, and quantum wire circuits [3, 30, 43, 42, 18, 52], [7, Section 5.1], [37, Section 6.1].

One of the standard ways to achieve the band-gap structure of the spectrum is by making the medium periodic, where the gaps may arise due to the Bragg scattering [3]. However, existence of spectral gaps in periodic media is not guaranteed and is not easy to achieve and manipulate (see, e.g., [37, Section 6.1]). Thus, a different, resonant gaps technique has been explored, where identical resonators are distributed throughout the medium to create spectral gaps [50]. This idea was implemented in the discrete situation in [1] by attaching to each vertex v of the graph Γ_0 (which is the medium in this case) an identical *decoration* (resonator) G (Fig. V.1).

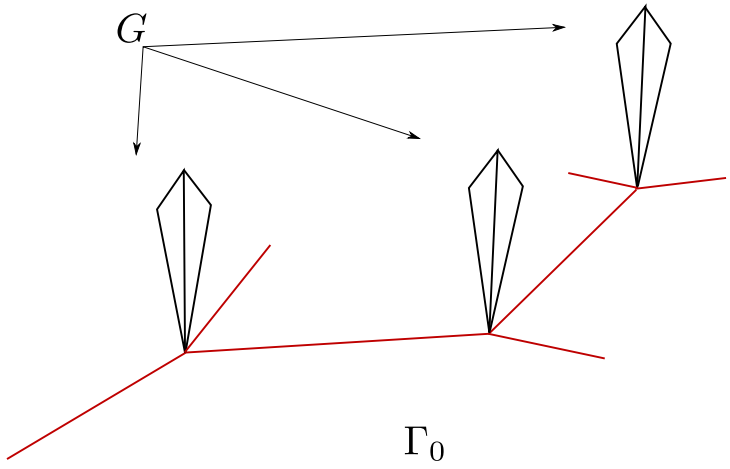

Figure V.1: Decorations used by Schenker and Aizenman in [1].

This technique has been extended to the case of quantum graphs, see [7, Section 5.1]. However, it would be desirable in many instances (e.g., in photonic crystal theory) to insert some internal structure into each vertex, rather than attach a decoration (resonator) to Γ_0 sideways. In other words, one is looking for a *spider decoration* (Fig. V.2)[1].

[1]Compare with the first step of the zig-zag construction of an expander [52].

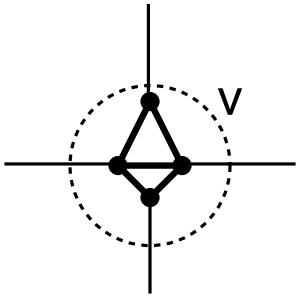

Figure V.2: A "spider" decoration replacing a vertex V.

Here one hits a snag. The nice procedure in [1] does not work nearly that well when the common "boundary" between Γ and G consists of more than one point, as in the case of a "spider" decoration.

When the boundary is a single point, by applying a rather standard technique used in considering the transmission problem between two media, one can rewrite the spectral problem on the decorated graph as the one on the original graph Γ with an additional energy (spectral parameter) dependent potential (*Dirichlet-to-Neumann operator* of the decoration, see [7, Section 5.1] for details). Poles of this potential arise at the spectrum of the decoration, which leads to the gap opening.

With the boundary consisting of more than one point, the arising potential term is now a meromorphic matrix function, whose poles may or may not show up, depending on the vector the matrix function is applied to. Some examples of spider decorations not leading to spectral gap opening were constructed in [47, Chapter 3]. On the other hand, it is also shown in [47, Chapter 3] that some special decorations do lead to gap openings.

In what follows, we will extend the result of [47]. We provide necessary notions and notations as well as some auxiliary results in Section V.1, and the main result on gap opening in Section V.2.

V.1 Preliminary results

In what follows, we consider only infinite periodic metric graph Γ_0 (see Section I.2). Let us also assume that Γ_0 is a d-regular graph (i.e. the degree of each vertex is equal to d), G is a finite metric graph with at least d vertices and a singled out subset $B \subset V(G)$ consisting of d vertices. The set B will be called the *boundary* of G. For each vertex $v \subset V(\Gamma_0)$ we establish a 1-to-1 correspondence between the edges adjacent to v and the elements of B. One can now decorate in a natural way the vertex v with the internal structure, which is

a copy of G (see again Fig. V.2). Doing this for all vertices of Γ_0, we obtain the *decorated graph* Γ.

We now introduce differential operators H_0 in $L^2(\Gamma_0)$ and H in $L^2(\Gamma)$ as follows: on each edge they act as $-d^2/dx^2$ with the domain consisting of functions f such that

1. $f \in H^2(e)$ for each edge e;
2. $\sum\limits_e \|f\|^2_{H^2(e)} < \infty$;
3. f is continuous on the whole graph;
4. at each vertex, the sum of the outgoing derivatives of f along all adjacent edges is equal to zero (Kirchhoff condition).

Here, $H^2(e)$ is the standard Sobolev space on the segment $e = [0, l_e]$.

We also denote by H_G the analogous operator on G, with the exception that at the boundary vertices $v \in B$ of the boundary, Dirichlet conditions $f(v) = 0$ are imposed instead of Kirchhoff ones. The spectrum $\sigma(H_G)$ of this operator is discrete [7, Theorem 3.1.1]. All defined operators H_0, H, and H_G are self-adjoint [7, Section 1.4.4].

We denote by Σ_D the discrete set of Dirichlet eigenvalues of all edges of Γ_0, i.e. $\Sigma_D := \{(n\pi l_e^{-1})^2, n \in \mathbb{N}, e \in E(\Gamma_0)\}$.

Let us also denote by $N : \bigoplus\limits_{e\in E(G)} H^2(e) \to l^2(B)$ the *Neumann* operator that for any function $f \in \bigoplus\limits_{e\in E(G)} H^2(e)$ and a vertex $v \in B$ produces the value at v equal to the sum of the outgoing derivatives of f along the edges of G adjacent to v. Here, we denote by $l^2(B)$ the d-dimensional Hilbert space of functions on B.

We can now define, for any $\lambda \notin \sigma(H_G)$, the *Dirichlet-to-Neumann operator* (in fact, a $d \times d$-matrix) $\Lambda(\lambda)$ as follows: for any $\phi \in l^2(B)$ let u be the (existing and unique) solution of the following problem:

$$\begin{cases} -u'' = \lambda u \text{ on each } e \in E(G), \\ u \text{ satisfies continuity and Kirchhoff condition at each vertex } v \notin B, \\ u|_B = \phi. \end{cases} \tag{V.1}$$

Then, $\Lambda(\lambda)\phi := Nu$. It is clear that $\Lambda(\lambda)$ is a meromorphic functions with poles at $\sigma(H_D)$ only (see [7, Section 3.5] for more detailed consideration of Dirichlet-to-Neumann operator in the quantum graph case and its relation to the resolvent of H_G).

Let $\lambda_0 \in \sigma(H_G)$. As it was indicated before, and as we will see clearly in the next section, it will be important for us that for any non-zero $\phi \in l^2(B)$ the vector function $\Lambda(\lambda)\phi$ still has a pole at λ_0. It is clearly sufficient to consider vectors ϕ that belong to the unit sphere S of $l^2(B) \approx \mathbb{C}^d$.

We recall and extend some auxiliary results from [47] that are crucial for our work. The proofs (with some minor changes) of these results are reproduced here for readers' convenience. From now on, unless otherwise specify, we use the notation $\|.\|$ to denote the L_2-norm.

Theorem V.1.1. *1. If for a given $\phi \in S$ and $\lambda = \lambda_0$ the problem (V.1) has a solution, then $\Lambda(\lambda)\phi$ does not have singularity at λ_0;*

2. If the problem (V.1) has no solution for $\lambda = \lambda_0$ and any $\phi \in S$, then for any ϕ, the following estimate holds in an (independent on ϕ) neighborhood of λ_0:

$$\|\Lambda(\lambda)\phi\| \geq \frac{C}{|\lambda - \lambda_0|}\|\phi\| \tag{V.2}$$

with a constant C independent of ϕ.

This result was established in [47, Theorem 20] for decoration graphs with no internal vertices (i.e. $V(G) \setminus B = \emptyset$). This unessential assumption can be removed as we see below.

Proof. 1. For $\lambda \neq \lambda_0$ we want to solve the spectral problem (V.1). Let $\tilde{\phi}$ be defined on G, twice differentiable on each edge, and satisfy continuity and Kirchhoff condition on $V(G) \setminus B$ such that $\tilde{\phi}|_B = \phi$. Such a function is easy to construct. Then $w = u - \tilde{\phi}$ solves the following problem

$$\begin{cases} -w'' - \lambda u = \tilde{\phi}'' + \lambda\tilde{\phi} \text{ on each } e \in E(G), \\ w \text{ satisfies continuity and Kirchhoff condition at each vertex } v \notin B, \\ w|_B = 0. \end{cases} \tag{V.3}$$

As for $\lambda = \lambda_0$ the problem (V.1) has a solution, let $\tilde{\phi}$ be that solution. Then, the solution of (V.3) can be written as

$$w = R(\lambda)(\tilde{\phi}'' + \lambda\tilde{\phi}) = R(\lambda)(\lambda - \lambda_0)\tilde{\phi} = (\lambda - \lambda_0)R(\lambda)\tilde{\phi}.$$

Since $\lambda_0 \in \sigma(H_G)$ and H_G is self-adjoint, $R(\lambda)$ has a pole of order one. This pole is eliminated by $(\lambda - \lambda_0)$, which implies that $\|\lambda(\lambda)\phi\| = \|N((\lambda - \lambda_0)R(\lambda)\tilde{\phi} + \tilde{\phi})\| < C$ for some constant C independent on λ.

2. Let $\{\psi_j\}$ be the orthonormal complete set of eigenfunctions of H_G corresponding to eigenvalues λ_j and $\Psi_j(v_i)$ be the sum of outgoing derivatives of ψ_j at v_i along all edges in $E(v_i)$, where $v_i \in B, i = \overline{1,d}$. Let us also denote by Ψ_j the vector $(\Psi_j(v_1), \ldots, \Psi_j(v_d))$.

For $\lambda \neq \lambda_0$ and $\phi \in S$, let $\tilde{\phi}$ be smooth on each edge of G, $\tilde{\phi}|_B = \phi$ that vanishes together with its first derivative on $V(G) \setminus B$. Then, $w = u - \tilde{\phi}$ solves the problem (V.3).

$$\begin{aligned}
w &= R(\lambda)(\tilde{\phi}'' + \lambda\tilde{\phi}) \\
&= \sum_j \langle R(\lambda)(\tilde{\phi}'' + \lambda\tilde{\phi}), \psi_j\rangle\psi_j = \sum_j \langle \tilde{\phi}'' + \lambda\tilde{\phi}, R(\overline{\lambda})\psi_j\rangle\psi_j \\
&= \sum_j \langle \tilde{\phi}'' + \lambda\tilde{\phi}, \frac{1}{\overline{\lambda} - \lambda_j}\psi_j\rangle\psi_j = \sum_j \frac{1}{\lambda - \lambda_j}\langle \tilde{\phi}'' + \lambda\tilde{\phi}, \psi_j\rangle\psi_j \\
&= \sum_j \frac{1}{\lambda - \lambda_j}\left(\sum_{i=1}^{d}\sum_{e\in E(v_i)} -\tilde{\phi}(v_i)\overline{\frac{d\psi_j}{dx_e}}(v_i)\psi_j + (\lambda - \lambda_j)\langle\tilde{\phi}, \psi_j\rangle\psi_j\right) \\
&= -\sum_j \frac{1}{\lambda - \lambda_j}\langle\phi, \Psi_j\rangle_{\mathbb{C}^d}\psi_j + \sum_j \langle\tilde{\phi}, \psi_j\rangle\psi_j \\
&= -\frac{1}{\lambda - \lambda_0}\sum_{\lambda_j = \lambda_0}\langle\phi, \Psi_j\rangle_{\mathbb{C}^d}\psi_j - \sum_{\lambda_j \neq \lambda_0}\frac{1}{\lambda - \lambda_j}\langle\phi, \Psi_j\rangle_{\mathbb{C}^d}\psi_j + \sum_j \langle\tilde{\phi}, \psi_j\rangle\psi_j.
\end{aligned}$$

In [47, Theorem 20] the assumption that there is no internal vertices was used to prevent unnecessary boundary terms from appearing after doing integration by part. With our choice of $\tilde{\phi}$, these terms go away even under the presence of internal vertices.

As $\sum_{e\in E(v_k)} \frac{d\tilde{\phi}}{dx_e}(v_k)$ is analytic with respect to λ for any v_k, it is sufficient to consider $\sum_{e\in E(v_k)} \frac{dw}{dx_e}(v_k)$. Computing the latter, we have

$$-\frac{1}{\lambda - \lambda_0}\sum_{\lambda_j = \lambda_0}\langle\phi, \Psi_j\rangle_{\mathbb{C}^d}\Psi_j(v_k) - \sum_{\lambda_j \neq \lambda_0}\frac{1}{\lambda - \lambda_j}\langle\phi, \Psi_j\rangle_{\mathbb{C}^d}\Psi_j(v_k) + \sum_j \langle\tilde{\phi}, \psi_j\rangle\Psi_j(v_k). \quad \text{(V.4)}$$

The last two terms are both analytic on a small neighborhood around λ_0. If the sum in the first term is nonzero at some v_k, then $\lambda(\lambda)\phi$ will blow up at $\lambda = \lambda_0$ for all nonzero ϕ. We now show that if (V.1) has no solution for all nonzero $\phi \in \mathbb{C}^n$ for $\lambda = \lambda_0$, then this will indeed happen. If the problem (V.1) has no solution u for non-zero ϕ, then the problem (V.3) also has no solution w for non-zero ϕ. By Fredholm alternative, there exists j such that

$$\lambda_j = \lambda_0 \text{ and } \langle\tilde{\phi}'' + \lambda_0\tilde{\phi}, \psi_j\rangle \neq 0, \text{ i.e. } 0 \neq \langle\tilde{\phi}'' + \lambda_0\tilde{\phi}, \psi_j\rangle = \sum_{i=1}^{d}\tilde{\phi}(v_i)\psi_j(v_i) = \langle\phi, \Psi_j\rangle_{\mathbb{C}^d}.$$

Therefore,

$$\langle \phi, \sum_{\lambda_j=\lambda_0} \langle \phi, \Psi_j \rangle_{\mathbb{C}^d} \Psi_j \rangle = \sum_{\lambda_j=\lambda_0} |\langle \phi, \Psi \rangle_{\mathbb{C}^d}|^2 > 0 \text{ for all } \phi \neq 0,$$

which implies $\sum_{\lambda_j=\lambda_0} \langle \phi, \Psi_j \rangle_{\mathbb{C}^d} \Psi_j \neq 0, \text{ for all } \phi \neq 0.$

Thus, there exists v_i such that $\sum_{\lambda_j=\lambda_0} \langle \phi, \Psi_j \rangle_{\mathbb{C}^d} \Psi_j(v_i) \neq 0.$

The first statement of case 2 of the theorem is proven. We now show the inequality (V.2).

From above we know that $\sum_{\lambda_j=\lambda_0} |\langle \phi, \Psi_j \rangle|^2 > 0$. This sum of square is a positive continuous function on the compact set S, there exists a positive constant C_1 such that

$$\sum_{\lambda_j=\lambda_0} |\langle \phi, \Psi_j \rangle|^2 \geq C_1 \text{ for all } \phi \in S. \tag{V.5}$$

Analogously, there exists a positive constant C_2 such that

$$\sum_{\lambda_j=\lambda_0} |\langle \phi, \Psi_j \rangle| \leq C_2 \text{ for all } \phi \in S.$$

For each j let us define function f_j as follows

$$f_j(\lambda) = \begin{cases} 1 \quad \text{if } \lambda_j = \lambda_0, \\ 1 + \frac{1}{\lambda - \lambda_j} \text{ if } \lambda_j \neq \lambda_0 \end{cases}$$

Function $f_j(\lambda)$ is analytic in some small neighborhood U of λ_0 not containing any $\lambda_j \neq \lambda_0$. Then, for $\lambda \in U$, there exists a constant $C_3 > 0$ such that

$$|f_j(\lambda)| \leq 1 + \frac{1}{|\lambda - \lambda_j|} \leq C_3 \text{ for all } j \in \mathbb{N} \text{ such that } \lambda_j \neq \lambda_0.$$

The following estimate is true for ϕ from S

$$\sum_j |f_j(\lambda)||\langle \tilde{\phi}, \psi_j \rangle||\langle \phi, \Psi_j \rangle_{\mathbb{C}^d}| \leq C_3 \|\tilde{\phi}\| \sum_j |\langle \phi, \Psi \rangle_{\mathbb{C}^d}| \leq C_2 C_3 \|\tilde{\phi}\|. \tag{V.6}$$

Using the expression (V.4) and $u = w + \tilde{\phi}$, we get

$$|\langle \Lambda(\lambda)\phi, \phi \rangle| \geq \frac{1}{|\lambda - \lambda_0|} \sum_{\lambda_j=\lambda_0} |\langle \phi, \Psi_j \rangle_{\mathbb{C}^d}|^2 - \sigma_j |f_j(\lambda)||\langle \tilde{\phi}, \psi_j \rangle||\langle \phi, \Psi_j \rangle_{\mathbb{C}^d}| - \langle \phi, \Phi \rangle_{\mathbb{C}^d},$$

where $\Phi = \left(\sum_{e \in E(v_1)} \frac{d\tilde{\phi}}{dx_e}(v_1), \ldots, \sum_{e \in E(v_d)} \frac{d\tilde{\phi}}{dx_e}(v_d) \right)$.

From (V.5) and (V.6), we have

$$|\langle \Lambda(\lambda)\phi, \phi \rangle| \geq \frac{C_1}{|\lambda - \lambda_0| - C_2 C_3 \|\tilde{\phi}\| - \|\Phi\|_{\mathbb{C}^d}}.$$

Since function $\tilde{\phi}$ is smooth on each edge, it is in $H^2(e)$ for all $e \in E(G)$. By Sobolev trace theorem on each edge, $\|\tilde{\phi}\|$ and $\|\Phi\|$ are bounded above by $C_4\|\phi\|$ for some positive constant C_4. Thus,

$$|\langle \Lambda(\lambda)\phi, \phi \rangle| \geq \frac{C_1}{|\lambda - \lambda_0|} - (C_2 C_3 + 1) C_4, .$$

For λ sufficiently close to λ_0, i.e. $|\lambda - \lambda_0| < \frac{C_1}{2C_5}$, where $C_5 = (C_2 C_3 + 1) C_4$,

$$\frac{C_1}{|\lambda - \lambda_0|} - (C_2 C_3 + 1) C_4 = \frac{1}{|\lambda - \lambda_0|}(C_1 - C_5|\lambda - \lambda_0|) > \frac{C_1}{2|\lambda - \lambda_0|}.$$

The desired estimate follows from here as $|\langle \Lambda(\lambda)\phi, \phi \rangle| \leq \|\Lambda(\lambda)\phi\|$. □

Thus, we will be looking at graphs G with boundary B such that the problem (V.1) has solution only for zero Dirichlet data ϕ. The following theorem describes some graphs with this property, and thus provides the desired gap-opening tool.

Theorem V.1.2. *Let $l_0 > 0$ and n be an odd natural number. Suppose that the pair G, B satisfies the following conditions:*

1. *Graph G contains a non-self-intersecting cycle Z consisting of an odd number of edges of the length l_0;*
2. *Each boundary vertex $v \in B$ either belongs to Z, or is connected to a vertex of Z by a path of edges of length l_0 each.*

Then, for $\lambda_0 = (n\pi/l_0)^2$, there exist a neighborhood U of λ_0 and a constant C such that the inequality (V.2) holds for any ϕ and $\lambda \in U$.

Proof. Assume on the contrary that there exists function $\phi \in S$ such that the problem (V.1) has a solution for $\lambda = \lambda_0$.

We first consider a special case. Suppose the cycle Z contains all the vertices in B_v which we denote as $(v_1, \ldots, v_d)$. On each edge connecting v_i to v_{i+1} the solution is of the form

$c_i \cos(\sqrt{\lambda_0}x) + b_i \sin(\sqrt{\lambda_0}x)$ with $x = 0$ representing v_i and $x = l_0$ representing v_{i+1}. Then $c_i = u(0) = \phi_i$ and $-c_i = u(l_0) = \phi_{i+1}$ since n is odd. Hence, $\phi_i = -\phi_{i+1}$.

Since there is an odd number of vertices in B_v, we have $\phi_1 = -\phi_2 = \ldots = \phi_n = -\phi_1$, which makes $\phi_i = 0, i = \overline{1,d}$ and thus $\phi = 0$ - contradiction.

Now let us consider the general case. Suppose at $\phi(v_{j_0}) \neq 0$ for some j_0. If v_{j_0} belongs to the cycle Z then by a similar argument we arrive at the contradiction. Otherwise, there is a l_0-path $(v_{j_0}, \ldots, v_{j_k})$ connects to a vertex v_c ($v_c \equiv v_{j_k}$) belonging to Z. Let e_{j_i} be the edge connecting vertices v_{j_i} and $v_{j_{i+1}}, i = 0, \ldots, k-1$. On each of these edge, the solution of (V.1) has the form $c_i \cos(\sqrt{\lambda_0}x) + b_i \sin(\sqrt{\lambda_0}x)$ with $x = 0$ representing v_{j_i} and $x = l_0$ representing $v_{j_{i+1}}$. Again, we have $\phi_{j_0} = -\phi_{j_1} = \ldots = (-1)^k \phi_{j_k} = 0$. Thus, $\phi = 0$ which is contradict to $\phi \neq 0$. Problem (V.1) therefore cannot have a solution for non-zero ϕ for $\lambda = \lambda_0$. □

V.2 Spectral gaps opening

The main result of this chapter is the following

Theorem V.2.1. *Let $l_0 > 0$ and n be an odd natural number. Let also the infinite periodic d-regular graph Γ_0, finite graph G with boundary B, $|B| = d$, and the decorated graph Γ be as before. Suppose that the following conditions are satisfied:*

1. *$\lambda_0 = (n\pi/l_0)^2$ is not in the Dirichlet spectrum Σ_D of Γ_0, with $dist(\lambda_0, \Sigma_D) = \delta > 0$;*
2. *The decoration (resonator) (G, B) satisfies the conditions of Theorem V.1.2.*

Then, there exists a punctured neighborhood of λ_0, depending on G, topology of Γ_0, and δ only, which does not belong to the spectrum $\sigma(H)$.

Proof. As before, by H_θ we denote Bloch Hamiltonian operator that acts in the same way as H does and has domain consisting of functions u such that

1. $u \in H^2(e)$ for each edge e;
2. u is continuous on the whole graph;
3. at each vertex, the sum of the outgoing derivatives of u along all adjacent edges is equal to zero (Kirchhoff condition);
4. u satisfies Floquet condition, i.e. $u(x + pe) = e^{ip\theta}u(x)$, for all $x \in G$ and $p \in \mathbb{Z}^n$.

If $\lambda \in \sigma(H)$, then there exists a quasimomentum $\theta \in [-\pi, \pi)^n$ and a corresponding non zero quasi-periodic Floquet-Bloch eigenfunction u_θ of H_θ.

Removing all internal edges and vertices from each of the decorations in Γ, one gets a disjoint union of edges of Γ_0 (see Fig V.3), since each former vertex $v \in \Gamma_0$ is replaced by d vertices $v_1, \ldots, v_d$. We denote this new graph $\widetilde{\Gamma}$. By $\widetilde{W}$ we denote the fundamental domain of $\tilde{\Gamma}$.

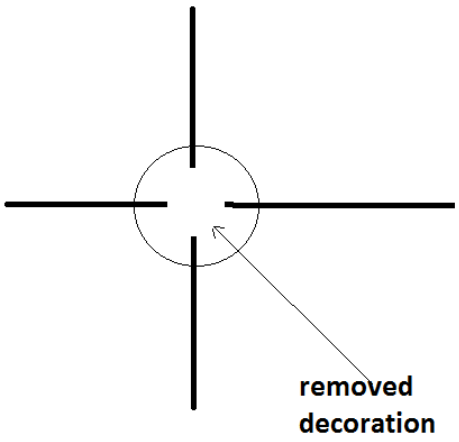

Figure V.3: Decoration removed from a former vertex of degree 4.

Denoting

$$\phi_v := (u_\theta(v_1), \ldots, u_\theta(v_d))^t,\ \phi'_v := (du_\theta/dx_{e_1}(v_1), \ldots, du_\theta/dx_{e_d}(v_d))^t,$$

where $e_1, \ldots, e_d$ are the edges formerly adjacent to vertex v and coordinates x_{e_j} increase from the value zero at vertex v, one can rewrite the equation for u on Γ as the following one on $\widetilde{\Gamma}$:

$$\begin{cases} -u''_\theta = \lambda u_\theta \text{ on each edge } e \in \tilde{\Gamma}, \\ \phi'_v = -\Lambda(\lambda)\phi_v \text{ for all vertices } v \in V(\tilde{\Gamma}). \end{cases} \tag{V.7}$$

From now on, we write u instead of u_θ when there is no confusion.

We consider only λ from the neighborhood of λ_0 with radius less than $\delta/2 = dist(\lambda_0, \Sigma_D)/2$. Then, it does not intersect with Σ_D and for all λ from this neighborhood we have

$$(1 + |\lambda|^2) \leq 1 + (|\lambda_0| + \delta/2)^2.$$

Let $x \in [0, l_e]$ be the coordinate defined on the edge e. By u_e we denote the solution of $-u'' = \lambda u$ on edge e. As $\|u\|_{H^2(e)}$ is equivalent to the norm defined by $(\|u\|^2 + \|u''\|^2)^{1/2}$,

for some positive constant C_1 depending only on the topology of Γ_0 we have

$$\|u\|^2_{H^2(e)} \le C_1 \int_e (\|u\|^2 + \|u''\|^2) = C_1 \int_e (1+|\lambda|^2)|u|^2 dx \le 1 + (|\lambda_0| + \delta/2)^2) C_1 \|u\|.$$

We have three cases depending on λ.

Case 1: Suppose that $\lambda > 0$. On each edge e in Γ_0 we have $\sin\sqrt{\lambda} l_e \neq 0$ because $\lambda \notin \Sigma_D$. The solution of $-u'' = \lambda u$ on e has the following form:

$$u_e(x) = \frac{u(0)\sin\sqrt{\lambda}(l_e - x) + u(l_e)\sin\sqrt{\lambda}x}{\sin\sqrt{\lambda} l_e}.$$

We then have

$$\|u\|^2_{H^2(e)} \le (1 + (|\lambda_0| + \delta/2)^2) C_1 \|u\| \le \frac{2(1+|\lambda|^2) C_1 l_e}{\sin^2\sqrt{\lambda} l_e} \sum_{v_i \in e} |u(v_i)|^2$$

In order to estimate the term $\sin\sqrt{\lambda} l_e$, we inscribe a triangle inside each hump of $|\sin\sqrt{\lambda} l_e|$ with vertices of triangle at $((n-1)\pi, 0), (n\pi, 0)$, and $((2n-1)\pi/2, 1)$ for some $n \in \mathbb{N}$ (see Fig. V.4), then we obtain

$$|\sin\sqrt{\lambda} l_e| \ge \frac{2l_e}{\pi} \min_n |\sqrt{\lambda} - \frac{n\pi}{l_e}|.$$

There exists a positive constant C_2 depending on λ_0 and δ only such that

$$\frac{2l_e}{\pi} \min_n |\sqrt{\lambda} - \frac{n\pi}{l_e}| \ge \frac{2l_e C_2}{\pi} \min_n |\lambda - \left(\frac{n\pi}{l_e}\right)^2 |. \tag{V.8}$$

On the other hand,

$$\min_n |\lambda - \left(\frac{n\pi}{l_e}\right)^2 | \ge \min_n |\lambda_0 - \left(\frac{n\pi}{l_e}\right)^2 | - |\lambda - \lambda_0| \ge \frac{\delta}{2}. \tag{V.9}$$

From (V.8) and (V.9) we have

$$|\sin\sqrt{\lambda} l_e| \ge \frac{C_2 \delta l_e}{\pi}.$$

Therefore, for some constant C_3 depending only on λ_0, δ, and Γ_0 we have

$$\|u\|^2_{H^2(e)} \le C_3 \sum_{v \in e} |u(v)|^2.$$

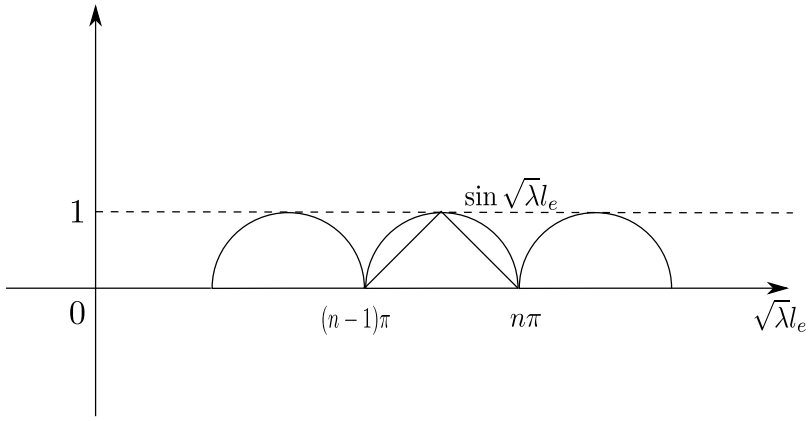

Figure V.4: Inscribe a triangle inside each hump of $|\sin\sqrt{\lambda}l_e|$

Summing this over all the edges e from the fundamental domain, we obtain

$$\sum_{e\in\widetilde{W}} \|u\|^2_{H^2(e)} \leq dC_3 \sum_{v\in\widetilde{W}} |u(v)|^2$$

Case 2: If $\lambda = 0$, then

$$u_e(x) = \frac{u(0)(l_e - x) + u(l_e)x}{l_e}$$

There exist C_4, C_5 depending on λ_0, δ, and Γ_0 such that

$$\sum_{e\in\widetilde{W}} \|u\|^2_{H^2(e)} \leq \sum_{e\in\widetilde{W}} (1 + (|\lambda_0| + \delta/2)^2) C_1 \|u\| \leq \sum_{e\in\widetilde{W}} C_4 \sum_{v\in e} |u(v)|^2 \leq C_5 \sum_{v\in\widetilde{W}} |u(v)|^2.$$

Case 3: If $\lambda < 0$, then

$$u_e(x) = \frac{u(0)\sinh\sqrt{-\lambda}(l_e - x) + u(l_e)\sinh\sqrt{-\lambda}x}{\sinh\sqrt{-\lambda}l_e}.$$

Again, we have that

$$\sum_{e\in\widetilde{W}} \|u\|^2_{H^2(e)} \leq \sum_{e\in\widetilde{W}} (1 + (|\lambda_0| + \delta/2)^2) C_1 \sum_{v\in e} |u(v)|^2 \leq C_6 \sum_{v\in\Gamma_0} \sum_{v_i\in B_v} |u(v_i)|^2$$

for some C_6 constant depending on $\lambda_0, \delta, \Gamma_0$.

Hence, in all cases, we end up with

$$\sum_{e\in\widetilde{W}} \|u\|_{H^2(e)} \leq C \sum_{v\in\widetilde{W}} \|\phi_v\|^2_{\mathbb{C}^d},$$

where the constant C depends on $\lambda_0, \delta, \Gamma_0$ only.

Combining that with the trace estimate (e.g., [7, Theorem 1.3.8]), we have

$$\sum_{v\in\widetilde{W}} \|\phi'_v\|^2_{\mathbb{C}^d} \leq M \sum_{v\in\widetilde{W}} \|\phi_v\|^2_{\mathbb{C}^d}. \tag{V.10}$$

for a constant M that only depends on λ_0, δ, and the topology of Γ_0.

On the other hand, when λ is sufficiently close to λ_0, according to Theorem V.1.2, one has

$$\sum_{v\in\widetilde{W}} \|\phi'_v\|^2_{\mathbb{C}^d} \geq \frac{C^2}{|\lambda-\lambda_0|^2} \sum_{v\in\widetilde{W}} \|\phi_v\|^2_{\mathbb{C}^d} > M \sum_{v\in\widetilde{W}} \|\phi_v\|^2_{\mathbb{C}^d}. \tag{V.11}$$

The contradiction obtained from (V.10) and (V.11) proves the claim of the theorem. □

V.3 Some remarks

(1) Although it is not easy to understand the general case of spider decoration, the main result of this chapter provides a way to create spectral gaps rather easily at prescribed locations. The spectral value $(n\pi/l_0)^2$ involves an arbitrary positive length l_0 and an odd natural number n, which gives one a significant freedom of choosing location (one just needs to avoid the Dirichlet spectrum of Γ_0). When such a value is specified, one can easily produce a spider decoration G that creates the gap. An example of such a procedure is shown in Fig.V.5 for the case $d = 4$. The structure of decoration graph is also quite flexible, for example, there is no constraint on its inner vertices or edges as long as the listed conditions from Theorem V.1.2 are satisfied.

(2) The regularity assumption on the graph Γ_0 can be removed. Indeed, one can still open a spectral gap in the case of non-regular periodic graph by choosing different spider decorations adjusted to each vertex such that the corresponding resonant value λ_0 agree.

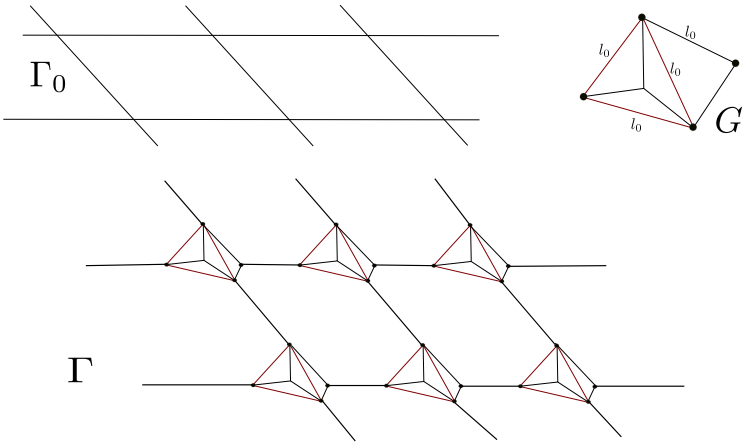

Figure V.5: An example of spider decoration. The decorated graph Γ is obtained from the periodic 4-regular graph Γ_0 and the decoration graph G

CHAPTER VI

SUMMARY

In chapter II and chapter III we analyzed dispersion relations of periodic Schrödinger operators with real and even potentials on graphyne and its related nanotubes respectively. Various information about singular continuous spectra, absolutely continuous spectra, and pure point spectra of the operators was extracted from here. Unlike similar periodic operators in $\mathbb{R}^n$, the quantum graph operators on these structures were proven to have nonempty point spectra (i.e., bound states). We found these parts of the spectra and provided explicit description of the corresponding eigenspaces. Spectral gaps and Dirac cones for a graphyne structure were described. The formulations of the results involved the discriminant of the Hill operator with the potential obtained by the periodic extension of the 1D potential on a single edge. The presence of Dirac cones makes some of graphynes, which do not have honeycomb symmetry, fascinating in terms of their electrical properties.

In chapter IV, we investigated the conjecture that the extrema of dispersion relation of a generic periodic Schödinger operator have only non-degenerate Hessian. We studied a simpler version of the conjecture using the graph approach. In particular, we proved the conjecture for periodic difference operators on a class of discrete (combinatorial) graphs.

In the last chapter V, we studied the creation of gaps in the spectra of some periodic operators. Namely, we extended the technique that was used in [47] to open and manipulate the spectral gaps in the finite quantum graph case. It was proven that inserting some internal structure into each vertex will indeed open a gap. We were able to remove the unessential condition that prohibits internal vertices of the decoration graph. Moreover, we proved that the same technique works well in the infinite periodic quantum graph case.

REFERENCES

[1] M. Aizenman and J. Schenker, *The creation of spectral gaps by graph decoration*, Lett. Math. Phys. **53** (2000), 253–262.

[2] C. Amovilli, F. Leys, and N. March, *Electronic Energy Spectrum of Two-Dimensional Solids and a Chain of C Atoms from a Quantum Network Model*, Journal of Mathematical Chemistry **36** (2004), no. 2, 93–112.

[3] N. Ashcroft and D. Mermin, *Solid state physics*, Holt, Rinehart and Winston, 1976.

[4] D. Bardhan, *Novel New Material Graphyne Can Be A Serious Competitor To Graphene*, 2012, http://techie-buzz.com/science/graphyne.html.

[5] D. J. Bates et al., *Bertini: Software for Numerical Algebraic Geometry*, 2013, http://bertini.nd.edu.

[6] G. Berkolaiko and A. Comech, *Symmetry and Dirac points in graphene spectrum*, (2014). arXiv: 1412.8096.

[7] G. Berkolaiko and P. Kuchment, *Introduction to quantum graphs*, American Mathematical Society, 2012.

[8] E. Bierstone and P. D. Milman, *Semianalytic and subanalytic sets*, Inst. Hautes Etudes Sci. Publ. Math. **67** (1988), 5–42.

[9] G. Borg, *Eine Umkehrung der Sturm-Liouvillischen Eigenwertaufgabe*, Acta Mathematica **78** (1946), 1–96.

[10] M.J. Bucknum and E.A. Castro, *The squarographites: A lesson in the chemical topology of tessellations in 2- and 3-dimensions*, Solid State Sciences **10** (2008), 1245–1251.

[11] N. Do, *On the quantum graph spectra of graphyne nanotubes*, Analysis and Mathematical Physics **5.1** (2015), 39–65.

[12] N. Do and P. Kuchment, *Spectra of Schrödinger operators on a graphyne structure*, Nanoscale Systems: Mathematical Modeling, Theory and Applications **2** (2013), 107–123.

[13] N. Do, P. Kuchment, and B. S. Ong, *On resonant spectral gap opening in quantum graph networks*, to appear (2016). arXiv: 1601.04774.

[14] N. Do, P. Kuchment, and F. Sottile, *On generic properties of dispersion relations of periodic operators*, in preparation.

[15] M.S.P. Eastham, *The Spectral Theory of Periodic Differential Equations*, Scottish Academic Press Ltd., 1973.

[16] A. Enyanshin and A. Ivanovskii, *Graphene Alloptropes: Stability, Structural and Electronic Properties from DF-TB Calculations*, Physics Status Solidi (b) **248** (2011), no. 8, 1879–1883.

[17] P. Exner and O. Post, *Convergence of spectra of graph-like thin manifolds*, Journal of Geometry and Physics **54** (2005), 77–115.

[18] P. Exner. et al., eds., *Analysis on graphs and its applications*, vol. 77, Proceedings of Symposia in Pure Mathematics, American Mathematical Society, Providence, RI, 2008, Papers from the program held in Cambridge, January 8–June 29, 2007.

[19] C.L. Fefferman and M.I. Weinstein, *Honeycomb latice potentials and Dirac points*, Journal of American Mathematical Society **25** (2012), 1169–1220.

[20] C.L. Fefferman and M.I. Weinstein, *Waves in Honeycomb Structures*, (2012). arXiv: 1212.6684.

[21] N. Filonov and I. Kachkovskiy, *On the structure of band edges of 2d periodic elliptic operators*, (2015). arXiv: 1510.04367.

[22] A. Geim, *Nobel lecture: Random walk to graphene*, Reviews of Modern Physics **83** (2011), 851–862.

[23] I. M. Gelfand, *Expansion in eigenfunctions of an equation with periodic coefficients*, Dokl. Akad. Nauk. SSSR **73** (1950), 1117–1120.

[24] E.A. Gorin, *Asymptotic properties of polynomials and algebraic functions of several variables*, Russian Mathematical Surveys **16** (1961), no. 1, 91–118.

[25] *Graphene*, https://en.wikipedia.org/wiki/Graphene, Accessed: 2016-05-12.

[26] *Graphene nanotubes*, http://commons.wikimedia.org/wiki/File:Types_of_Carbon_Nanotubes.png, Accessed: 2016-05-12.

[27] *Graphynes*, http://physicsworld.com/cws/article/news/2012/mar/01/could-graphynes-be-better-than-graphene, Accessed: 2016-05-12.

[28] P. Harris, *Carbon Nano-tubes and Related Structures*, Cambridge University Press, 2002.

[29] J. M. Harrison et al., *On occurrence of spectral edges for periodic operators inside the Brillouin zone*, Journal of Physics A: Mathematical and Theoretical **40** (2007), no. 27, 75–97.

[30] J. D. Joannopoulos et al., *Photonic Crystals: Molding the Flow of Light*, 2nd, Princeton University Press, Princeton, N.J., 2008.

[31] T. Kato, *Perturbation theory for linear operators*, Springer-Verlag, Berlin, 1995.

[32] M.I. Katsnelson, *Graphene. Carbon in two dimensions*, Cambridge University Press, 2012.

[33] W. Kirsch and B. Simon, *Comparison theorems for the gap of Schrödinger operators*, Journal of Functional Analysis **75** (1985), no. 2, 396–410.

[34] F Klopp and J. Ralston, *Endpoints of the spectrum of periodic operators are generically simple*, Methods and Application in Analysis **7** (2000), 459–464.

[35] E. Korotyaev and I. Lobanov, *Schrödinger operators on zigzag graphs*, Annales Henri Poincaré **8** (2007), no. 6, 1151–1176.

[36] E. Korotyaev and I. Lobanov, *Zigzag periodic nanotube in magnetic field*, (2006). arXiv: `1012.0814v2 [math.QA]`.

[37] P. Kuchment, *An overview of periodic elliptic operators*, Bulletin of the American Math. Soc. (2016).

[38] P. Kuchment, *Floquet Theory for Partial Differential Equations*, Birkhauser Verlag, 1993.

[39] P. Kuchment, *On some spectral problems of mathematical physics*, Contemporary Mathematics **362** (2004).

[40] P. Kuchment, *Quantum graphs I. Some basic structures*, Waves in Random media **14** (2004), S107–S128.

[41] P. Kuchment, *Quantum graphs II. Some spectral properties of quantum and combinatorial graphs*, Journal of Physics A: Mathematical and Theoretical **38** (2005), no. 22, 4887–4900.

[42] P. Kuchment, "The mathematics of photonic crystals", *Mathematical modeling in optical science*, ed. by G. Bao, L. Cowsar, and W. Masters, vol. 22, Frontiers Appl. Math. SIAM, Philadelphia, PA, 2001, pp. 207–272.

[43] P. Kuchment and L. Kunyansky, *Spectral properties of high-contrast band-gap materials and operators on graphs*, Experimental Mathematics **8** (1999), no. 1, 1–28.

[44] P. Kuchment and O. Post, *On the Spectra of Carbon Nano-Structures*, Communications in Mathematical Physics **275** (2007), no. 3, 805–826.

[45] D. Malko et al., *Competition for Graphene: Graphynes with Direction-Dependent Dirac Cones*, Physical Review Letters **108** (2012).

[46] K. Novoselov, *Nobel lecture: Graphene: Materials in the flatland*, Reviews of Modern Physics **83** (2011), 837–849.

[47] B.-S. Ong, *Spectral Problems of Optical Waveguides and Quantum Graphs*, PhD thesis, Texas A&M University, 2006.

[48] K. Pankrashkin, *Spectra of Schrödinger operators on equilateral quantum graphs*, Letters in Mathematical Physics **77** (2006), no. 2, 139–154.

[49] L. Pauling, *The diamagnetic anisotropy of aromatic molecules*, Journal of Chemical Physics **4** (1936), no. 10, 673–677.

[50] B. Pavlov, *The theory of extensions, and explicitly solvable models*, Uspekhi Mat. Nauk **42** (1987), no. 6(258), 99–131, 247.

[51] M. Reed and B. Simon, *Methods of Modern Mathematical Physics: Functional analysis*, vol. 4, Academic Press, 1972.

[52] O. Reingold, S. Vadhan, and A. Wigderson, *Entropy waves, the zig-zag graph product, and new constant-degree expanders*, Ann. of Math. (2) **155** (2002), no. 1, 157–187.

[53] J. Rubinstein and M. Schatzman, *Variational problems on multiply connected thin strips. I. Basic estimates and convergence of the Laplacian spectrum*, Archive for Rational Mechanics and Analysis **160** (2000), no. 4, 271–308.

[54] K. Ruedenberg and C.W. Scherr, *Free-electron network model for conjugated systems*, The Journal of Chemical Physics: I. Theory **21** (1953), no. 9, 1565–1581.

[55] Y. Saito, *The limiting equation for Neumann Laplacians on shrinking domains*, Electronic Journal of Differential Equations **31** (2000), 1–25.

[56] B. Simon, *On the genericity of nonvanishing instability intervals in Hills equation*, Annales Henri Poincaré **24** (1976), no. 1, 91–93.

[57] L.E. Thomas, *Time dependent approach to scattering from impurities in a crystal*, Communications in Mathematical Physics **33** (1973), 335–343.

[58] Y. Colin de Verdiere, *Sur les singularites de van Hove generiques*, Mem. Soc. Math. France (1991), no. 46, 99–109.

[59] P. R. Wallace, *The band theory of graphite*, Phys. Rev. **71** (1973), 622.